TDP-43 IS DIRECTED TO STRESS GRANULES BY SORBITOL, A NOVEL PHYSIOLOGICAL OSMOTIC AND OXIDATIVE STRESSOR

APPROVED BY SUPERVISORY COMMITTEE

Gang Yu, Ph.D.
P. Robin Hiesinger, Ph.D.
Joachim Herz, Ph.D.
Kimberly Huber, Ph.D.

DEDICATION

I would like to thank the members of my graduate committee for their guidance, support and encouragement throughout this process, and Gang and all Yu lab members for their scientific critiques and discussions. I would also like to thank my parents, my siblings and brother in law for encouragement and support, and my grandparents for inspiring me to become a scientist. Finally, I thank Brett A. Johnson for many scientific discussions, and his support, advice and love.

TDP-43 IS DIRECTED TO STRESS GRANULES BY SORBITOL, A NOVEL PHYSIOLOGICAL OSMOTIC AND OXIDATIVE STRESSOR

by

COLLEEN MARIE DEWEY

DISSERTATION

Presented to the Faculty of the Graduate School of Biomedical Sciences

The University of Texas Southwestern Medical Center at Dallas

In Partial Fulfillment of the Requirements

For the Degree of

DOCTOR OF PHILOSOPHY

The University of Texas Southwestern Medical Center at Dallas

Dallas, Texas

August, 2011

TDP-43 IS DIRECTED TO STRESS GRANULES BY SORBITOL, A NOVEL PHYSIOLOGICAL OSMOTIC AND OXIDATIVE STRESSOR

COLLEEN MARIE DEWEY, Ph.D.

The University of Texas Southwestern Medical Center at Dallas, 2011

GANG YU, Ph.D.

TDP-43, or TAR DNA-binding protein 43, is a pathological marker of a spectrum of neurodegenerative disorders including amyotrophic lateral sclerosis (ALS) and frontotemporal lobar degeneration with ubiquitin-positive inclusions (FTLD-U). TDP-43 is an RNA/DNA-binding protein implicated in transcriptional and post-transcriptional regulation. Recent work also suggests that TDP-43 associates with cytoplasmic stress granules, which are transient structures that form in response to stress. In this study, we establish sorbitol as a novel stressor that directs TDP-43 to stress granules in Hek293T cells and primary cultured glia. We quantify TDP-43 association with stress granules over time and show that stress granule association and size are dependent on the glycine-rich region of TDP-43, which harbors the majority of pathogenic mutations. Moreover, we

establish that cells harboring wild-type and mutant TDP-43 have distinct stress responses: mutant TDP-43 forms significantly larger stress granules and incorporates into stress granules more early; in striking contrast, wild-type TDP-43 forms more stress granules over time, but granule size remains relatively unchanged. We propose that mutant TDP-43 alters stress granule dynamics, which may contribute to the progression of TDP-43 proteinopathies.

TABLE OF CONTENTS

PRIOR PUBLICATIONS

Sheu-Fen Lee, Bhooma Srinivasan, Chantelle F. Sephton, Daniel R. Dries, Wang, Cong Yu, Yun Wang, Colleen M. Dewey, Sanjiv Shah, Jin Jiang and Gang Yu. Gamma-secretase-regulated proteolysis of notch by mitochondrial intermediate peptidase. **Journal of Biological Chemistry.** 2011, doi:10.1074/jbc.M111.243154.

Basar Cenik, Chantelle F. Sephton, Colleen M. Dewey, Xunde Xian, Shuguang Wei, Kimberley Yu, Wenze Niu, Giovanni Coppola, Sarah E. Coughlin, Suzee E. Lee, Sandra Almeida, Daniel H. Geschwind, Fen-Biao Gao, Bruce L. Miller, Robert V. Farese, Bruce A. Posner, Gang Yu and Joachim Herz. SAHA (VORINOSTAT) upregulates progranulin transcription: a rational therapeutic approach to frontotemporal dementia. **Journal of Biological Chemistry**. 2011, doi: 10.1074/jbc.M110.193433.

Colleen M. Dewey, Basar Cenik, Chantelle F. Sephton, Daniel R. Dries, Shannon K. Good, Brett A. Johnson, Joachim Herz and Gang Yu. TDP-43 is directed to stress granules by sorbitol, a novel physiological osmotic and oxidative stressor. **Molecular and Cellular Biology**, 2011, 31(5):1098-1108.

Chantelle F. Sephton, Can Cenik, Alper Kucukural, Eric B. Dammer, Basar Cenik, YuHong Han, Colleen M. Dewey, Fritz P. Roth, Joachim Herz, Junmin Peng, Melissa J. Moore and Gang Yu. Identification of neuronal RNA targets of TDP-43-containing ribonucleoprotein complexes. **Journal of Biological Chemistry**. 2011, 286:1204-1215.

Paul R. Mayer, Nian Huang, Colleen M. Dewey, Daniel R. Dries, Hong Zhang and Gang Yu. Expression, localization, and biochemical characterization of nicotinamide mononucleotide adenyltransferase 2. **Journal of Biological Chemistry**. 2010, 285(51):40387-96.

Chantelle F. Sephton, Shannon K. Good, Stan Atkin, Colleen M. Dewey, Paul Mayer III, Joachim Herz and Gang Yu. TDP-43 is a developmentally regulated protein essential for early embryonic development. **The Journal of Biological Chemistry**. 2010, 285(9):6826-6834.

Suprabha Pulipparacharuvil, William Renthal, Carly F. Hale, Makoto Taniguchi, Guanghua Xiao, Arvind Kumar, Scott J. Russo, Devanjan Sikder, Colleen M. Dewey, Maya Davis, Paul Greengard, Angus C. Nairn, Eric J. Nestler and Christopher W. Cowan. Cocaine regulates MEF2 to control synaptic and behavioral plasticity. **Neuron**. 2008, 59:621-33.

Gabriela Lavezzari, Jennifer McCallum, Colleen M. Dewey, and Katherine W. Roche. Subunit-specific regulation of NMDA receptor endocytosis. **The Journal of Neuroscience**. 2004, 24(28):6383-6391.

LIST OF FIGURES

LIST OF TABLES

LIST OF ABBREVIATIONS

TDP-43, TAR DNA-binding protein 43

ALS, amyotrophic lateral sclerosis

FTLD-U, frontotemporal lobar degeneration with ubiquitinated inclusions

RRM, RNA recognition motif

GRR, glycine-rich region

hnRNP, heterogeneous ribonucleoprotein

wt, wild-type

TIA-1, T-cell-restricted intracellular antigen-1

TIAR, TIA1 cytotoxic granule-associated RNA binding protein-like 1

PARP, poly(ADP-ribose) polymerase

ROS, reactive oxygen species

VCP, valosin containing protein

CHMP2B, Chromatin modifying protein 2B

VABP, vesicle associated membrane protein associated protein B

sALS, sporadic ALS

fALS, familial ALS

eIF3, elongation initiation factor 3

AD, Alzheimer's disease

PD, Parkinson's disease

HD, Huntingtin's disease

APP, amyloid precursor protein

SOD1, superoxide dismutase 1

ANG, angiogenin

FTD-ALS, frontotemporal lobar degeneration with amyotrophic lateral sclerosis

FTD-MND, frontotemporal lobar degeneration with motor neuron disease

DIV, days in vitro

CHAPTER ONE
Introduction

THE IMPORTANCE OF STUDYING NEURODEGNERATION

Combating neurodegeneration in an aging society

The United States is the third largest country in the world in 2011 behind China and India. With respect to the US age structure, only 20.1% of its population is in the 0-14 year age bracket, while 66.8% fall in the 15-64 bracket and 13.1% are 65 and older bracket. A troubling issue is that our nation's "baby boomer" population (the birth boom from 1946 through 1964) is only now approaching age 65(3). Beginning in 2011, and spanning the next 20 years, the US expects an unprecedented number of its citizens to transition from middle-aged to elderly(44, 136).

The United States is not alone: many countries experienced the post-world war II baby boom(50, 61, 98). As a result, many countries have a relatively large aging population. As this demographic bulge ages, susceptibility to dementias and other age-related disorders like cancers, type-II diabetes and cardiovascular diseases increase(136). Yet, neurodegenerative disorders are not restricted to the 65 years and older age bracket. Depending on genetic predisposition, exposure to high levels of environmental toxins, or leading a "high risk" lifestyle, disease onset can occur at a much younger age(134).

Two examples of neurodegenerative diseases affecting the middle-aged and elderly include amyotrophic lateral sclerosis or ALS (age 40-60 yrs)(134) and frontotemporal lobar degeneration with ubiquitinated aggregates or FTLD-U (age 46-78)(57). Middle-age onset of these diseases is particularly devastating for younger families. Why and how the central nervous system is both temporally and spatially susceptible to degeneration is unknown. What is understood however, is that now in the industrialized world there exists an urgent need to understand the etiology of neurodegenerative diseases. As more data becomes available, it is imperative that clinicians and scientists work together to define common clinical symptoms and pathologies leading to neurodegeneration, both in the middle-aged and elderly.

Common pathological features across neurodegenerative diseases

There are some broad similarities among different neurodegenerative disorders, including increased risk with age. But another common feature is the presence of aggregated, ubiquitinated proteins. Just to name a few examples, ubiquitinated aggregates are found in Alzheimer's disease (AD), Parkinson's disease (PD), Huntington's disease (HD), amyotrophic lateral sclerosis (ALS) and frontotemporal lobar degeneration with ubiquitinated aggregates (FTLD-U). Commonly, these aggregated proteins have mutations in the gene encoding them. For example, amyloid precursor protein composes the amyloid plaques found in AD and mutations have been found in its gene. Likewise, alpha synuclein and huntingtin aggregates are found in PD and HD patients respectively, and

mutations have been found in both genes. In contrast, for many years, the proteins composing the ubiquitinated aggregates in ALS and FTLD-U were unknown.

Clearly, in multiple neurodegenerative disorders, there is some problem in clearing these aggregating proteins. In contrast, healthy cells are able to clear unwanted proteins by labeling them with ubiquitin chains, the degradation signal of the cell. These ubiquitin chains attract a proteasome that chops up and recycles the amino acids present in the degraded protein. Alternatively, another degradative process called autophagy exists in the cell to degrade unwanted cellular matter. Hence, a common hypothesis in neurodegenerative disorders is an impairment in the ubiquitin-proteasome system, autophagy or both. Yet some questions remain: are these processes less efficient in people with neurodegenerative disorders, or are the proteins aggregating too quickly for the cell to clear them away?

Thus, many neurodegenerative diseases are broadly united by increased risk with age and the presence of ubiquitinated protein aggregates. Previously, it was argued that the mechanism behind each neurodegenerative disease was distinct, as there was a "selective vulnerability" of these brain cells to degrade. Yet, as more neurodegenerative research is conducted, it is becoming evident that the underlying mechanism behind this neurodegeneration may be more "common" than distinct. As new data emerges, perhaps many neurodegenerative diseases are more similar in onset than previously believed. Additional common features across different diseases must be investigated.

ALS and FTLD-U are clinically linked neurodegenerative diseases

In addition to increased risk with age and the presence of ubiquitinated aggregates, some neurodegenerative diseases also have overlapping symptoms. For example, for many years it was a widely accepted belief that ALS only affected motor neurons, sparing higher cognitive functions. However, it is now understood that ALS patients have dementia overlapping clinically with FTLD-U(85). This finding may be surprising to some scientists, as ALS and FTLD-U were previously believed to affect neurons in disparate regions of the central nervous system: the brain in FTLD-U and the spinal cord in ALS.

To better understand the common underlying symptoms in these diseases, an introduction into ALS and FTLD-U is essential. First, ALS is a progressive, neurodegenerative disease affecting the upper and lower motor neurons; incidence is rare with only one to two people per 100,000(86). The duration of the disease can vary, but on average lasts 3-5 years(85). During this time, patients undergo symptoms of muscle atrophy and paralysis before dying of respiratory failure or pneumonia(60, 113).

In contrast, FTLD is a progressive neurodegenerative disease affecting frontal and temporal cortical neurons(52, 85). FTLD is typically diagnosed between 40-65 years of age, and is second only to Alzheimer's disease in its prevalence in those aged 65 and younger(53, 62). FTLD is a clinically, genetically and pathologically heterogeneous disease, and the FTLD-U subtype has ubiquitin immunoreactive aggregates(102).

The clinical symptoms arising from FTLD-U can be divided into three subtypes: behavioral variant frontotemporal dementia, semantic dementia, and progressive non-fluent aphasia(29). The behavioral variant is a consequence of frontal cortex neuron degeneration where personality changes manifest including lethargy, apathy and disinhibition(53). The semantic dementia (SD) variant develops as temporal cortex neurons degenerate, producing symptoms including aphasia (inability to articulate or understand spoken or written language). Finally, progressive non-fluent aphasia is marked by impaired speech production, including hesitant speech, stuttering and incorrect tense or word order(62, 115).

Thus, the type of overlapping symptoms between ALS and FTLD-U patients include motor impairments in FTLD-U patients and both behavioral and speech problems in ALS patients(47). In patients with FTD, this variant is called "FTD-MND" or "FTD-ALS", meaning FTD with motor neuron disease, or FTD with amyotrophic lateral sclerosis, respectively. In one report, among 36 patients with sporadic FTD, ~14% were diagnosed with ALS, while 36% had some symptoms consistent with ALS(89). In patients with ALS, this variant is called "ALS-FTD", meaning ALS with frontotemporal lobar degeneration. In one report, from 44 ALS patients in the study, ~52% were diagnosed with FTD(90). As this area of research is relatively new, these statistics will undoubtedly change as more clinical data is published.

Importantly, patients diagnosed with ALS-FTD not only have overlapping clinical symptoms between ALS and FTD, but the ubiquitinated aggregates are found in both the spinal cord and the brain(34, 106). Despite the presence of

these ubiquitinated aggregates in affected brain *and* spinal cord regions, and the presence of overlapping symptoms in these patients, for many years there was no known protein that overlapped in these two diseases.

ALS and FTLD-U are pathologically linked through a common ubiquitinated protein called TAR DNA Binding Protein 43 or TDP-43

ALS and FTLD-U appeared to be clinically linked with overlapping CNS regions presenting ubiquitinated aggregates, but could a single protein underlie the pathology observed in both diseases? To determine whether ALS and FTLD-U were pathologically linked, ubiquitinated aggregates were solubilized from pathological tissues, and antibodies were generated against its proteinaceous components(102). These antibodies were then used to stain ALS and FTLD-U tissues, and overlapping pathology was assessed. Finally, in 2006 two independent research groups identified a common aggregated, ubiquitinated protein: TAR DNA binding protein 43 or TDP-43(9, 102).

TDP-43 is a highly conserved RNA-binding protein

Prior to 2006, limited information was known about TDP-43 cell biology, but it was known that TDP-43 is a 414 amino acid, 43 kDa protein encoded by the TARDBP gene located on chromosome 1(67). TDP-43 is highly conserved and ubiquitously expressed, and it was first identified in a screen where it bound the TAR region of HIV DNA, hence its name *TAR* DNA binding protein 43(105). Initial studies in the TDP-43 field also discovered that it also binds to single-

stranded RNA through UG-rich sequences in cystic fibrosis transmembrane receptor (CFTR) pre-mRNA(23, 27). The TDP-43-mediated exclusion of exon 9 generates an inactive CFTR protein, implicating TDP-43 in the onset of the disease cystic fibrosis(28). Yet, even basic data about TDP-43 localization and function in different cell types was unknown, especially as it related to the central nervous system. Thus, in the first attempts to further characterize TDP-43 cell biology in 2006, it became essential to compare TDP-43 structure and function with similar proteins: the heterogeneous ribonucleoprotein (hnRNP) class of RNA-binding proteins.

TDP-43 is a member of the heterogeneous nuclear ribonucleoprotein (hnRNP) family

Structurally, TDP-43 is classified as a heterogeneous nuclear ribonucleoprotein (hnRNP) family member(23). TDP-43 is sub-categorized in this family as a 2x-RBD-Gly protein(48, 83, 100), meaning it has two RNA recognition motifs (RRM1 and RRM2), and one glycine-rich region (GRR) at the distal C-terminus. The structure of TDP-43 (as it was understood in 2006) is shown below in Figure 1.1.

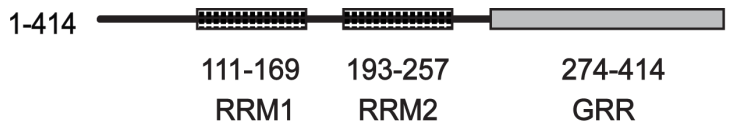

Important functional regions:			Function(s):
RRM1		RNA Recognition Motif 1	Binds RNA/DNA
RRM2		RNA Recognition Motif 2	Binds RNA/DNA
GRR		Glycine Rich Region	protein:protein interactions

Figure 1.1, Structural and functional schematic of TDP-43

TDP-43 is a heterogeneous nuclear ribonucleoprotein (hnRNP) family member and is classified as a 2x RBD-Gly hnRNP as it has two RNA recognition motifs (1 and 2) and a glycine rich region (GRR). This schematic was current in 2006; updated schematics are shown throughout my thesis, but the simplicity of this figure underscores the limited understanding of TDP-43 at the beginning of this project.

Both RRM1 and RRM2 domains are highly conserved, and mediate TDP-43 interactions with single-stranded RNA and DNA(23). In contrast, the GRR is not well conserved, but is known to mediate protein:protein interactions. These protein interactors include other hnRNP proteins, specifically hnRNPs A1, A2/B1, C1/C2 and A3(26). Interactions with hnRNP family members make it possible for TDP-43 to contribute to exon splicing without binding mRNA. This limited understanding of TDP-43 structure and function would be greatly expanded upon in the years to come (2006-2011), but forced the neurodegenerative field to initially focus on characterizing the disease, or forming cell culture models to better understand basic TDP-43 functions in cellular biology.

TDP-43 pathology is heterogeneous in ALS and FTLD-U

Pathological TDP-43 is characterized by its ubiquitination, hyperphosphorylation, cleavage, mislocalization and aggregation(9, 102). As previously mentioned, FTLD is a heterogeneous disease with multiple genetic origins, each culminating in distinct clinical symptoms. Interestingly, as more sub-types of FTLD-U were stained for TDP-43, four distinct TDP-43

immunoreactivity profiles were discovered, which varied by genetic origin(9, 54, 102). These sub-types are shown in the Figure 1.2 below.

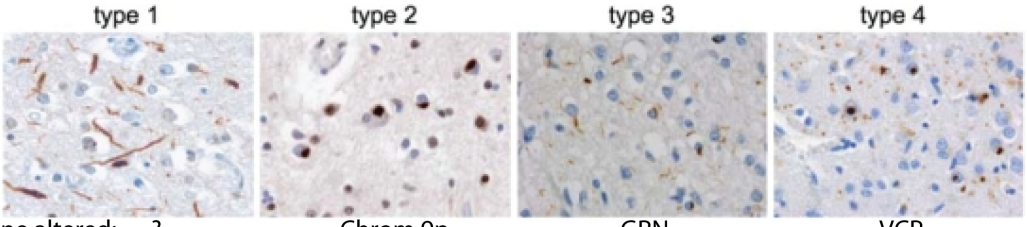

Subtype:	TDP-43 immunoreactivity profile:
type 1:	Abundant long dystrophic neurites (layers II/III) Few NCIs; Rare NIIs
type 2:	Abundant NCIs (superficial and deep cortical layers Few DNs; Few NIIs
type 3:	Abundant NCIs and short dystrophic neurites Variable NIIs in superficial cortical layers
type 4:	Abundant NIIs and dystrophic neurites Rare NCIs in neocortex

Figure 1.2, TDP-43 pathology in FTLD-U is heterogeneous. We summarize the heterogeneous TDP-43 pathology observed in four sub-types of FTLD-U. TDP-43 pathology is found in both neurons and glial cells. Also, the TDP-43 immunoreactivity profile is dependent on underlying genetic mutations, including an unknown gene on chromosome 9p (subtype 2), the granulin gene (subtype 3) and the VCP gene (subtype 4). Abbreviations used are: NCIs, neuronal cytoplasmic inclusions; NIIs, neuronal intranuclear inclusions; DNs, dystrophic neurites. This figure was adapted from Kwong et. al(84).

Subtype I pathology is observed in superficial cortical layers, and TDP-43 is found mislocalized to cytoplasmic inclusions with long neuritic profiles(31, 54). Type II TDP-43 pathology is found in both the superficial and deep cortical layers, type III is in superficial cortical layers with cytoplasmic inclusions and nuclear TDP inclusions are present in type IV(31, 54). Therefore, depending on the genetic mutation underlying FTLD-U, TDP-43 pathology is distinct. These

findings reinforce the importance of understanding determinants of TDP-43 localization in different cell types.

TDP-43 is a secondary histopathological feature in other neurodegenerative disorders

TDP-43 is a primary histopathological feature in ALS and FTLD-U because the majority of the ubiquitinated aggregate is composed of TDP-43. However, TDP-43 has also been observed as a secondary histopathological feature in other neurodegenerative diseases. As a secondary histopathological feature, TDP-43 is not the primary component of the ubiquitinated aggregate, however it is still associated with the ubiquitinated aggregates. These secondary histopathological features have been observed in AD, PD, HD, and more rare disorders including Guam ALS and Guam ALS-PD(31).

To describe this spectrum of neurodegenerative disorders with TDP-43 pathology, an umbrella term "TDP-43 proteinopathies" was generated(48, 83, 100). A consequence of these findings that TDP-43 is present as both a primary and secondary feature of multiple neurodegenerative diseases made some researchers doubt that TDP-43 caused neurodegeneration. Instead, it was argued that TDP-43 was an "innocent bystander", as no genetic mutations were discovered to date. As such, many researchers began looking for pathological mutations in the TARDBP gene to definitively prove that TDP-43 was initiates disease onset.

Pathological mutations implicate the glycine-rich region of TDP-43 in neurodegeneration

TDP-43 is genetically linked to ALS and FTLD-U

To definitively prove that TDP-43 is a mediator of disease, scientists needed to identify pathological TARDBP mutations in both ALS and FTLD-U patients. Approximately 20-25% of patients with ALS have overlapping symptoms with FTLD-U, and are defined as ALS-FTD. From this pool of ALS-FTD patients, the first TARDBP mutations linked to ALS were reported in 2008 (41, 67, 81, 114, 130). In contrast, fewer patients (10-15%) have been diagnosed with FTLD-U overlapping motor neuron disease or FTD-MND. Why more ALS patients have ALS-MND relative to the number of FTLD-U patients with FTD-MND is not yet clear. Regardless, genetic mutations in FTD-MND patients were finally discovered in 2009(18, 56, 79). It can be argued that this smaller pool of patient samples explains the delay in identifying TARDBP mutations in FTD-MND relative to ALS-FTD. In conclusion, TARDBP mutations are found in both ALS and FTLD-U patients; and these findings strengthen the argument that genetic TARDBP mutations alter TDP-43 protein function or localization, mediating onset of these neurodegenerative diseases.

Pathological mutations are concentrated in the glycine-rich region (GRR)

Over the last few years, an increasing number of TARDBP mutations have been found in ALS and FTLD-U patients. To date (2011), ~40 TARDBP mutations have been identified in ALS patients, while ~3 have been identified in

FTLD-U patients(85). Most ALS mutations are located in the distal-C-terminus, the region known as the glycine-rich region (GRR)(85, 86). In Figure 1.3 below, the region where the majority of mutations are clustered is underlined, and ALS mutations are highlighted in blue text.

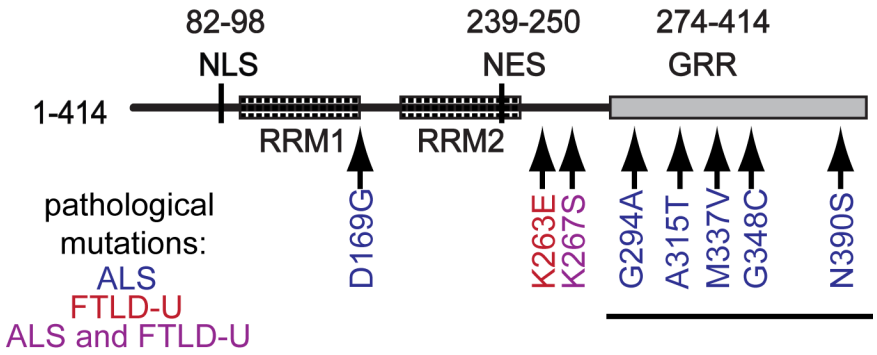

Figure 1.3, TDP-43 pathological mutations are concentrated in the GRR. The majority of pathological mutations in ALS patients localize to the glycine-rich region (GRR), emphasized by the black line beneath some of the mutations. An exception to this general rule is the D169G mutation, which is located in the RRM1. Three mutations have been identified in FTLD-U patients, including the K267S (purple), K263E (red) mutations and a 3' UTR mutation (not indicated). One mutation (K267S) has been identified in both ALS and FTLD-U patients.

However, some mutations lie outside the GRR. These mutations include the K263E mutation, which was discovered in an FTLD-U patient (red text)(79), and the N267S mutation, which was discovered in both ALS and FTLD-U (purple text)(18). Pathological mutations that have been tested in cell culture models have been highlighted in Figure 1.2, including the G294A, A315T, M337V, G348C and N390S mutations.

Proposed cellular processes affected by genetically-linked mutations

To determine viable hypotheses about how TDP-43 mediates neurodegeneration, I approached this question by outlining each mutation found in both ALS and FTLD-U. Next, I listed each gene, protein, and known functions of each protein, leading to both ALS and FTLD-U. From these functions, I formed subcategories that might explain how neurons in ALS and FTLD-U become susceptible to neurodegeneration. Table 1 has been generated to summarize ALS mutations, alongside disease hypotheses.

Table 1. Genes linked to familial amyotrophic lateral sclerosis (ALS)

Gene	Protein	Function(s)	Disease hypothesis
			Increased susceptibility to stress
SOD1	Superoxide dismutase 1	catalyzes the dismutation of O_2^- into O_2 and H_2O_2	Reactive oxygen species (ROS) generate oxidative stress, DNA damage and cell death?
VAPB	Vesicle-associated membrane protein-associated protein B	membrane protein - involved in lipid transport	Mutations cluster in the ER and result in unique restructuring of the ER that increase susceptibility to stress?
			Impaired neurite growth
ALS2	Alsin	GEF promotes neurite outgrowth	Truncated alsin causes impaired neurite outgrowth?
ANG	Angiogenin	stimulates formation of new blood vessels	Angiogenin LOF results in decreased neurite outgrowth/increased motor neuron susceptibility to stress?
			Impaired protein degradation
CHMP2B	Chromatin modifying protein 2B	ESCRT-III pathway	Inhibition of autophagy leads to more ubiquitinated proteins and cell death?
			Aberrant RNA processing
TARDBP	TAR DNA binding protein 43	RNA splicing Transcript stability Stress response	Altered RNA splicing increases susceptibility to stress? Nuclear loss of function? Cytoplasmic toxic gain of function? Impaired stress response?
FUS	Fused in sarcoma		

Table 1, The genes linked to ALS have been grouped into four categories, according to how their dysfunction may lead to neurodegeneration. Susceptibility to ALS may stem from an increased susceptibility to stress

through SOD1 or VAPB, impaired neurite growth through ALS2 or ANG, impaired protein degradation through CHMP2B or aberrant RNA metabolism through TARDBP or FUS.

Currently, genetic linkage studies have identified multiple sporadic and familial mutations in: *SOD1, ANG, VAPB, ALS2, CHMP2B, TARDBP* and *FUS*. These genes encode the proteins: superoxide dismutase 1 (SOD1), angiogenin, vesicle associated membrane protein associated protein B (VAMP), alsin, chromatin modifying protein 2B, TAR DNA binding protein 43 (TDP-43) and fused in sarcoma (FUS), respectively. By examining the function of these proteins a number of disease hypotheses can be proposed, including: oxidative stress (SOD1, VAPB), neurite outgrowth and maintenance (ANG, ALS2), cellular degradation pathways (CHMP2B) and RNA processing (TARDBP, FUS).

Next, the same approach was taken for genes linked to FTLD-U. These genes are listed in table 2, alongside the protein encoded by that gene and its functions. A list of disease hypotheses follows each gene, and common mechanisms are grouped by green boxes.

Table 2. Genes linked to familial frontotemporal lobar degeneration with ubiquitinated aggregates (FTLD-U)

Gene	Protein	Function(s)	Disease Hypothesis
			Inhibition of degradative pathways
CHMP2B	Chromatin modifying protein 2B	ESCRT-III pathway	Inhibition of autophagy leads to more ubiquitinated proteins and cell death?
VCP	Valosin containing protein	Required for ubiquitin-proteasome degradation	Inhibition of the ubiquitin-proteasome system results in cytoplasmic aggregates leading to cell death?
			Increased inflammation
PGRN	Progranulin	Growth factor Inflammation	PGRN is cleaved by elastases to form granulins that induce inflammatory response?
			Altered RNA metabolism
TARDBP	TAR DNA binding protein 43	RNA splicing Transcript stability Stress response	Altered RNA splicing increases susceptibility to stress? Nuclear loss of function? Cytoplasmic toxic gain of function? Impaired stress response?
FUS	Fused in sarcoma		

Table 2, The genes linked to FTLD-U have been grouped into three categories according to how their dysfunction may lead to neurodegeneration. Increased susceptibility to FTLD-U may be through inhibition of degradative pathways through CHMP2B or VCP, increased inflammation through PGRN, or altered RNA metabolism through TARDBP or FUS.

Currently, FTLD-U is genetically linked with: CHMP2B, VCP, GRN, TARDBP, FUS, and an undetermined gene on chromosome 9p(126). These genes encode the proteins: chromatin-modifying protein 2B, valosin-containing protein, progranulin, TDP-43 and FUS, respectively. By examining the function of these proteins, multiple disease hypotheses have emerged, including: aberrant protein degradation (via autophagy and/or the 26S proteasome; VCP, CHMP2B), inflammation (GRN), and aberrant RNA metabolism/stress response (TDP-43, FUS).

As ALS and FTLD-U have overlapping pathologies, we compared these genetic lists for similar categories in both diseases. Three genes overlap between ALS and FTLD-U including: TARDBP, FUS and CHMP2B. This strongly implicates RNA-processing defects, or impairments of cellular degradative pathways, in the pathogenesis of these neurodegenerative disorders.

Disease hypotheses of TDP-43-mediated neurodegeneration

To understand how pathological mutations in TDP-43 increase susceptibility to neurodegeneration, three hypotheses have been proposed: a nuclear loss of TDP-43 function (LOF), a cytoplasmic toxic gain of function (GOF), or both a nuclear LOF and toxic cytoplasmic GOF hypothesis. In the nuclear LOF hypothesis, a deficiency in nuclear TDP-43 results in mis-splicing events. Because TDP-43 represses exon inclusion, the argument is that "mis-splicing" would result in novel isoforms that may be toxic to the cell. In the cytoplasmic toxic gain of function hypothesis, the cytoplasmic accumulation of TDP-43 may alone be toxic, or its aggregation may impede cellular trafficking networks resulting in cell death. Finally, the third hypothesis argues that both a nuclear LOF and a cytoplasmic toxic GOF need to work together to impair cellular viability or induce cell death.

MOTIVATION FOR STUDIES

Testing the cytoplasmic toxic gain of function hypothesis

Some of the most prominent TDP-43 disease hallmarks include its cytoplasmic mislocalization and aggregation, truncation, and reduced solubility. Understanding how TDP-43 is mislocalized and aggregated in the cytoplasm is confounded by TDP-43's pathological heterogeneity, as distinct immunoreactivity profiles are generated by different genetic origins underlying FTLD-U. Moreover, TDP-43 pathology is observed in both neurons and glia, and its aggregation can occur in both the nucleus and cytoplasm of cells. These observations have led to the hypothesis that the cytoplasmic mislocalization of TDP-43 is a mediator of neurodegeneration, hence a "cytoplasmic toxic gain of function" hypothesis has been proposed.

When TDP-43 was established as the pathological link between ALS and FTLD-U in 2006, the primary issue in understanding its role in neurodegeneration was the lack of information about its localization and function. As previously stated, very few research articles had been published on TDP-43 in 2006. Of the articles published, the focus was on TDP-43 nuclear functions, including pre-mRNA splicing and nuclear body organization, and TDP-43 was in fact believed to be a nuclear-restricted protein(132). As such, one of the first arguments proposed under the "cytoplasmic toxic gain of function" hypothesis was that TDP-43 is nuclear-restricted, and increased TDP-43 levels in the cytoplasm are toxic and lead to cell death. Because of the limited information available on TDP-43, our approach was to conduct an extensive characterization of its basic cellular biology (with an emphasis on localization and function) in both central nervous system and somatic cells.

Our study objectives

Our first objective was to characterize the cellular localization of TDP-43 in multiple cell types, including primary and immortalized cell lines both in and outside of the CNS. Our second objective was to identify cellular processes resulting in increased cytoplasmic TDP-43 protein levels, and use this process to develop a cell culture localization model. Third, using this cell culture model, we wanted to test for differences in the localization or aggregation of overexpressed wild-type and pathological TDP-43 protein.

CHAPTER TWO
Results

CHARACTERIZATION OF TAR DNA BINDING PROTEIN 43 (TDP-43) LOCALIZATION IN MULTIPLE CELL TYPES FOR THE DEVELOPMENT OF CELL CULTURE AND ANIMAL DISEASE MODELS

ABSTRACT

TDP-43, or TAR DNA-binding protein 43, is a pathological marker of a spectrum of neurodegenerative disorders including amyotrophic lateral sclerosis and frontotemporal lobar degeneration with ubiquitin-positive inclusions. TDP-43 is a highly conserved, ubiquitously expressed, RNA/DNA-binding protein implicated in transcriptional regulation. TDP-43 is structurally and functionally classified as a member of the heterogeneous nuclear ribonucleoprotein (hnRNP) family. Many hnRNP proteins are sub-classified as either nuclear-restricted or nucleo-cytoplasmic shuttling proteins. At the beginning of this project, TDP-43 was classified as a nuclear-restricted hnRNP protein, and reports focused on TDP-43 nuclear localization and function, and ignored any possible role for TDP-43 in the cytoplasm. This limited understanding of TDP-43 localization and function in the cytoplasm of both central nervous system tissues and somatic cells impeded progress in testing the cytoplasmic toxic gain of function hypothesis. In this study, I determine TDP-43 subcellular localization in multiple cell types, including primary cultured neurons and glia, as well as immortalized cell lines

derived from human glia and kidney. I hypothesized that TDP-43 is not a nuclear-restricted protein, and its localization varies by physiological processes including cell cycle progression and hyperosmotic stress. I find that TDP-43 is not a nuclear-restricted protein in either central nervous system cells or immortalized cell lines. While TDP-43 is a predominantly nuclear protein, a subpopulation of TDP-43 is diffusely-localized to the cytoplasm. I furthermore find that TDP-43 localization can shift during cell cycle progression and stress. As my goal is to test the cytoplasmic toxic gain of function hypothesis of TDP-43 mediated neurodegeneration, I conclude that stress can be used to establish a cell culture localization model for future studies. Moreover, for future studies, my lab and I have established conditional transgenic mice overexpressing wild-type and mutant (G348C) TDP-43 to establish an *in vivo* model of disease.

INTRODUCTION

"TDP-43 proteinopathies" encompass a spectrum of neurodegenerative diseases with ubiquitinated aggregates primarily composed of TDP-43 (31, 52). Ubiquitinated TDP-43 is especially prevalent in patients with amyotrophic lateral sclerosis (ALS) and frontotemporal lobar degeneration with ubiquitinated inclusions (FTLD-U). In these diseases, many mutations have been identified within the glycine-rich region (GRR) of TDP-43 (~forty mutations in ALS (81, 85, 107, 114, 121, 130) and three in FTLD-U (18, 31, 56, 79)). How TDP-43 contributes to neurodegeneration is unknown, but other pathological alterations to

TDP-43 implicate aberrant proteolysis, hyperphosphorylation and mis-accumulation in the cytoplasm (9, 24, 31, 52, 102).

It is unclear how cytoplasmic accumulation of TDP-43 contributes to neurodegeneration at the molecular and cellular level. Existing evidence is compatible with the hypothesis that TDP-43 proteinopathies arise from a gain of TDP-43 function in the cytoplasm, due to its mis-accumulation in the cytoplasm. This may indirectly or directly impact its nuclear function, as cytoplasmic mis-accumulation would reduce the amount of functional TDP-43 in the nuclear compartment. In this study, as a first step toward testing this hypothesis, I characterize the localization of TDP-43 in central nervous system and somatic cells. Furthermore, I examine processes that drive TDP-43 cytoplasmic accumulation, including cell cycle progression and hyperosmotic stress. I conclude that hyperosmotic stress can be used in future studies to test TDP-43 cytoplasmic accumulation. Finally, I establish a conditional transgenic model for the future study of TDP-43 proteinopathies.

Aims and hypothesis

For my thesis, I wanted to test the cytoplasmic toxic gain of TDP-43 function hypothesis. However, at the start of my study in 2006, the localization and function of TDP-43 in central nervous system tissues was poorly characterized. Therefore, my first aim became the determination of TDP-43 localization in multiple cell types, including nervous system cells. I hypothesized that TDP-43 is not nuclear-restricted in either central nervous system tissues or somatic cells, and

TDP-43 localization can shift between the nucleus and cytoplasm during physiological processes including cell cycle progression and exposure to stress.

MATERIALS AND METHODS

Cell and Primary Cultures

Commercial cell lines used in this study (Hek293T and U343, ATCC) were maintained in standard growth medium: 10% fetal bovine serum in DMEM (Invitrogen). For primary mixed glial cultures, rat cortices were dissected from postnatal (D1-4) pups in ice-cold dissection medium (Gibco-Invitrogen) as described previously (118). Glia (~21-28 DIV) were split onto poly-*D*-lysine and matrigel-coated coverslips. For primary cortical neurons, rat cortices were dissected from E18 rat brains. Cortical neurons were dissociated with papain (20 units/ml) for 7 min at 37 °C, triturated with a Pasteur pipette, and plated at 100,000/200 mm^2 onto nitric acid-etched coverslips coated with poly-D-lysine (Sigma) and Matrigel (BD Biosciences). Cultures were maintained for 21 days *in vitro* (DIV) in Neurobasal medium (Invitrogen) supplemented with 2% B27 (Invitrogen) and 1% L-glutamine (Sigma).

Western Blot

Cells were solubilized in a high salt buffer (50mM Tris-HCl, pH 7.5, 0.5 M NaCl, 1% NP-40, 1% DOC, 0.1% SDS, 2 mM EDTA and 1 Roche Complete protease-

inhibitor tablet). Protein concentrations were determined using the Bio-Rad Dc protein assay kit.

Immunofluorescence and Confocal Microscopy

Cells were fixed for 15 minutes in 4% PFA, 2% sucrose in PBS, followed by a 5 minute permeabilization with 0.2% TX-100 in PBS. Coverslips were blocked for one hour with 10% NGS/PBS, followed by an overnight incubation with primary antibody as specified in the text: anti-TDP-43 (1:200, ProteinTech Group); anti-p70 S6K or Hedls (1:500, Santa Cruz), anti-hnRNP A1 (1:3200, Sigma), anti-hnRNP C1/C2 (1:1600, Sigma), anti-tubulin (1:300, BD Biosciences). The next day, cells were rinsed with PBS, and incubated with secondary antibody and dye for 30 minutes at room temperature in a humidified chamber: Alexa 488-conjugated anti-rabbit IgG (1:500), Alexa 546-conjugated anti-mouse IgG (1:500), Alexa 568 phalloidin-conjugated anti-rabbit IgG, and the DNA-staining dye ToPro-3 (1:1000, Invitrogen). Images were captured using a Zeiss 510 confocal microscope and images were processed using LSM software and ImageJ.

Design and Transfection of siRNA

Three siRNAs (designated in the text as H1, H2 and H3) directed against human TDP-43 (NM_007375) were designed using the MIT software database (http://jura.wi.mit.edu/bioc/siRNAext/tmp/2007-11-5/2007-11-5-62331-19128_0.tab.txt), and purchased from Dharmacon. Positive and negative controls (Lamin A/C and Dharmafect control #00031-04-I-01-U, respectively) were

purchased from Dharmacon. Oligos were resuspended according to the Dharmacon's online protocol using 5x resuspension buffer (Dharmacon) diluted to 1x with RNase-free water. Oligos were transfected into Hek293T cells using the Dharmafect 1,2,3,4 kit in serum-free medium (Opti-Mem, Invitrogen).

Cell Cycle Synchronization and Release

Hek293T cells were plated onto nitrogen-etched coverslips coated with PDL and matrigel (as described above) and synchronized in the G1 phase of the cell cycle by depriving the cells of serum for 24 hours. To release cells from this arrest, serum free medium was replaced by standard growth medium. Cells were allowed to proceed through the cell cycle for 3, 6, 9, 12 and 24 hrs, at which coverslips were removed from culture, fixed and processed for immunofluorescence (as previously discussed).

RESULTS

Characterization of TDP-43 expression and localization in multiple cell types

TDP-43 is not a nuclear-restricted RNA-binding protein

I determined the localization of TDP-43 in different cell types. At the time of this analysis, it was believed that TDP-43 is a nuclear-restricted protein. I examined the localization of TDP-43 in central nervous system tissues, starting with primary neurons, followed by primary mixed glial cultures. As shown in Figure 2.1 below, I confirmed that TDP-43 localizes to the nucleus in primary neurons, however TDP-43 is not confined to the nucleus and is also present in the cytoplasm.

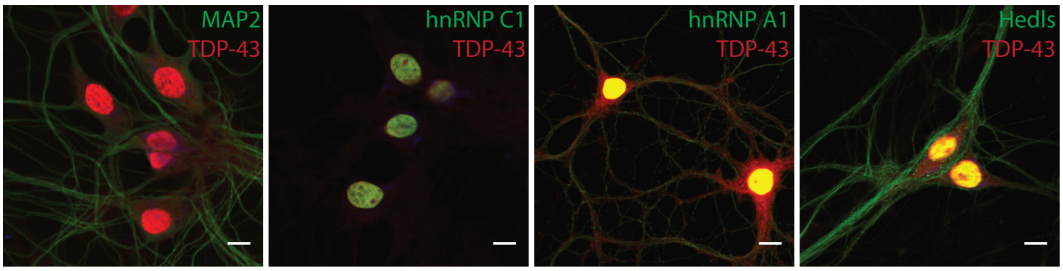

Figure 2.1, TDP-43 is not a nuclear restricted protein in primary cultured neurons. TDP-43 is a predominantly nuclear protein that is also present in the cytoplasm. Merged confocal images shows TDP-43 (red) signal in neurons stained by the neuronal marker MAP2, and by the nuclear-resident protein hnRNP C1, the nucleocytoplasmic shuttling protein hnRNP A1 and a p70 S6 kinase/Hedls antibody (shown in green). Scale bars: 10 μm.

First, I stained neurons with the dendritic marker protein microtubule-associated protein 2 or MAP2 (shown in green on the first image). TDP-43 (red staining) was found in $MAP2^{+}$ cells, and appeared to localize to the nucleus. As MAP2 is a neuronal marker but not a nuclear marker, I confirmed TDP-43 nuclear localization by colabeling TDP-43 (red) with hnRNP C1 (green), a nuclear-resident protein. In the third image, I used a longer exposure time, and detected a diffuse TDP-43 (red) cytoplasmic sub-population in addition to nuclear staining. This is confirmed by co-staining TDP-43 (red) with hnRNP A1 (green), a nucleo-cytoplasmic shuttling protein that is also predominantly nuclear. As a technical note, hnRNP A1 was not overexposed to the same extent as TDP-43 to emphasize TDP-43 cytoplasmic localization in the soma, although the colocalization of hnRNP A1 and TDP-43 is faintly detectable in the dendrites (yellow), in addition to robust nuclear colocalization (yellow). In the fourth image, we show TDP-43 (red) colocalization with p70 S6 kinase (green) antibody, an antibody that specifically detects p70 S6 kinase in the nucleus and processing bodies (a type of RNA granule) in the cytoplasm. I conclude that TDP-43 is predominantly

nuclear-localized, although a subpopulation is localized to the cytoplasm of healthy primary neurons.

I then sought to determine the localization of TDP-43 in another central nervous cell type found altered by disease: glial cells. I cultured mixed, primary glial cells, and used immunofluorescence to determine the localization of TDP-43 with phalloidin (red), hnRNP C1 (green), hnRNP A1 (green) and p70 S6 kinase/Hedls (green), respectively.

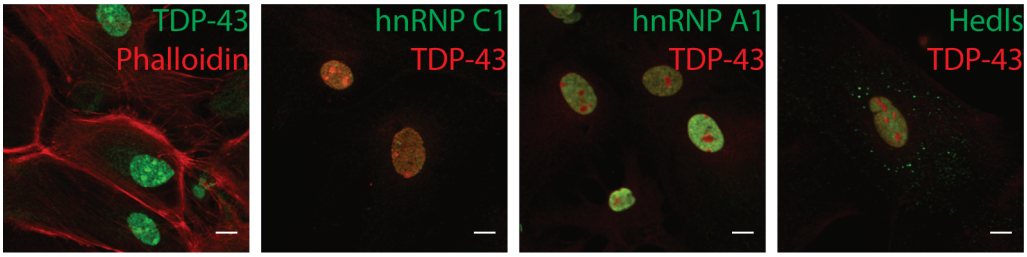

Figure 2.2, TDP-43 is not a nuclear-restricted protein in primary cultured glia. Glia were co-stained for TDP-43 and the actin stain phalloidin, the nuclear-resident protein hnRNP C1, the nucleocytoplasmic shuttling protein hnRNP A1, and p70 S6 kinase/Hedls, respectively. TDP-43 is a predominantly nuclear-localized protein, although a diffuse cytoplasmic population is detectable in glia (as seen in the TDP-43 phalloidin image). Scale bars = 10 μm.

Similar to what was observed in neurons, I found robust TDP-43 nuclear localization. However, TDP-43 is diffusely localized to the cytoplasm, as seen in the first data panel (TDP-43 and phalloidin, red and green respectively). Also, similar to primary neurons, TDP-43 (red) colocalizes with nuclear-resident protein hnRNP C1(green), the nucleocytoplasmic shuttling protein hnRNP A1 (green), as well as p70 S6 kinase/Hedls (green) nuclear staining.

I conclude that TDP-43 is a predominantly nuclear protein, with a sub-population in the cytoplasm of central nervous system cells. I next asked if the localization of TDP-43 is different in immortalized central nervous system

tissues, such as U343 cells, and in non-central nervous system cells such as Hek293T cells (Figure 2.3). Specifically, U343 cells are a human glioblastoma cell line and Hek293T cells are derived from human embryonic kidney.

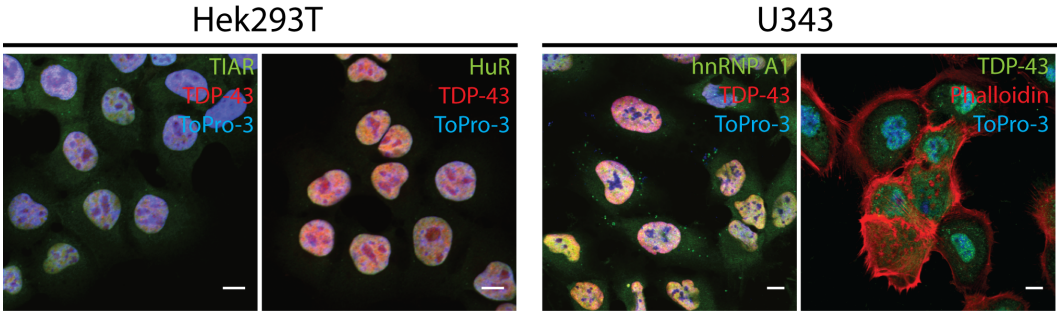

Figure 2.3, TDP-43 is not nuclear-restricted in immortalized cell lines. In Hek293T cells, I highlight TDP-43 nuclear localization, as TDP-43 (red) colocalizes with RNA-binding proteins TIAR and HuR strongly in the nucleus. TDP-43 cytoplasmic staining in Hek293T cells is more clearly shown in Chapter 3. In U343 cells, TDP-43 is strongly nuclear, as TDP-43 (red) colocalizes with hnRNP A1 (green) in the nucleus. Yet, TDP-43 cytoplasmic localization is obvious in the TDP-43 (green) and phalloidin (red) stained image. Scale bars: 10 µm.

I found that in these immortalized cell lines (U343 and Hek293T cells), TDP-43 is not nuclear-restricted, consistent with my observations in primary cultured neurons and glia. As shown in Figure 2.3, this conclusion can be drawn by examination of the U343 cells stained with TDP-43 (green) and the actin stain phalloidin (red). As previously observed in central nervous system cells, TDP-43 is a predominantly nuclear protein (Hek293T and U343 cell images with colocalization between TDP-43 (red) and RNA-binding proteins TIAR, HuR and hnRNP A1, green).

From this qualitative analysis, I conclude that TDP-43 is not a nuclear-restricted protein, and this observation is valid in multiple cell types spanning central nervous system cells and somatic cells. However, an alternative explanation for my findings is that the commercial TDP-43 antibody used in these

immunofluorescence experiments isn't specific to TDP-43, and this cytoplasmic staining is an artifact.

Cytoplasmic TDP-43 staining is not an antibody artifact

During my initial investigation, it was believed that TDP-43 is a nuclear-restricted protein. However, I observed cytoplasmic TDP-43 staining in multiple cell types including central nervous system cells (primary cortical neurons and glia), and immortalized cell lines (U343 and Hek293T cells). I questioned whether TDP-43 cytoplasmic localization was due to a specificity issue, or if TDP-43 is not a nuclear-restricted protein.

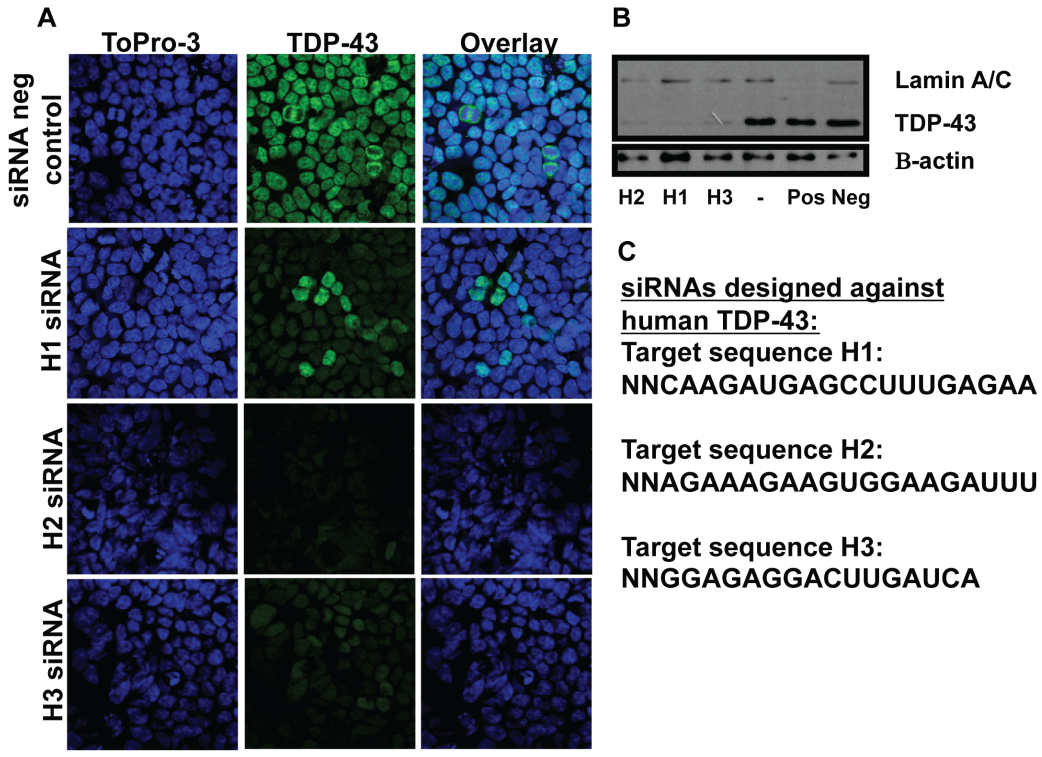

Figure 2.4, Determination of TDP-43 antibody specificity. c. To determine whether the commercial antibody from ProteinTech Group specifically detects TDP-43, three siRNAs were designed against human TDP-43 (labeled as H1, H2 and H3). b. These siRNAs were transfected into Hek293T cells

and knockdown was determined by western blot. All three siRNAs effectively knock down TDP-43, while robust TDP-43 protein levels are observed in controls: (neg) negative control designed by Dharmacon; (pos) positive control against Lamin A/C; and (-) is an untreated control. a. Antibody specificity is striking using immunofluorescence: detection of TDP-43 in control cells (green), versus knockdown cells in which the antibody fails to detect TDP-43 resulting in little to no staining. A DNA dye (ToPro-3, blue) was used to label nuclei.

I first tested the specificity of a commercial TDP-43 antibody (ProteinTech Group, Chicago IL) using siRNA. I designed three siRNAs targeting human TDP-43 (Figure 2.4c, H1, H2 and H3), and show they effectively knocked-down TDP-43 in Hek293T cells as assayed by western blot (Figure 2.4b). TDP-43 knockdown was also confirmed in Hek293T cells using immunofluorescence, where TDP-43 protein was labeled in control cells incubated with the ProteinTech Group TDP-43 antibody (labeled in green), while the antibody failed to detect TDP-43 protein in siRNA-treated cells. Taken together, these immunofluorescent and western blot results led us to the conclusion that the ProteinTech Group antibody is specific. Therefore, TDP-43 is not a nuclear-restricted protein, and its localization to the cytoplasm indicates a novel function for TDP-43 outside of just nuclear pre-mRNA splicing.

Other hnRNP proteins localizing to the cytoplasm have intrinsic structural motifs that mediate their nucleocytoplasmic shuttling. In less common cases, nucleocytoplasmic shuttling in hnRNP A1 and hnRNP K is mediated by the M9 or KNS motif, respectively(63, 64, 95, 109). However, most nucleocytoplasmic shuttling hnRNPs have more traditional motifs: the nuclear localization signal (NLS) and nuclear export signal (NES). My next objective was to determine the intrinsic signals in TDP-43 dictating its nucleocytoplasmic localization. Shortly

into this study, another laboratory published that TDP-43 is in fact a nucleocytoplasmic shuttling protein, and this shuttling is mediated by NLS and NES signals(14). These findings further validated that my cytoplasmic TDP-43 staining is real and not an artifact. I next sought to test the second half of my hypothesis: TDP-43 localization can shift between the nucleus and cytoplasm during physiological processes including cell cycle progression and exposure to stress.

Determination of Cellular Processes that Alter TDP-43 Localization

Hypothesis: TDP-43 localization is dependent on cell cycle stage

While characterizing the localization of TDP-43 in different cell types, I observed that in some cells, TDP-43 is predominantly localized to the cytoplasm instead of the nucleus (Figure 2.5b, 0 hr). I therefore hypothesized that TDP-43 localization is dependent on cell-cycle stage.

I characterized TDP-43 localization during the cell cycle using immunofluorescence. Hek293T cells were serum-deprived for 24 hours to sync the population in G1, and released from cell cycle arrest by addition of growth medium (indicated as "+ serum", this process is summarized in Figure 2.5a). TDP-43 localization during cell cycle progression is shown in Figure 2.5b, where cytoplasmic TDP-43 (red stain, 0 hr) shifts back into, and out of, the nucleus over time (3-24 hours).

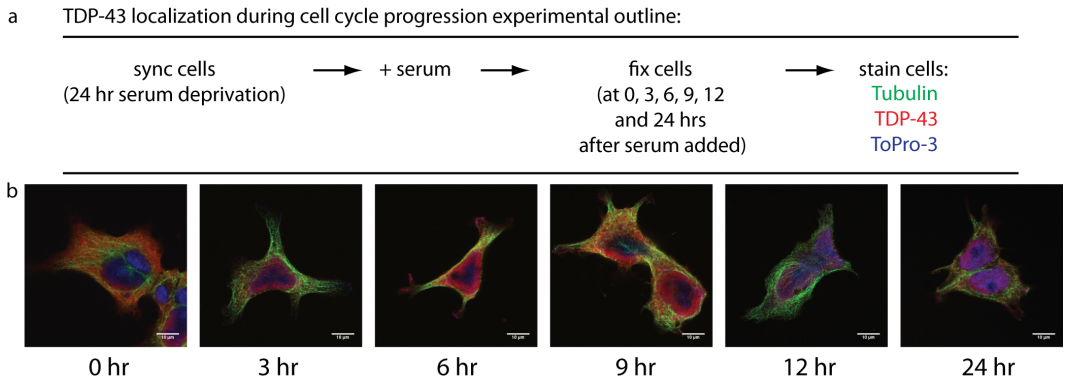

Figure 2.5, Characterization of TDP-43 subcellular localization during cell cycle progression. a. Hek293T cells are synchronized after a 24 hour serum-deprivation treatment (0 hr). Cells released from cell cycle arrest by addition of serum are captured at different timepoints (3, 6, 9, 12 and 24 hours) by immunofluorescence. b. TDP-43 localization at these timepoints is shown, where TDP-43 is stained red, tubulin is green and the DNA dye ToPro-3 is blue. Scale bars: 10 μm.

Hypothesis: TDP-43 relocalizes from the nucleus to the cytoplasm during stress

TDP-43 is structurally similar to hnRNP A1, another ubiquitously expressed hnRNP family member. This structural similarity is shown in Figure 2.6a, where both proteins have two RNA binding domains (RRM1 and RRM2) and one glycine rich region (GRR). Importantly, both proteins are nucleocytoplasmic shuttling proteins, mediated by the M9 domain in hnRNP A1, and localization signals (NLS and NES) in TDP-43(14, 63, 64).

An interesting property of many nucleocytoplasmic shuttling hnRNPs (including hnRNP A1), is their response to stress: they accumulate in the cytoplasm(4, 58). I sought to test whether TDP-43 responds to the same stressor that mediates hnRNP A1 cytoplasmic accumulation: hyperosmotic levels of the sugar sorbitol(4).

I wanted to determine if stress shifts nuclear TDP-43 populations into the cytoplasm. This was tested by treating Hek293T cells with sorbitol (0.4 M, 0-4 hrs), followed by subcellular fractionation (nuclear and cytoplasmic fractions) and visualized by western blot.

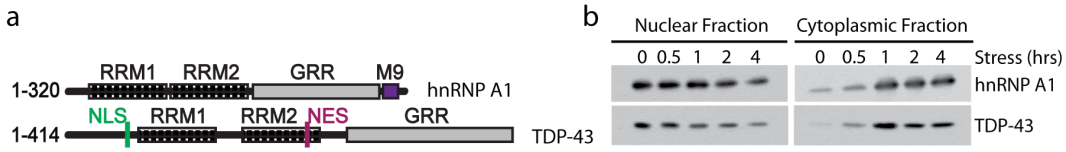

Figure 2.6, TDP-43 and hnRNP A1 cytoplasmic protein levels rise during sorbitol stress, at the expense of their nuclear protein levels. a. TDP-43 and hnRNP A1 are structurally similar hnRNP family proteins with two RNA Recognition Motifs (RRM1 and RRM2) and one Glycine Rich Region (GRR). Both proteins are also nucleocytoplasmic shuttling proteins, which is mediated by the M9 domain in hnRNP A1, and the Nuclear Localization Signal (NLS) and Nuclear Export Signal (NES) in TDP-43. b. Subcellular fractionation of Hek293T cells stressed with 0.4 M sorbitol for 0-4 hours. Both TDP-43 and hnRNP A1 show increased cytoplasmic protein levels with longer stress, and decreased nuclear levels with longer stress.

I found that the cytoplasmic protein levels of both hnRNP A1 and TDP-43 increased with longer stress duration, at the expense of their nuclear populations (Figure 2.6b). My findings are consistent with previously published subcellular fractionation data documenting the stress response of hnRNP A1 to 0.4 M sorbitol stress(4). I conclude that stress (specifically 0.4 M sorbitol) increases cytoplasmic TDP-43 protein levels at the expense of its nuclear levels, similar to the stress response of hnRNP A1, a structurally similar protein.

Development of transgenic mouse models to understand TDP-43 biology *in vivo*

My short-term approach to understanding mediators of TDP-43 cytoplasmic localization and accumulation is by thoroughly characterizing the localization of TDP-43 in different cell types and during different cellular processes including cell cycle progression and stress. However, in the long-term, it is essential to start establishing TDP-43 transgenic models, to elucidate the localization and function of TDP-43 *in vivo,* and to establish a murine model of the disease.

Using a previously established system, I generated conditional transgenic mice overexpressing wild-type and mutant (G348C) TDP-43 under the control of the CAG promoter in collaboration with the Olson lab. When not crossed with Cre, these mice do not overexpress TDP-43, rather LacZ is generated by cells expressing the construct. When crossed with a Cre line, these mice express TDP-43 alongside GFP, which is under the control of an IRES. This transgenic system is summarized in Figure 2.7a. Overexpressed TDP-43 is specifically detected using the human specific Abnova antibody, while both mouse and human TDP-43 are detected by an in-house antibody (generated by Chantelle Sephton and Basar Cenik) that recognizes the C-terminus of TDP-43 (748C) (Figure 2.7b). Expression of human TDP-43 is detected by western blot in transgenic mice crossed with a germline CRE (Meox) (screening and maintenance of these mouse lines was performed by Shannon Good, Mieu Brooks and Chantelle Sephton).

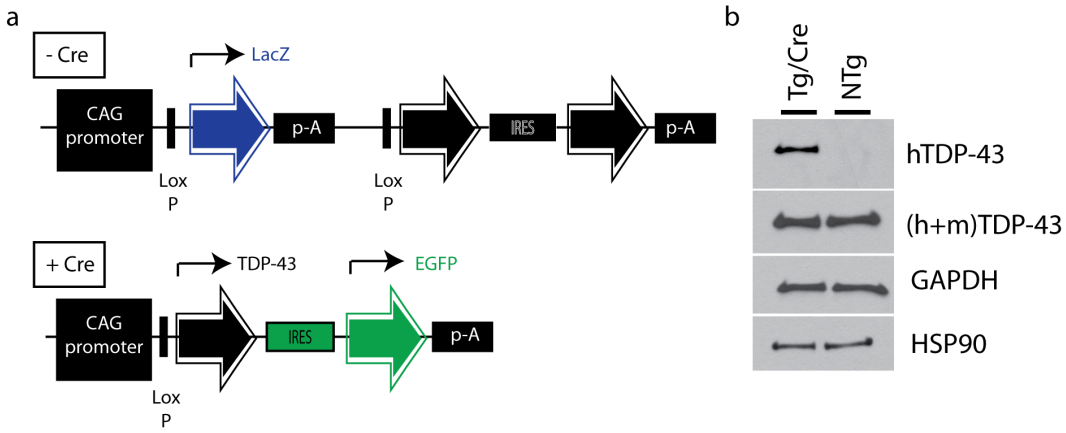

Figure 2.7, Generation of conditional TDP-43 transgenic mice. a. Summary of the transgenic system used to overexpress wild-type and mutant (G348C) human TDP-43. Without Cre, LacZ is expressed in cells expressing the construct. When crossed with a Cre mouse, the Cre removes the LacZ by the LoxP sites flanking this gene, and TDP-43 is expressed under the control of the CAG promoter. GFP is also expressed under the control of an IRES sequence, indicating successful expression of the transgene. b. Human TDP-43 is specifically detected by the Abnova TDP-43 antibody, while human and mouse TDP-43 is detected by an in-house antibody (748C, h+m TDP-43). GAPDH is shown as a loading control and HSP90 levels are consistent between the transgenic and NTg animals.

Hence, I have cloned both wild-type and mutant (G348C) human TDP-43 into the CAG vector system, and have established two lines of transgenic mice in collaboration with members of the Olson lab (Brett A. Johnson and John McNally) and Yu lab members (Chantelle Sephton, Mieu Brooks and Shannon Good). Although the system appears to be functional, in the future, additional lines will need to be established and screened before these animals are used for behavioral studies.

Thus, I have characterized TDP-43 localization in multiple cell types, including central nervous system cells and somatic cells. I have shown that TDP-43 is a robustly nuclear-localized protein with a diffuse cytoplasmic sub-population. Importantly, I have also identified two cellular processes that result in

TDP-43 accumulation in the cytoplasm: cell cycle progression and stress. In future experiments, the stress model can be applied to test how TDP-43 accumulation in the cytoplasm varies according to the wild-type or pathological protein. Also, the transgenic system I have introduced to the lab can be used in future studies for understanding disease pathogenesis.

DISCUSSION

TDP-43 function is dependent on its localization

TDP-43 is a nucleo-cytoplasmic shuttling protein

Using qualitative methods, I have determined that TDP-43 is not a nuclear-restricted protein. By immunofluorescence, TDP-43 localization is predominantly nuclear with a diffuse, weakly-staining cytoplasmic population. I have confirmed this observation in multiple cell types, including primary cultured central nervous cells (neurons and glia) and immortalized cell lines (U343 and Hek293T cells). I have furthermore confirmed that these observations are not due to antibody specificity issues, as our commercially purchased antibody detects TDP-43 in control, but not in knockdown cells.

Before I could identify intrinsic determinants of TDP-43 localization, another group published that TDP-43 has a nuclear localization signal (NLS) and nuclear export signal (NES)(14). This NLS is located between residues 82-98, while the NES is located between residues 239-250, which is located at the distal end of the RRM2. These signals are highlighted below in Figure 2.8. Importantly,

these findings confirmed and expanded upon my own localization studies that TDP-43 is not nuclear-restricted, and therefore TDP-43 must be functionally significant in both the nucleus and cytoplasm.

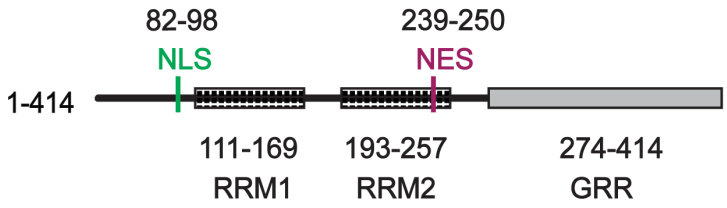

Important functional regions:			Function(s):
RRM1		RNA Recognition Motif 1	Binds RNA/DNA
RRM2		RNA Recognition Motif 2	Binds RNA/DNA
GRR		Glycine Rich Region	protein:protein interactions
NLS		Nuclear Localization Signal	nucleocytoplasmic shuttling
NES		Nuclear Export Signal	

Figure 2.8, Revised structural and functional schematic of TDP-43. Important TDP-43 structural regions are defined, including two RNA recognition motifs (1 and 2) and the glycine rich region (GRR). The nuclear localization signal (NLS) and nuclear export signal (NES) are also shown, which dictate TDP-43 cellular localization.

The functional significance of nuclear and cytoplasmic TDP-43 populations

In testing the cytoplasmic toxic gain of function hypothesis, one of the initial arguments was that TDP-43 localization to the cytoplasm was sufficient to induce cell death. The determination that TDP-43 has both an NLS and NES was extremely important, because this showed that TDP-43 is functionally relevant in the cytoplasm, and therefore the presence of cytoplasmic TDP-43 alone is not sufficient to induce cell death.

In order to test the cytoplasmic toxic GOF hypothesis, the normal function of TDP-43 in the cytoplasm must first be determined. To get an idea of what this

function is, it became important to first compare TDP-43 structure and function with other closely related proteins. As previously mentioned, TDP-43 is closely related to other hnRNP proteins, some of which are nuclear-restricted, while others are nucleocytoplasmic shuttling proteins(45). Functionally, nuclear-restricted hnRNP proteins (like hnRNP C1) participate in pre-mRNA splicing, while nucleo-cytoplasmic shuttling hnRNPs (like hnRNP A1) can participate in pre-mRNA splicing, mRNA export, as well as mature transcript stabilization in the cytoplasm(108). The discovery that TDP-43 is localized to the cytoplasm raised many functional questions, including: what transcripts are bound by TDP-43 in the nucleus and cytoplasm? To what functional categories do these TDP-43 bound transcripts belong? And if these transcripts are prevented from being translated in the cytoplasm (because they are aggregated), do they induce cell death pathways?

TDP-43 is a predominantly nuclear-localized protein

As is the case with many hnRNP class proteins, TDP-43 can participate in both pre-mRNA splicing and mRNA stability(23). While TDP-43 can localize to the cytoplasm, its immunoreactivity profile indicates that it is a predominantly nuclear-localized protein. TDP-43's predominantly nuclear localization makes sense in the context of its mRNA binding profile: the majority of TDP-43 mRNA targets are intronic sequences. Recently, RNA-deep sequencing has revealed the pre-mRNA targets of TDP-43. This is summarized in the schematic below: intronic targets compose nearly 73% of all TDP-43 binding targets. This

underscores the importance of TDP-43 in pre-mRNA splicing in cortical neurons, and its localization to the nucleus.

Exonic targets:	Intronic targets:
7.97% 3'UTR exon	72.87% CDS intron
7.86% CDS exon	9.71% 5'UTR intron
0.84% 5' UTR	0.73% 3'UTR intron
RNA metabolism	Synapse
Synapse	Development
Development	Cell morphology
Cell morphology	Cell signaling
Cell signaling	

Figure 2.9, TDP-43 targets indicate important functions for pre-mRNA processing. The majority of TDP-43 transcripts are intronic targets (72.87%), thus TDP-43 is very important in pre-mRNA splicing. Processes affected by TDP-43-mediated pre-mRNA splicing include synapse stabilization, development, cellular morphology and cellular signaling. This is adapted from the work of Sephton et. al.

Functions of TDP-43 in nuclear pre-mRNA splicing

These pre-mRNA transcripts bound by TDP-43 can be subdivided into three categories: intronic, exonic and both intronic and exonic pre-mRNA transcripts(116). The functional classes of TDP-43 bound RNAs (as determined in rat cortical neurons) are summarized in Figure 2.9 and 2.10.

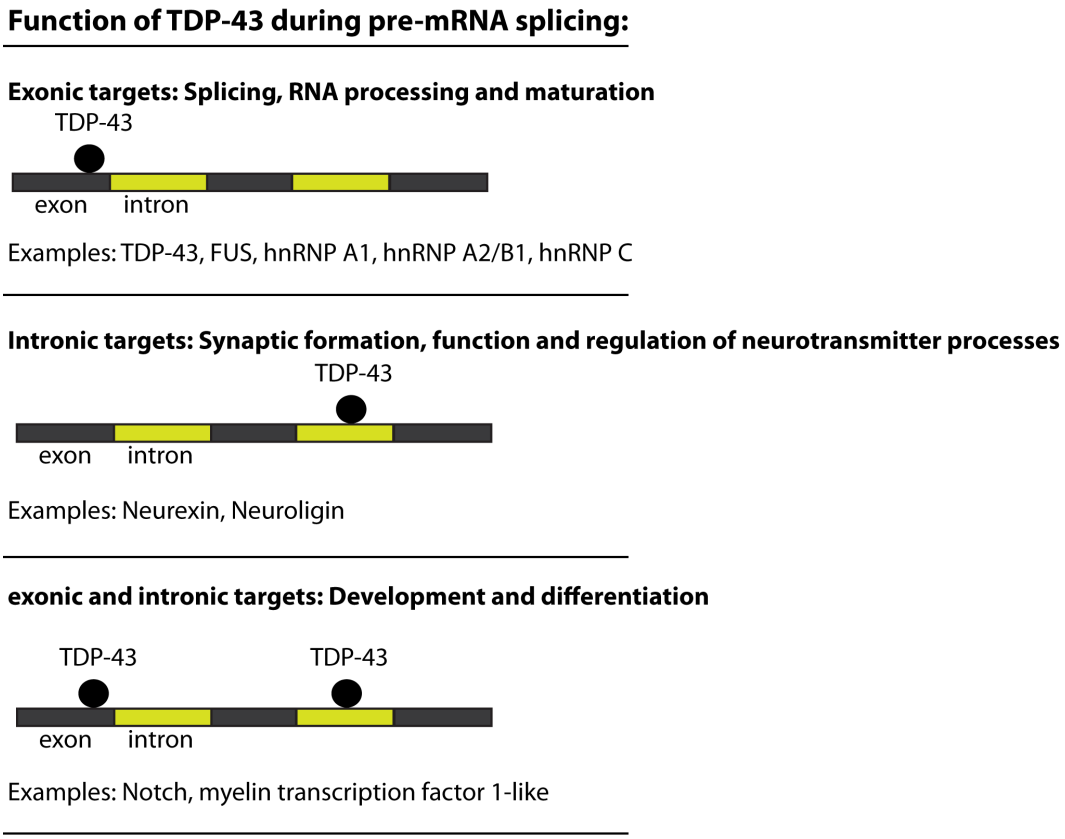

Figure 2.10, TDP-43 binds exonic, intronic and both exonic and intronic regions. The function of TDP-43 in pre-mRNA splicing varies according to the region bound: exonic, intronic and both exonic and intronic targets. TDP-43 exonic targets are involved in RNA metabolism, intronic targets are important for synaptic function while both exonic and intronic bound targets are important for development.

In addition to defining these functional categories, Sephton et. al. also determined profiles of TDP-43 binding frequency and discovered that TDP-43's RNA recognition site is perhaps more complicated than previously thought(116). I previously mentioned that TDP-43 was believed to bind $(TG)_6$-sequences, yet $(TG)_nTA(TG)_m$ sequences were found at a higher frequency(116). Whether TDP-43 has a higher affinity for the latter binding sequence relative to the former is unknown. However, an even more fascinating discovery from Sephton et. al. is the determination that many TDP-43 mRNA targets are already linked to other

neurodegenerative disorders. These targets include: presenilin 1 and 2, tau, TDP-43, VCP, GRN, Huntingtin, FUS, alpha-synuclein and APP(116). Thus, the nuclear functions of TDP-43 have been further defined by this study, however very little discussion concerning TDP-43 3' UTR targets was discussed in this paper. Additional deep sequencing results however, have shed light on this topic.

Cytoplasmic functions of TDP-43

As previously mentioned, some hnRNP class proteins stabilize cytoplasmic mRNA transcripts. TDP-43 is now understood to be a nucleocytoplasmic shuttling protein, yet what transcripts does TDP-43 bind? The list of cytoplasmic transcripts bound and stabilized by TDP-43 is much shorter than those identified in pre-mRNA splicing. Yet, the few targets that have been identified by RNA deep sequencing include: solute carrier family 1, syntaxin 1B and calmodulin 1(125). A mature mRNA transcript schematic is shown in Figure 2.11 below, as well as the 3' UTR bound by TDP-43.

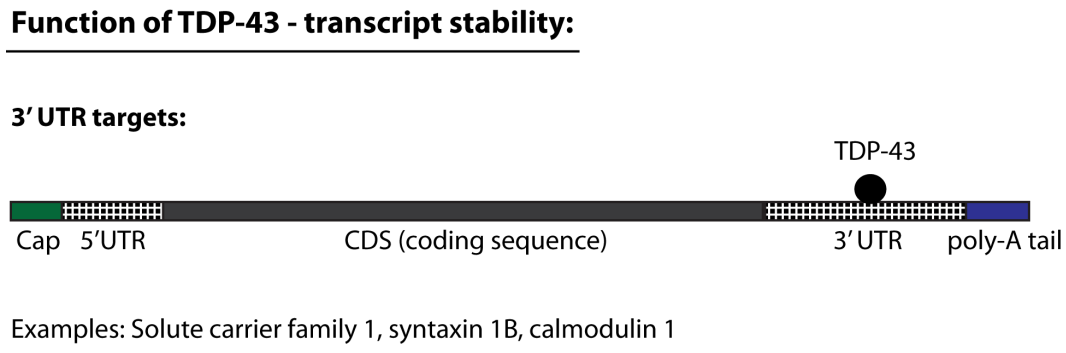

Figure 2.11, Schematic of a mature cytoplasmic mRNA transcript bound at its 3' UTR by TDP-43. Examples of 3' UTR bound TDP-43 targets include solute carrier family 1, syntaxin 1B, calmodulin 1, hNFL, and TDP-43.

These RNA deep sequencing targets indicate that TDP-43 stabilizes multiple transcripts in the cytoplasm. Additional 3' UTR TDP-43 targets have been identified in other studies and include: the light neurofilament protein (hNFL), β-actin, CamKII and TDP-43(87, 122, 133). Future studies will need to test how a depletion of these transcripts and the proteins they encode lead to the activation of cell death pathways.

Development of TDP-43 cell culture localization models and transgenic animal models

Determinants of TDP-43 localization: cell cycle progression and TDP-43 localization

The significance of my findings that TDP-43 localization is determined by cell cycle stage, as they relate to the toxic cytoplasmic gain of function hypothesis, is unknown. A complication in using these cell cycle findings to develop a cell culture degenerative or localization model is that neurons are quiescent cells. On the other hand, some controversial papers have documented that neurons in neurodegenerative patient brains can re-activate cell cycle or embryonic genes(78). Because TDP-43 exonic and intronic targets are developmental transcripts, there may be some credence to this argument. Additionally, TDP-43 is necessary for embryonic murine development, and its knockdown results in embryonic lethality by E3.5(117, 137).

However, another argument to study the function of TDP-43 during cell cycle is because some central nervous system cells are capable of cell division, including glial cells and immature neurons that haven't differentiated yet. One could propose that because glia offer trophic support for neurons, arrest at one stage of the cell cycle might prevent glia from providing that support, leading to the dystrophy observed in neurons in the disease. Glia also clear excitotoxic factors from the synaptic cleft (like the neurotransmitter glutamate), therefore any impairment of glial transport processes might lead to neuronal excitotoxicity. This too can be rationalized, as riluozole, the only drug currently used to treat the symptoms of ALS, works by reducing excitotoxicity, and excitotoxicity leads to neuronal death(96). Regardless, this initial insight into TDP-43 biology may prove significant as data accumulates on the function of TDP-43 in different cell types.

Determinants of TDP-43 localization: stress and TDP-43 localization

I found that 0.4 M sorbitol stress is able to increase TDP-43 cytoplasmic levels at the expense of its nuclear levels. These results were similar to previously published data on the stress response of hnRNP A1, a closely related protein to TDP-43. However, the significance of these findings is unknown as it relates to the cytoplasmic toxic gain of function hypothesis.

First, it is unknown at what timepoints sorbitol stress duration becomes toxic to the cell, and what role, if any, TDP-43 might play in mediating this toxicity. Second, additional pathological hallmarks of the disease must be

screened, including whether TDP-43 responds to stress by aggregating, and whether this process can occur in neurons and glial cells.

Regardless, my findings are significant toward establishing a cell culture model where sorbitol administration increases cytoplasmic TDP-43 levels. In this manner, this stress model can be used to test how TDP-43 localization is altered following overexpression of wild-type and pathologically mutated protein. Moreover, cellular stress is a good model for investigating localization, as both neuronal and glial stress responses have been characterized for multiple stressors including: sorbitol, ischemia-reperfusion, lipopolysaccharides (LPS), and tumor necrosis factor alpha (TNF-α). In future studies, the key is finding the right type of stress that recapitulates TDP-43 pathological hallmarks, including TDP-43 accumulation in the cytoplasm and aggregation.

CHAPTER THREE
Results

TDP-43 IS DIRECTED TO STRESS GRANULES BY SORBITOL, A NOVEL PHYSIOLOGICAL OSMOTIC AND OXIDATIVE STRESSOR

ABSTRACT

TDP-43, or TAR DNA-binding protein 43, is a pathological marker of a spectrum of neurodegenerative disorders including amyotrophic lateral sclerosis and frontotemporal lobar degeneration with ubiquitin-positive inclusions. TDP-43 is an RNA/DNA-binding protein implicated in transcriptional and post-transcriptional regulation. Recent work also suggests that TDP-43 associates with cytoplasmic stress granules, which are transient structures that form in response to stress. In this study, we establish sorbitol as a novel stressor that directs TDP-43 to stress granules in Hek293T cells and primary cultured glia. We quantify TDP-43 association with stress granules over time and show that stress granule association and size are dependent on the glycine-rich region of TDP-43, which harbors the majority of pathogenic mutations. Moreover, we establish that cells harboring wild-type and mutant TDP-43 have distinct stress responses: mutant TDP-43 forms significantly larger stress granules and incorporates into stress granules more early; in striking contrast, wild-type TDP-43 forms more stress granules over time, but granule size remains relatively unchanged. We propose that mutant TDP-43 alters stress granule dynamics, which may contribute to the progression of TDP-43 proteinopathies.

INTRODUCTION

TDP-43 is an RNA-binding protein with multiple cytoplasmic functions

TDP-43 is a highly conserved, ubiquitously expressed RNA-binding protein of the heterogeneous nuclear ribonucleoprotein (hnRNP) family (13, 80, 131). TDP-43 and other hnRNPs are multifunctional proteins that regulate gene expression in both the nucleus and cytoplasm (80, 135). In the nucleus, TDP-43 binds single-stranded DNA and RNA (12, 13, 27, 28, 82, 105) and can function as both a transcriptional repressor (1, 2, 105) and a splicing modulator (20, 25, 28, 94). Specifically, TDP-43 regulates pre-mRNA splicing by binding mRNA with $(UG)_{6\text{-}12}$ sequences (27) and by recruiting other hnRNP proteins into repressive splicing complexes (12, 26, 94). However, as a nucleocytoplasmic shuttling protein (14), TDP-43 also has distinct cytoplasmic functions, the first being mRNA stabilization (133). Additionally, TDP-43 is directed to cytoplasmic stress granules following heat shock, oxidative stress and chemical inducers of stress granules(35, 49). The next logical questions are: what are stress granules? How are they assembled? And what is their composition and function?

The assembly of stress granules (SGs)

Cytoplasmic stress granules form when translation is stalled at the initiation step, which occurs when a cell is exposed to chemicals (puromycin), environmental stressors (oxidative stress, heat shock, hyperosmolarity, viral infection and UV irradiation), or physiological stressors (increased cellular sorbitol concentration, as seen in diabetic retinopathy; ischemia-reperfusion, as seen in stroke)(5). Depending on the stressor

present, kinases are activated which target the active serine on eukaryotic initiation factor 2 alpha or eIF2α. This phosphorylation causes eIF2α to dissociate from the ternary initiation complex (composed of eIF2α-GTP-$tRNA_i^{Met}$), resulting in stalled translation initiation(73).

Stalled transcripts remain bound by small ribosomes and eukaryotic initiation factor complexes, but large ribosomes run off the transcripts. RNA-binding proteins also remain bound to the stalled transcripts, which nucleate into stress granules (SGs)(5). SG formation is dependent on microtubule tracts, at least at the early stages of SG formation, and treatment with the microtubule-disrupting agent nocodazole prevents SG formation(32).

However, eIF2α-phosphorylation is not always required to stall transcripts and initiate stress granule formation. An alternative route to forming SGs is through eIF4A helicase, which is targeted by the drugs hippuristanol and pateamine A(5). Another alternative route to SG formation is by the overexpression of a "core component". Examples of core SG components include the closely related proteins TIA-1 and TIAR(7, 74). When overexpressed, these proteins "nucleate" or "seed" stress granule assembly. TIA-1/TIAR have prion-like domains, and their aggregation is concentration-dependent; hence, overexpression of these components results in the formation of SGs(5, 7).

Disassembly of stress granules

Translation can be subdivided into three steps: initiation, elongation, and termination. As previously mentioned, stress granule assembly occurs when translation initiation is inhibited. In contrast, inhibition of translation at the elongation step results in

the prevention of stress granule assembly(5). Inhibition of elongation can be achieved using the drug cycloheximide, which not only prevents SG formation, but also promotes the disassembly of pre-formed SGs, even during stress exposure(70).

Importantly, SGs are transient structures that naturally disassemble following stress removal. According to the literature, the timecourse of this disassembly can occur as quickly as 15 minutes(5). In addition, just as overexpression of TIA-1/TIAR seeds SG assembly, the overexpression of staufen prevents SG assembly(124). Thus, the dynamics of SG assembly and disassembly, and the contribution of different proteins to the formation or dissolution of SGs, is being investigated, but it seems that many distinct steps within SG assembly and disassembly can be targeted to modulate their formation.

Composition of stress granules

SG composition and morphology vary according to stress and cell type (6, 22, 58), but some core components are conserved. As previously mentioned, SG core components include the RNA-binding protein TIAR and TIA-1, but also includes stalled translation initiation complex components eIF3 and eIF4G (71, 75). In contrast, the incorporation of RNA-binding proteins HuR, hnRNP A1, and FUS into SGs varies according to cell type and stress (6, 19, 58). Other types of proteins accumulating in SGs include transcription factors, RNA helicases, nucleases, kinases and signaling molecules(5). The recruitment of signaling proteins into SGs can alter cellular viability, although SGs are generally regarded as pro-survival structures(10).

Biological function of stress granules (SGs)

SGs are dynamic cytoplasmic structures that are believed to act as sorting stations for mRNAs(6). The fate of the mRNA localizing to the stress granule includes: mRNA is translation, degradation or sequestration within the granule(71, 72, 76). Figure 3.1 below summarizes this discussion of the formation of SGs, their composition as well as the fate of the mRNAs localizing to these structures.

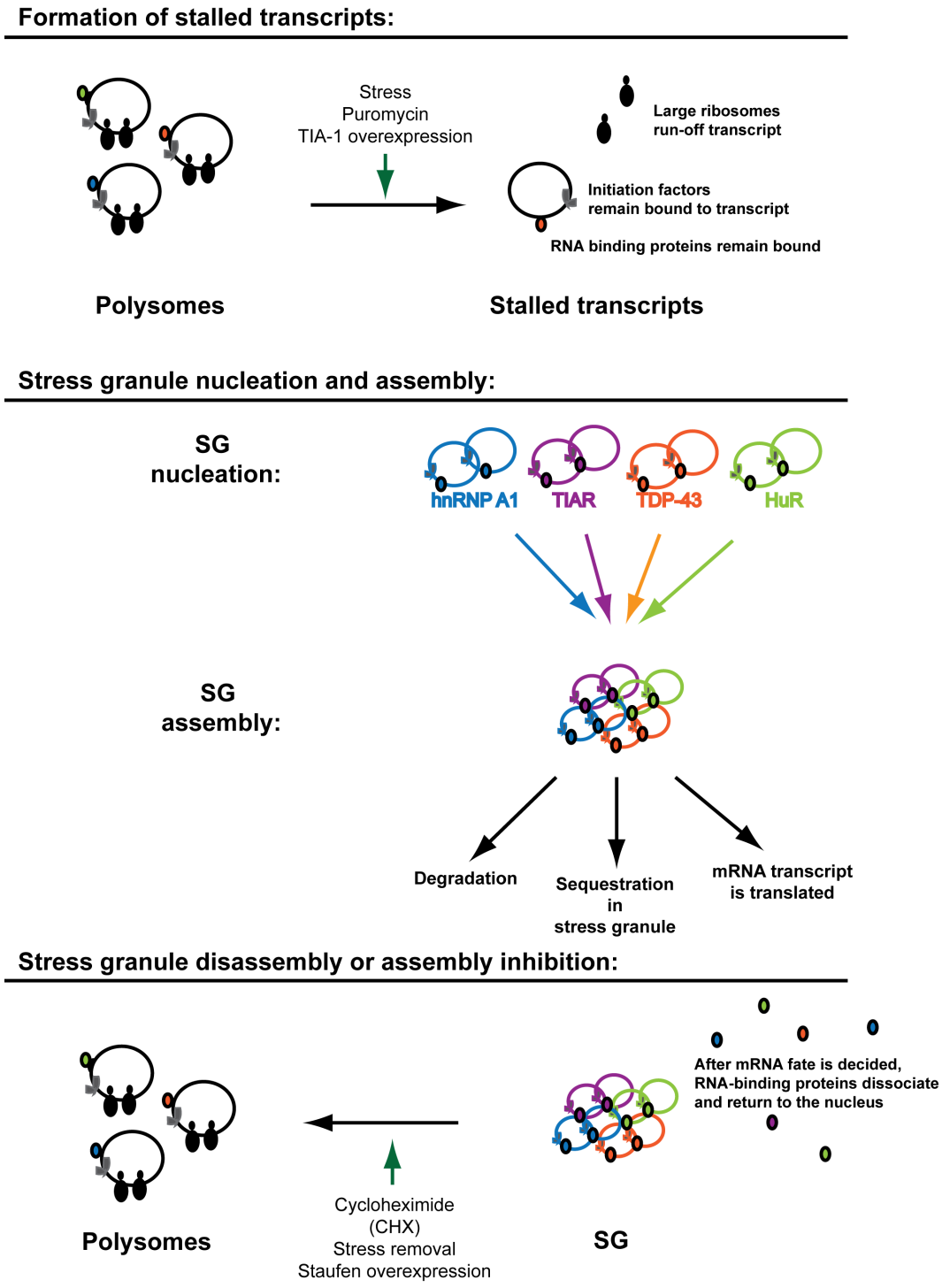

Figure 3.1, Stress granule (SG) assembly follows inhibition of translation initiation. SGs assemble when chemicals and stress prevent translation initiation, or following TIAR overexpression. Many hnRNP proteins bound to these stalled transcripts (including hnRNP A1, TIAR, TDP-43 and HuR) localize to SGs. The fate of mRNA transcripts bound by hnRNPs, small ribosomes and initiation factors is determined to be either: degradation,

sequestration or translation. When mRNA fate is determined, or when the stress is removed, RNA-binding proteins dissociate and return to the nucleus. Stress granules can also be prevented from forming by overexpressing Staufen or by treatment with the drug cycloheximide (CHX).

Testing the cytoplasmic toxic gain of function: TDP-43^{+} cytoplasmic aggregates are stress granules

One of the first questions asked when approaching the cytoplasmic toxic gain of function hypothesis are: what are the cytoplasmic aggregates found in the disease and how do they form? In a recent study, ubiquitinated aggregates in pathological tissues colocalize with stress granule (SG) markers TIA-1 and eIF3(88). Other labs have failed to detect TDP-43 colocalization with SG markers in pathological tissues, indicating that either not all pathological aggregates are stress granules(99), or that other proteins can somehow disassemble from the stress granule whereas TDP-43 cannot.

In this study, I build a robust, quantitative, and physiologically-relevant cellular model that allows us to establish the conditions under which TDP-43 accumulates in the cytoplasm, such as those seen in TDP-43 proteinopathies. I continue my previous study of sorbitol, but describe in greater detail how elevated levels of the sugar sorbitol, an intermediate in the polyol pathway (an ATP-independent metabolic route that generates fructose from glucose) (33), directs TDP-43 localization to SGs in Hek293T cells and, similarly, primary cultured glia. Furthermore, I use this new cellular model to examine the dynamic assembly of TDP-43^{+} SGs, including the control of SG size and the molecular determinants within TDP-43 necessary for its assembly into SGs. Finally, I use this model to

distinguish between the responses of wild-type and pathological mutant TDP-43 to stress. Mutant TDP-43 variants are incorporated into stress granules earlier than wild type, and these mutants form significantly larger stress granules. In striking contrast, wild-type TDP-43 forms more cytoplasmic granules over time, but granule size remains relatively unchanged. Thus, I establish in this study a simple, yet rigorous, quantitative, physiologically-relevant measurement of TDP-43 aggregate formation *in vivo*, and I use this novel assay to identify the regions of TDP-43 that contribute to this pathological phenomenon.

MATERIALS AND METHODS

Constructs and primers

We used TDP-43 mouse cDNA (Image clone #5346061) as template with the following primers: 5'-(HindIII):tttaagcttatgtctgaatatattcgggtaacagaagatgagaacg and a 3'-(BamHI): tttggatccattccccagccagaagacttagaatccatgc. The insert was sequentially digested with BamHI and HindIII and subcloned into vector pcDNA4 myc-His B (Invitrogen) to generate TDP-43 with C-terminal myc and 6x-His tags. Site-directed mutagenesis on template pcDNA4B-TDP-43 was used to generate the following mutations with the following primers using Quikchange (Qiagen): (G348C): 5'-cagcagaaccagtcgtgcccatctgggaata and 3'-tattcccagatgggcacgactggttctgctg; (A315T): 5'-ggatgaactttggtacttttag cattaacc and 3'-ggttaatgctaaaagtaccaaagttcatcc; (G294A): 5'-ggtaacagtagagcg ggtggagctggcttgg and 3'-ccaagccagctccacccgctctactgttacc; (N390S): 5'-

gttgggggtcagcatcaagtgcaggatcgg and 3'-ccgatcctgcacttgatgctgacccccaac. Truncated TDP-43 constructs were subcloned into the pcDNA4b vector using HindIII and BamHI using the following primer sets, (1-114): 5'-tttaagcttatgtctgaatatattcgggtaacagaagatgagaacg and 3'-tttggatcctttccaggggagacccaacactatgaggtcagatgttttctggac; (1-179): 5'-tttaagcttatgtctgaatatattcgggtaacagaagatgagaacg and 3'-tttggatccgttgggaagtttacagtcacaccatcgcccatctatcatatgtcg; (1-267): 5'-tttaagcttatgtctgaatatattcgggtaacagaagatgagaacg and 3'-tttggatccattgctattatgcttaggttcagcattggatatatgcacgctgat; (1-324): 5'-tttaagcttatgtctgaatatattcgggtaacagaagatgagaacg and 3'-tttggatccagccatcatcgctgggttaatgctaaaagcaccaaagttcatccc. Primers used to generate the ΔNLS and F147L/F149L mutants were previously described(14). Sequences were confirmed by the UT Southwestern sequencing facility using T7 and BGH primers.

Cell and primary cultures

Hek293T cell lines used in this study were maintained in standard growth medium: 10% fetal bovine serum in DMEM (Invitrogen). Low-passage number cells were used for analyzing stress granule formation due to their robust response to stress. For primary mixed glial cultures, rat cortices were dissected from postnatal (D1-4) pups in ice-cold dissection medium (Gibco-Invitrogen) as described previously (118). Glia (~21-28 DIV) were split onto poly-*D*-lysine and

matrigel-coated coverslips and were subjected to stress the next day with 0.4 M sorbitol (Sigma).

Transfection and stable cell selection

pcDNA4B-TDP-43-myc/6x-His and pcDNA4B-TDP-43-G348C-myc/6x-His were transfected into Hek293T cells with Fugene HD (Roche), according to the manufacturer's instructions. After two days, 800 μg mL^{-1} zeocin was added to growth medium to select for transformants. Following selection, cells were maintained in 400 μg mL^{-1} zeocin growth medium.

Induction of osmotic stress and TDP-43 clustering optimization

D-sorbitol (Sigma) was diluted in standard growth medium to yield a 0.4 M concentration. For Hek293T cells, optimal endogenous TDP-43 clustering was observed between passages 3-8. In stable cell lines, we observed robust TDP-43 clustering 6-8 passages after zeocin-selection. For all experiments, immunofluorescent validation of cellular TDP-43 clustering was performed alongside western blot analysis.

shRNA-mediated knockdown of TDP-43

Sigma Mission shRNAs were purchased against human TDP-43 (NM_007375) cloned into backbone vector plko.1 puro. shRNA constructs (#1261, 666, 1333, 931 and 177) were co-transfected with helper plasmids pspax2 and VSVG using Fugene HD (Roche) according to the manufacturer's specifications. Optimal

knockdown of TDP-43 was obtained using shRNA plasmid #1333, and stable selection of viral-infected cells was achieved using 1 μg mL^{-1} puromycin (Sigma). Control stable cell lines were generated expressing shRNA directed against EGFP (Sigma).

PARP cleavage and western blots

Hek293T cells were seeded the night before into 10 cm plates and treated with 0.4 M sorbitol stress the following day alongside untreated control. Cells were resuspended in a high salt buffer (50mM Tris-HCl, pH 7.5, 0.5 M NaCl, 1% NP-40, 1% DOC, 0.1% SDS, 2 mM EDTA and 1 Roche Complete protease-inhibitor tablet), freeze-thawed in liquid nitrogen, sonicated using a Diagenode Bioruptor 3 x 30s on high setting, and lysates were pre-cleared with centrifugation at 4ºC (14,000 x *g*). Protein was quantified using the Pierce BCA reagent; 75 μg of protein was loaded per lane.

MTS assay

Hek293T cells were plated at 20k/well in a 96-well plate. The next day, MTS assay was performed using the CellTiter 96 Aqueous Non-Radioactive Cell Proliferation Assay kit (Promega). Experiments were conducted in triple quadruplicates, according to the manufacturer's protocol. To analyze the recovery of cells after stress, stress was applied for the time indicated in the text and then washed off. Medium was immediately supplemented with PMS/MTS reagent and a baseline reading was determined after 4 hrs of color development. This assay

was repeated 24 and 48 into the recovery and percent cellular viability was determined as 100(490 $nm_{stressed}$/490 $nm_{unstressed}$).

Immunocytochemistry

Briefly, Hek293T cells were plated at 0.50-1.0 x 10^5 cells $well^{-1}$ onto nitric acid-etched coverslips coated with poly-D-lysine and matrigel. Cells were stressed with 0.4 M sorbitol (Sigma) medium for 0.5, 1, 2, or 4 hrs. Cells were fixed for 15 min. with 4% PFA/2% sucrose/PBS at room temperature and permeabilized for 5 min. with 0.25% Triton X-100 or 3 min. with 100% methanol. Coverslips were blocked for 1 hr in 10% normal goat serum in PBS (Jackson ImmunoResearch and Vector Labs). Primary antibodies were used at the following dilutions overnight at 4ºC: TDP-43 1:200 (polyclonal, ProteinTech Group); TDP-43 C-terminal antibody (polyclonal, 748C clone, in-house) 1:500; myc 1:500 (monoclonal, Santa Cruz); myc 1:5000 (polyclonal, Abcam); hnRNP A1 1:3200 (monoclonal, Sigma); HuR 1:100 (monoclonal, Santa Cruz); TIAR 1:500 (BD Transduction Laboratories). The next day, secondary antibodies were incubated 30 minutes at room temperature at the following dilutions: goat-anti-rabbit-488, goat-anti-rabbit-546, goat-anti-mouse-488, goat-anti-mouse-546 1:250; rhodamine-conjugated phalloidin 1:500; ToPro-3 1:1000 (Invitrogen). All antibodies were diluted in 3% normal goat serum in PBS. Coverslips were mounted in ProLong Gold Antifade Reagent (Invitrogen).

Microscopy and image processing

Images were collected on a Zeiss LSM 510 confocal microscope using LSM software. Images were analyzed using ImageJ, MetaMorph and Zen 2007 Light Edition software. Quantification of cytoplasmic granule size was determined with two programs: Metamorph and ImageJ. Nuclei were quantified using the ImageJ "cell counter" plug-in. Nuclear subtraction was performed in MetaMorph and further processed in ImageJ. ImageJ plug-in "analyze particles" was used to filter the granule size (size: 0-25). ImageJ plug-in "distribution" then determined the total area of cytoplasmic puncta and the total number of puncta. Average granule size was then determined by: $\text{puncta}_{\text{area}}/\text{puncta}_{\#}$. The number of granules/cell was determined by: $\text{puncta}_{\#}/\text{nuclei}_{\#}$. The percent of cells with stress granules was determined by: 100(cells with TDP-43^{+} granules/$\text{nuclei}_{\#}$).

Statistical analysis

All data is the result of (at least) three independent experiments. All results are recorded/graphed as the mean ± SEM. *p*-values are defined as the following: ns ($p > 0.05$); * ($p < 0.05$); ** ($p < 0.01$); *** ($p < 0.001$). For the endogenous TDP-43 study and transient transfections, Excel and GraphPad Prism were used to log data, determine statistical significance, and graph data. Statistical significance was determined by: student's *t*-test (Excel), one-way ANOVA, two-way ANOVA, and Bonferroni multiple-comparison post-tests (Prism) where appropriate. For wild-type and mutant TDP-43 stable cell line analysis, statistical significance was determined using R software package v2.6.0. Significance of average granule size was determined using the Wilcoxon rank sum test with continuity correction,

using a one-sided *p*-value. The statistical significance of the number of puncta per cell was determined using Excel and student's *t*-test.

RESULTS

Development of stress-based models to understand TDP-43 localization and function

Sorbitol is a novel stressor that directs TDP-43 to stress granules in Hek293T cells

TDP-43 is structurally similar to hnRNP A1: both have two RNA recognition motifs (RRM1 and 2), a glycine rich region (GRR), and NLS and NES signals allowing both proteins to undergo nucleocytoplasmic shuttling (Figure 2.6a). Also, both hnRNP A1 and TDP-43 can localize to stress granules (SGs) during heat shock and oxidative stress (14, 35, 58, 120). Another stressor, sorbitol (Figure 3.3) has been shown to drive hnRNP A1 to SGs (4). Sorbitol is a sugar intermediate in the polyol pathway, and is both a hyperosmotic and oxidative stressor. Importantly, sorbitol is regarded as a physiological stressor, because increased sorbitol levels have been found in patients with diabetic retinopathy. Below, I summarize how increased sorbitol concentrations can lead to both osmotic and oxidative stress (Figure 3.2).

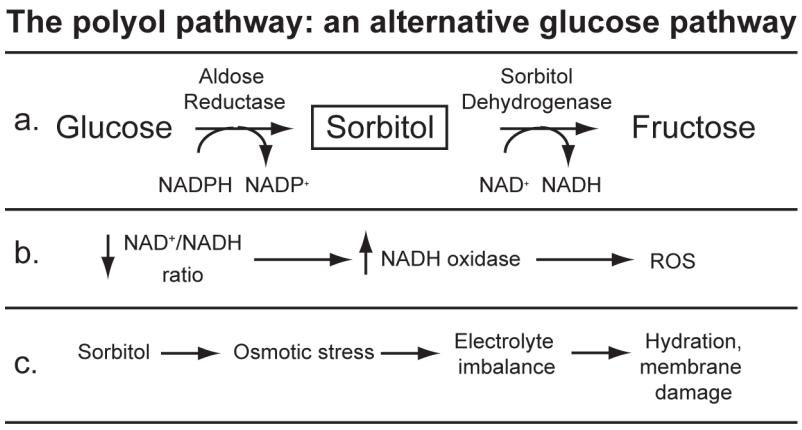

Figure 3.2, Sorbitol is an intermediate in the polyol pathway. a. The polyol pathway is an alternative pathway for the conversion of glucose into fructose. b. In the oxidation of sorbitol to fructose in, the NAD^+/NADH cofactor ratio is disturbed, leading to an increase of NADH oxidase resulting in oxidative stress by increased reactive oxygen species (ROS). c. Sorbitol is an osmotic stressor that causes electrolyte imbalances leading to membrane damage. Sorbitol is therefore both a hyperosmotic and oxidative stressor.

I previously described how 0.4 M sorbitol increases the cytoplasmic levels of both hnRNP A1 and TDP-43 in Hek293T cells. I next hypothesized that sorbitol stress directs TDP-43 to stress granules. In the literature, both 0.4 and 0.6 M sorbitol concentrations can generate stress granules in multiple cell types. I administered 0.4 M sorbitol in U343 and HeLa cells to determine if TDP-43 localized to cytoplasmic granules at this concentration and again used hnRNP A1 as control (Figure 3.3).

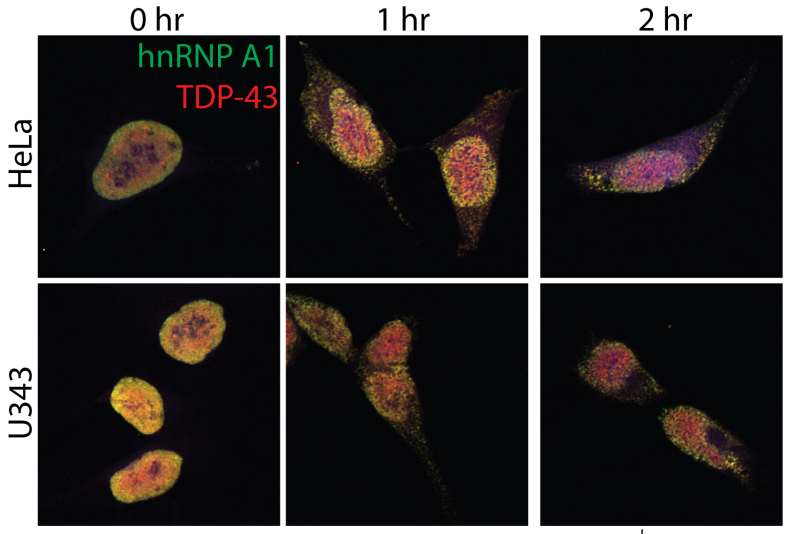

Figure 3.3, TDP-43 colocalizes with hnRNP A1$^+$ cytoplasmic granules during sorbitol stress. HeLa and U343 cells were treated with 0.4 M sorbitol for 0, 1 and 2 hrs (stress duration is labeled at the top of the images). In response to sorbitol, TDP-43 (red) localizes to cytoplasmic granules at both timepoints examined. Also, TDP-43 (red) colocalizes with hnRNP A1 (green) in the nucleus of unstressed cells (0 hr), and with cytoplasmic hnRNP A1 granules in stressed cells (colocalized proteins stain yellow). All images taken with the 63x objective.

I found that TDP-43 localized to hnRNP A1$^+$ cytoplasmic granules at the 0.4 M sorbitol concentration. Both TDP-43 (red) and hnRNP A1 (green) localized to these cytoplasmic granules in response to one and two hours of sorbitol stress (Figure 3.3).

To determine whether these TDP-43$^+$ granules are stress granules, I repeated the experiment in Hek293T cells and co-stained TDP-43 with TIAR, a stress granule marker. I found that TDP-43$^+$ granules colocalized with TIAR, therefore TDP-43 localizes to stress granules in response to one hour of 0.4 M sorbitol stress. Interestingly, I also tested an artificial oxidative stressor called sodium arsenite (ARS), however TDP-43$^+$ granules failed to form in response to arsenite stress (Figure 3.4 a and b).

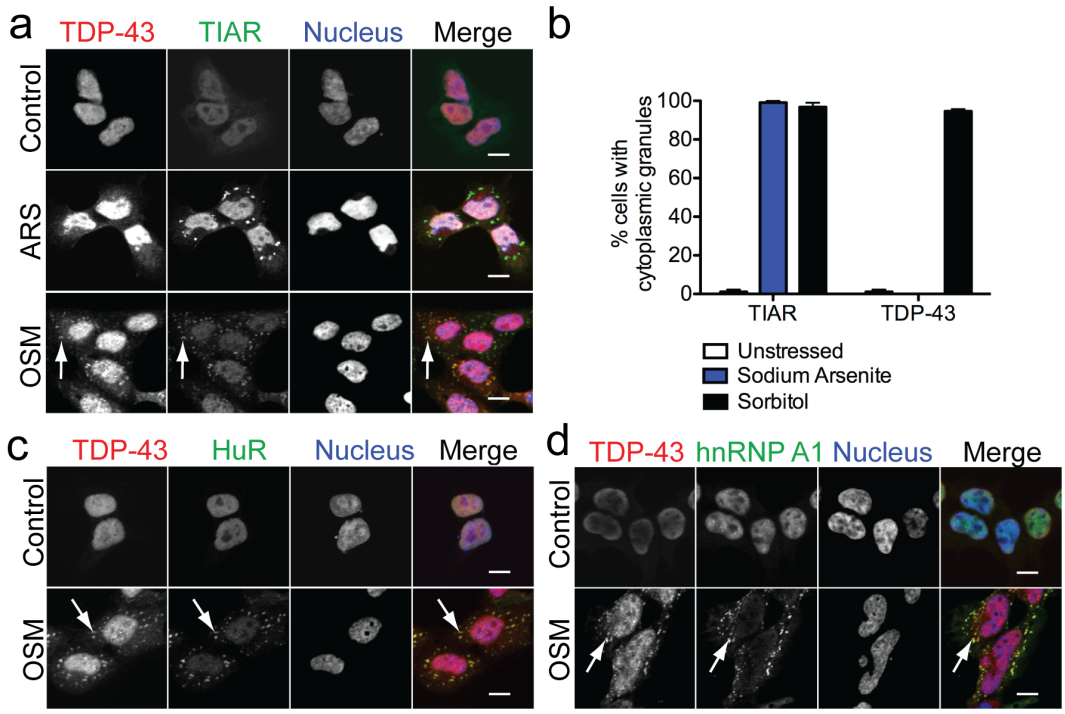

Figure 3.4, Hyperosmotic stress is a novel stressor that directs TDP-43 to stress granules. a. TDP-43 forms cytoplasmic granules (arrows) in Hek293T cells in response to sorbitol stress but not sodium arsenite stress. b. Quantification of TDP-43^{+} and TIAR^{+} granules in Hek293T cells stressed for 1 hr with sorbitol (osmotic stressor, OSM) or sodium arsenite (oxidative stressor, ARS) as demonstrated in panel (a). Data is the result of three experimental sets and presented as the mean ± SEM. c and d. Osmotic stress of Hek293T cells directs TDP-43 to HuR- and hnRNP A1-containing stress granules (c and d, respectively). Scale bars = 10 µm.

Although TDP-43 localizes to SGs in NSC34 cells following a 1 hr treatment with 0.5 mM sodium arsenite (35, 58), in Hek293T cells under the same conditions, I failed to detect TDP-43 at TIAR^{+} stress granules (Figure 3.4a and b). However, previous studies have shown that the composition of SGs can be distinct in different cell types (5, 6). Cells generate distinct SGs in response to different stressors, and these SGs can appear morphologically distinct (5, 6). This phenomenon is readily observed in Figure 3.4a, where arsenite and sorbitol stress generate TIAR^{+} granules that appear distinct in morphology, as well as in both

number and size (unquantified observations). Thus, TDP-43 is recruited to SGs during osmotic stress induced by 0.4 M sorbitol but not during oxidative stress induced by 0.5 mM sodium arsenite in Hek293T cells. This indicates that, unlike TIAR, TDP-43 is not a core component of stress granules and that its localization to SGs is stressor-dependent.

Sorbitol is a novel stressor that directs TDP-43 to stress granules in mixed primary cultured glia

Specifically, I examined glia, as TDP-43^{+} pathological inclusions have been observed in glial cells (51). Cortex-derived glia were isolated and subjected to 0.4 M sorbitol stress. I found that TDP-43^{+} granules are generated after 1 hr of stress in multiple types of morphologically-distinct glia (Figure 3.5). Additionally, these TDP-43^{+} granules colocalized with stress granule markers hnRNP A1, TIAR and HuR (a-c, respectively). Thus, TDP-43 is directed to stress granules by osmotic stress in both Hek293T cells and primary cultured glia. This indicates that in these cells a common signaling pathway exists that directs TDP-43 to SGs.

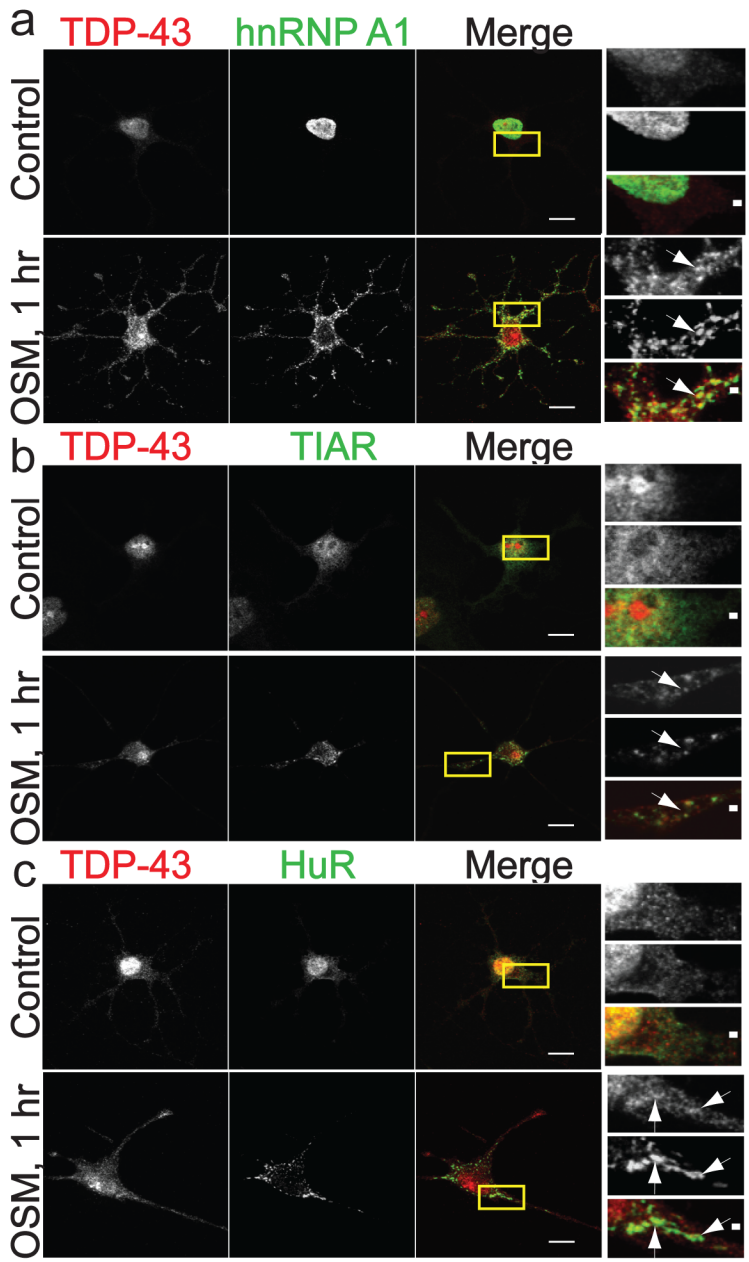

Figure 3.5, Hyperosmotic stress directs TDP-43 to stress granules in primary cultured glia. a-c. Mixed primary cultured glia stressed for 1 hr with 0.4 M sorbitol. TDP-43 was detected with the PTG antibody, and nuclei were stained using ToPro-3. Right panels show TDP-43 cytoplasmic clustering and colocalization (arrows) with hnRNP A1 (a), TIAR (b), and HuR (c). Scale bars = 10 µm (left); = 1 µm (right).

0.4 M sorbitol and 0.5 μM sodium arsenite fail to direct TDP-43 to SGs in primary cultured cortical neurons

As the formation of SGs can also be cell type-dependent, I next asked whether the sorbitol-induced localization of TDP-43 to SGs occurs in neurons. I cultured primary rat cortical neurons, as frontal and temporal cortical neurons display pathological TDP-43 hallmarks in FTLD-U and subjected these cells to both sorbitol (OSM) and arsenite (ARS) stress (Figure 3.6).

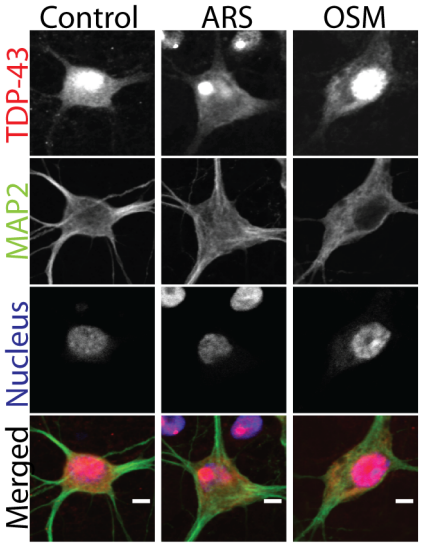

Figure 3.6, Neither 0.4 M sorbitol nor 0.5 μM arsenite induce TDP-43^{+} granule formation in primary cultured cortical neurons. 18 DIV cortical neurons were treated with 0.5 mM sodium arsenite (oxidative stressor) or 0.4 M sorbitol for 1 hour before immunofluorescent analysis. TDP-43 (red) fails to form cytoplasmic granules after treatment with these stressors. Neurons are labeled by MAP2, a dendritic marker protein, and the DNA-labeling dye ToPro-3 (nuclear). Scale bar: 5 μm.

The finding that TDP-43 is not directed to SGs by either sorbitol or sodium arsenite stress in neurons reinforces how distinct SG composition is, depending on cell type. Also, these results reinforce how neuronal stress responses are distinct from the glial and Hek293T cell response.

Timecourse of TDP-43 stress granule assembly in Hek293T cells

The previous data show that TDP-43 localizes to stress granules in response to specific stress conditions in different cell types. The next question I wanted to

ask was, what is the timecourse of TDP-43 localization to SGs? And, does TDP-43 persist in SGs during sorbitol stress, or does it leave SGs after one hour? To answer these questions, I exposed Hek293T cells to 0.4 M sorbitol for four hours, and determined TDP-43 localization at different timepoints using immunofluorescence.

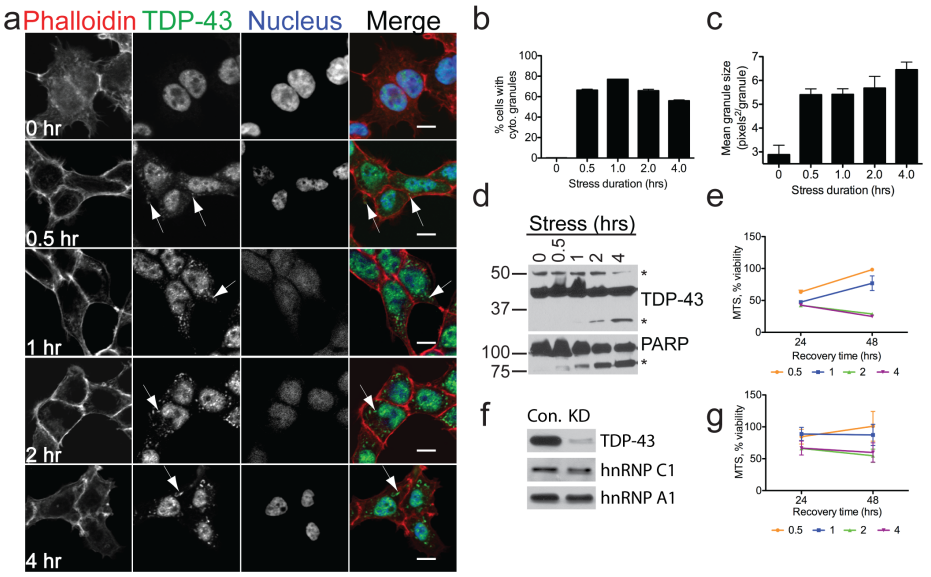

Figure 3.7, Characterization of the formation of endogenous TDP-43^{+} stress granules. a. Immunofluorescence of TDP-43 throughout 4 hrs of 0.4 M sorbitol administration in Hek293T cells. Arrows highlight TDP-43 cytoplasmic granules. b and c. Quantification of cells as in panel (a); shown are the percentage of cells with granules (b) and the mean granule size (c). Data are presented as mean ± SEM. d. Prolonged sorbitol stress results in PARP cleavage. Cross-reactive bands (*) in the upper panel show TDP-43 cleavage products (35 kDa) following 2-4 hrs of stress and a higher molecular weight TDP-43 species (50 kDa) that declines with longer stress treatment. PARP cleavage (*) is shown in the lower panel. e. Recovery of Hek293T cells from 0.5 to 4 hrs of sorbitol stress. Percent cell viability was determined 24 and 48 hours after 0.5, 1, 2, or 4 hrs of sorbitol stress. Viability was determined using the MTS assay in triplicate and presented as mean ± SEM. f. shRNA-mediated knockdown (KD) of TDP-43 in Hek293T cells. Con., EGFP shRNA control. g. Recovery of Hek293T cells in which TDP-43 expression was knocked down as in panel f. Experiments were performed in triplicate as in panel (e) and presented as mean ± SEM.

As previously shown in Chapter 2, TDP-43 is strongly nuclear-localized in unstressed Hek293T cells. Treatment of Hek293T cells with sorbitol however, indicated that by 0.5 hrs into the stress response, TDP-43 localized to discrete cytoplasmic granules (arrows, Figure 3.7a). Also, TDP-43 continued to localize to these cytoplasmic granules throughout the stress timecourse (2 and 4 hrs). Quantification showed that within 0.5 hrs of sorbitol stress, TDP-43 maximally localizes to cytoplasmic granules of a relatively uniform size throughout 4 hrs of sorbitol stress.

As the length of sorbitol stress continued, cells had a greater number of condensed nuclei (unquantified observations), leading us to speculate that these cells were undergoing apoptosis. Indeed, apoptosis is induced following prolonged sorbitol exposure in other cell types (8, 65, 123). A biological readout of this increased apoptosis is PARP cleavage, which follows caspase-3 activation (104). To examine when Hek293T cells induce apoptosis, we examined PARP cleavage in our stressed lysates (western blot by Basar Cenik). We found PARP cleavage throughout 4 hrs of stress, with the highest amount of cleavage at 2 and 4 hrs (Figure 3.7d). By 2 and 4 hrs into the stress response, we also detected a 35 kDa truncated TDP-43 species using an N-terminal (PTG) TDP-43 antibody. This is significant since TDP-43 is a known caspase-3 target, with an N-terminal cleavage product of 35 kDa (43, 139, 140).

To investigate whether Hek293T cells are irreversibly committed to apoptosis following sorbitol exposure, I performed a cellular recovery assay. I stressed the cells for 0.5 to 4 hrs and determined cellular viability using MTS

assay. Cells were able to recover from 0.5 and 1 hr of sorbitol stress but not after 2 or 4 hrs of stress (Figure 3.7e). Moreover, this recovery from sorbitol-induced stress required TDP-43, as cells did not improve their recovery following stress upon knockdown of TDP-43 (Figures 3.6g). Taken together, our data suggest that sorbitol-induced osmotic and oxidative stress directs TDP-43 to uniformly sized cytoplasmic granules within 30 minutes of stress and that TDP-43 allows for cellular recovery in response to acute sorbitol stress.

How does decreased cellular viability impact the composition of TDP-43$^+$ granules?

A previous report indicates that TDP-43$^+$ pathological granules fail to costain with hnRNP A1 and SMN in FTLD-U brain(99). In the last experiment, I showed that TDP-43$^+$ granules persisted in Hek293T cells exposed to both "recoverable" and "irrecoverable" stress timepoints (0.5-1 hr and 2 or more hours of 0.4 M sorbitol, respectively). I began to wonder how the granule composition changes over time: can some hnRNP proteins sense the viability of the cell? And if so, do they cease to localize to stress granules when the cell enters an "irrecoverable" stress exposure? I hypothesized that SG composition varies by duration of stress, and that TDP-43 persists in SGs throughout the stress, while hnRNP A1 and SMN localize to SGs only during viable stages of stress.

To test this hypothesis, I used the timepoints previously established in Hek293T cells: 0.5 hours of 0.4 M stress is recoverable, whereas 4 hrs is not. I then stressed Hek293T cells at these timepoints, and examined the localization of

TDP-43 with hnRNP A1 (Figure 3.8). Because hnRNP A1 is not found in pathological TDP-43^{+} cytoplasmic granules, I expected to observe hnRNP A1^{+} granules at 0.5 hrs stress, but not at 4 hours of stress. I found that TDP-43 (red) and hnRNP A1 (green) colocalized in the nuclei (yellow, merged) of unstressed cells. Yet, at both 0.5 and 4 hours of stress, TDP-43 and hnRNP A1 remain colocalized to cytoplasmic granules. I conclude that in Hek293T cells, hnRNP A1 is not sensitive to the viability of the cell.

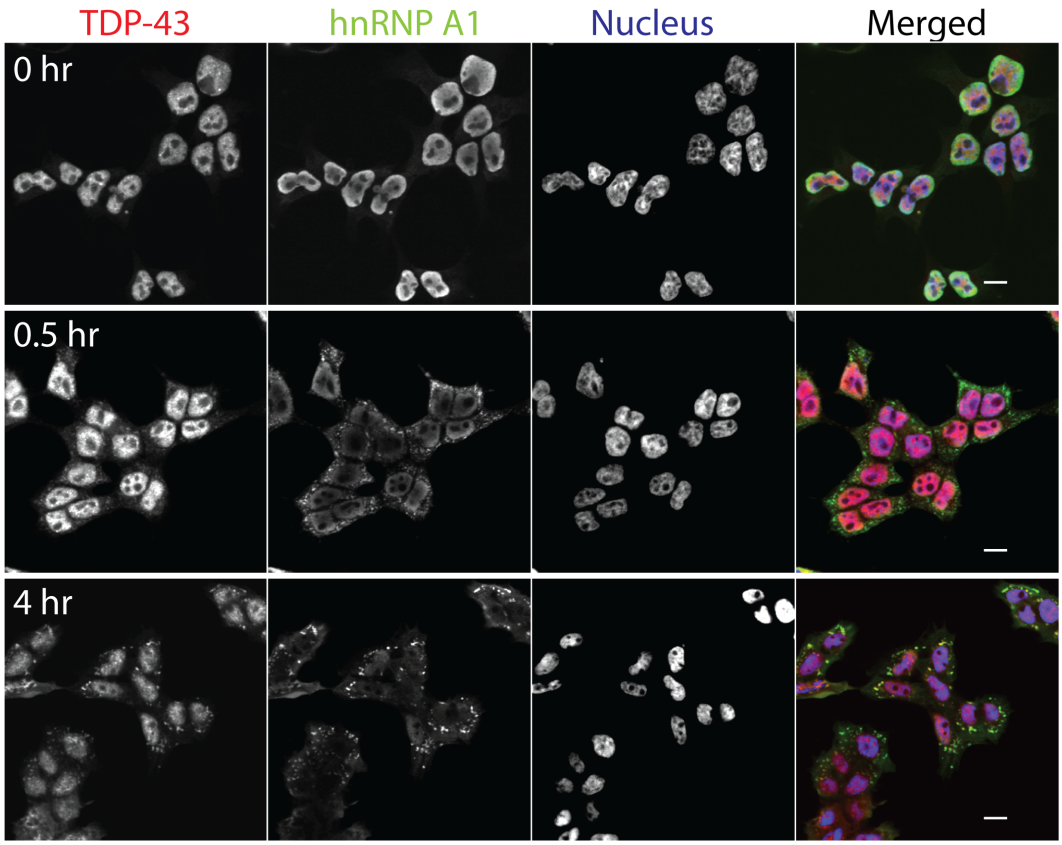

Figure 3.8, TDP-43 and hnRNP A1 colocalize to cytoplasmic granules in response to 0.5 and 4 hours of 0.4 M sorbitol stress. TDP-43 is stained in red, hnRNP A1 in green and the DNA dye ToPro-3 stains the nucleus in blue. Scale bars = 10 µm.

I then repeated this experiment in Hek293T cells, examining the response of SMN to a recoverable stress (0.5 hrs) versus an irrecoverable stress (4 hrs, 0.4

M sorbitol) in Figure 3.9. In unstressed cells, SMN is strongly localized to the cytoplasm, and excluded from the nucleus. In stressed cells, SMN localizes to cytoplasmic granules within 30 minutes, but does not appear to colocalize with TDP-43. Also, SMN persists in these granules up until the 4 hour timepoint. This indicates that SMN is not sensitive to the viability of the cell, and persists in cytoplasmic granules at all timepoints, similar to hnRNP A1.

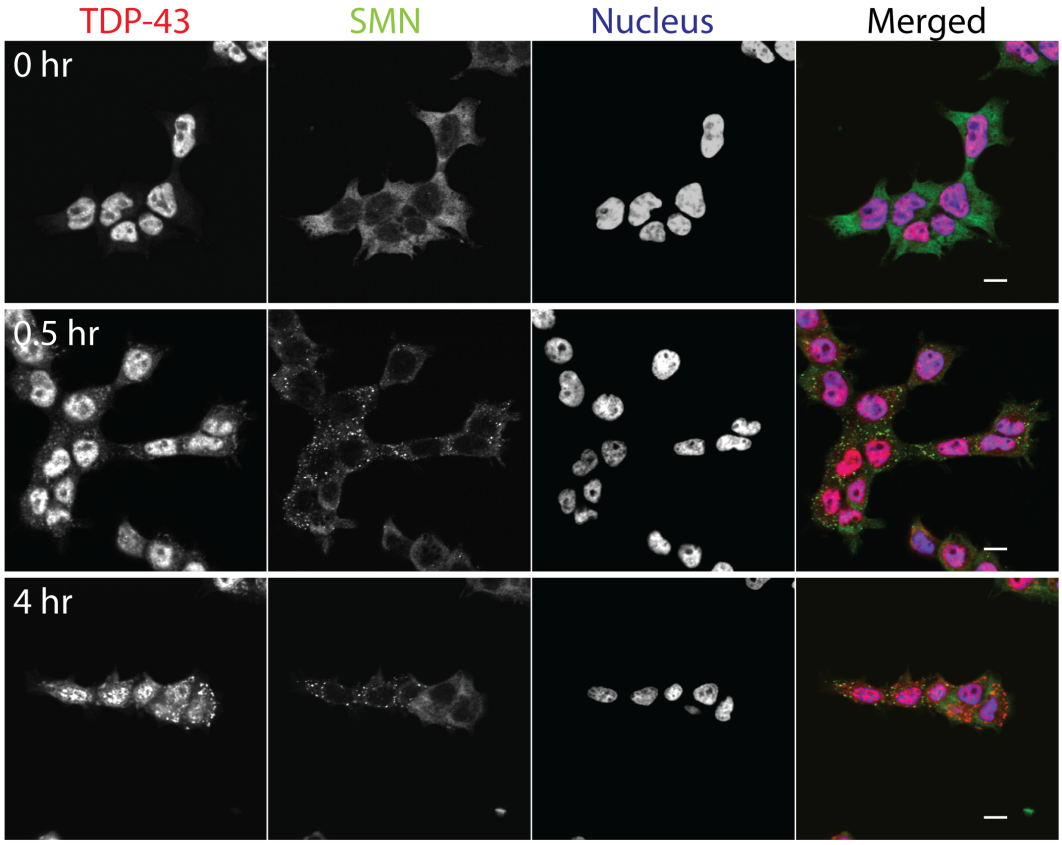

Figure 3.9, TDP-43 and SMN fail to colocalize to the same cytoplasmic granules in response to 0.5 and 4 hours of 0.4 M sorbitol stress. TDP-43 is stained in red, SMN in green and the DNA dye ToPro-3 stains the nucleus in blue. Scale bars = 10 µm.

Next, I wanted to gain a better understanding of how SG composition changes after a toxic exposure to stress. I wanted to test how a nuclear restricted protein like hnRNP C1, responds to a recoverable stress (0.5 hrs) versus an

irrecoverable stress (4 hrs, 0.4 M sorbitol) in Hek293T cells. I expect that hnRNP C1 will remain nuclear-localized during stress, although a previous report indicates that hnRNP C1 is sensitive to cellular viability, and will localize to the cytoplasm if the nuclear envelope is compromised. I find that hnRNP C1 remains nuclear-restricted after 0.5 hours of stress, but is diffusely localized to the cytoplasm after 4 hours of stress. Thus, even if hnRNP C1 encounters a stress that increases its cytoplasmic levels due to lowered cellular viability, it fails to localize to cytoplasmic granules.

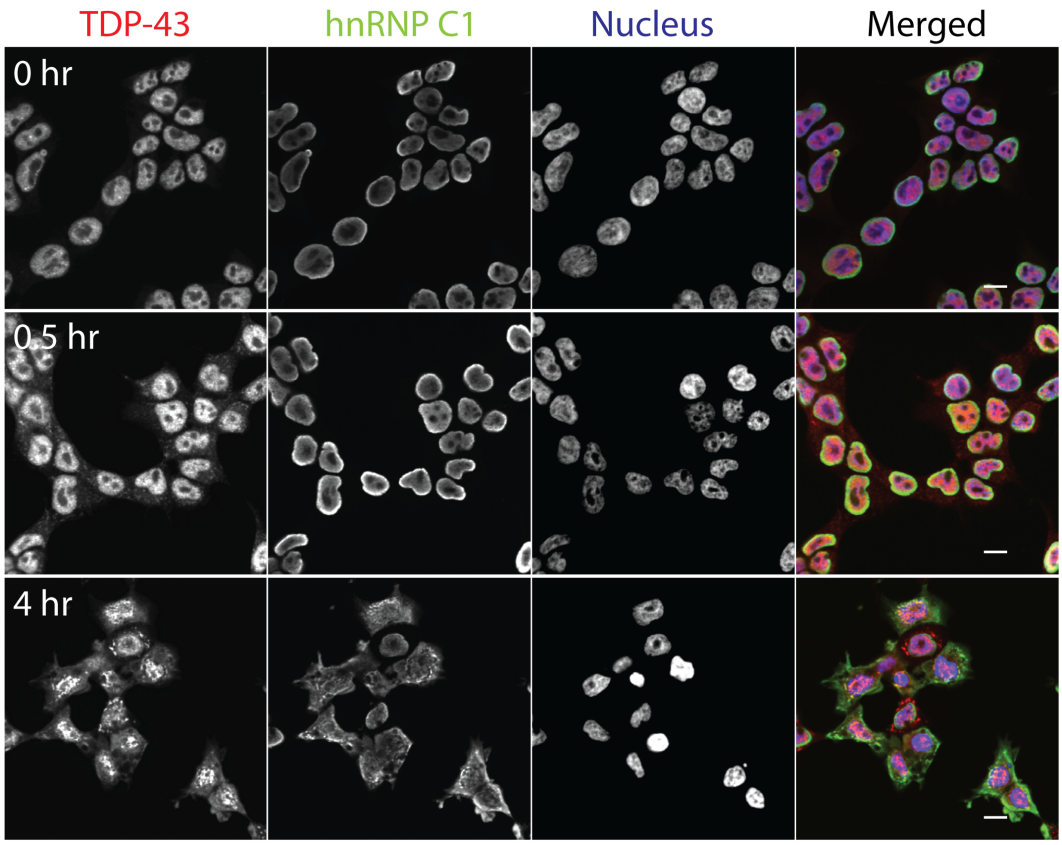

Figure 3.10, TDP-43 and hnRNP C1 do not colocalize to cytoplasmic granules in response to 0.5 and 4 hours of 0.4 M sorbitol stress. TDP-43 is stained in red, hnRNP C1 in green and the DNA dye ToPro-3 stains the nucleus in blue. The nuclear-resident protein hnRNP C1 remains nuclear after 0.5 hours of stress, but is diffusely localized to the cytoplasm after 4 hours of stress. Scale bars = 10 µm.

Finally, I wanted to test whether TDP-43^{+} granules localized to processing bodies (Hedls) when exposed to a recoverable stress (0.5 hrs) versus an irrecoverable stress (4 hrs, 0.4 M sorbitol) in Hek293T cells (Figure 3.11).

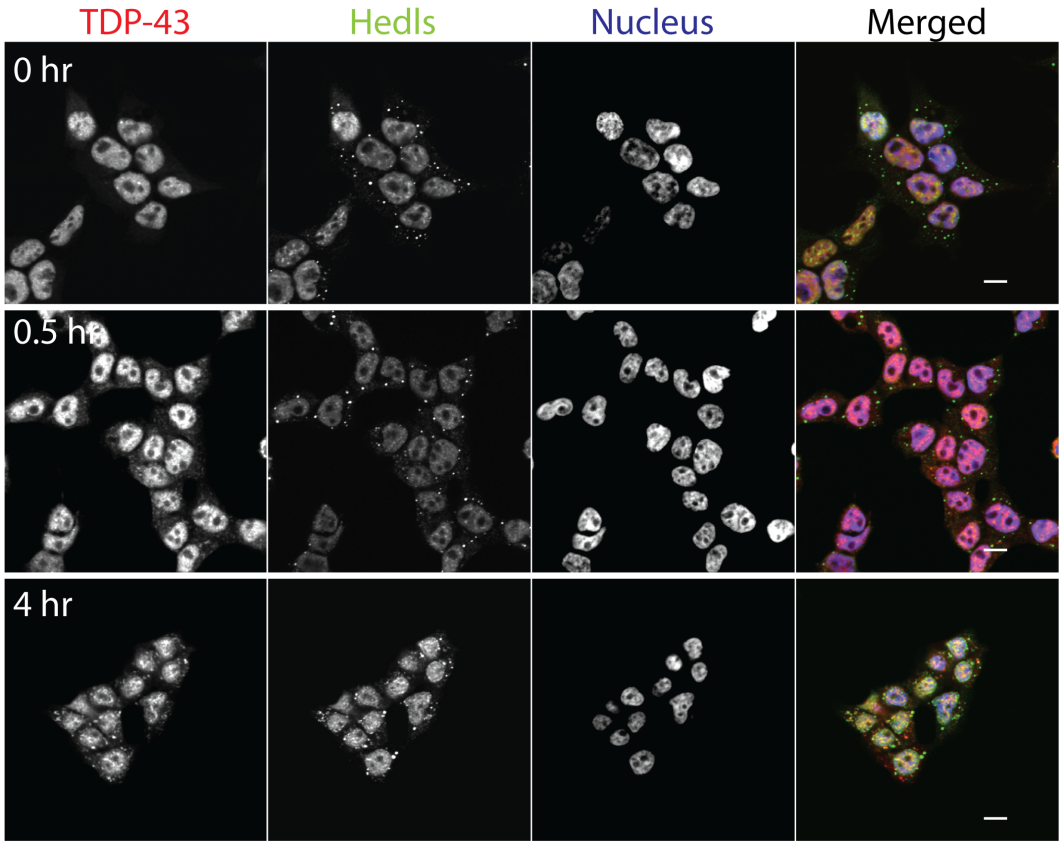

Figure 3.11, TDP-43 and Hedls do not colocalize to cytoplasmic granules in response to 0.5 hours of sorbitol stress. However, at 4 hours of stress, some TDP-43^{+} granules colocalize with processing bodies. The Hedls antibody also labels nuclear p70 S6 kinase, and TDP-43 and p70 S6 kinase colocalize in the nucleus. TDP-43 is stained in red, Hedls in green and the DNA dye ToPro-3 stains the nucleus in blue. Scale bars = 10 μm.

Previous studies have indicated that TDP-43 fails to colocalize with processing bodies during stress(35, 88). However, these studies examined a single timepoint instead of examining a timecourse. This approach is problematic, as SGs are dynamic and not static structures. We observed no colocalization of TDP-43 with Hedls (processing body marker) in response to 0.5

hours of stress. However, a few TDP-43^{+} granules appear to colocalize with Hedls after 4 hours of stress. Our results makes sense in the context of previous reports where mRNAs that are targeted for degradation are delivered to processing bodies, which seem to localize next to the stress granule to mediate this exchange(21). We conclude that TDP-43 colocalization with Hedls is dependent on the stress timepoint.

In conclusion, SMN and hnRNP A1 are not sensors of cellular viability, as these proteins persist in cytoplasmic granules spanning both recoverable and irrecoverable sorbitol stress timepoints. This doesn't match with the data observed in FTLD-U pathological tissues, however this discrepancy may be due to the cell type (Hek293T cells versus neurons or glia). Also, TDP-43 fails to colocalize to processing bodies, although this observation is consistent with the literature. Thus, it appears that both hnRNP A1 and SMN are not sensors of cellular viability in Hek293T cells; the explanation behind the absence of these proteins in pathological tissues are not understood at this time. Future studies will need to investigate how SG composition, perhaps only TDP-43, can lower cellular viability leading to neurodegeneration.

TDP-43 localization to stress granules is RNA-dependent

There are multiple ways a protein can be directed to a stress granule. First, the protein can bind to an mRNA and be directed to the stress granule during the stress response. Second, the protein can bind to another hnRNP protein bound to

an mRNA. Third, the protein can "piggyback" onto a SG if it is localized in the cytoplasm(15, 17, 21, 71).

In the case of TDP-43, TDP-43 must bind RNA to localize to stress granules(35). We show this below in Figure 3.12 b and d. We observe that mutations in TDP-43 that disrupt RNA binding (RRM1 mutations in FI47L/F149L) are sufficient to prevent cytoplasmic stress granule assembly (F147L/F149L construct was generated by Chantelle Sephton).

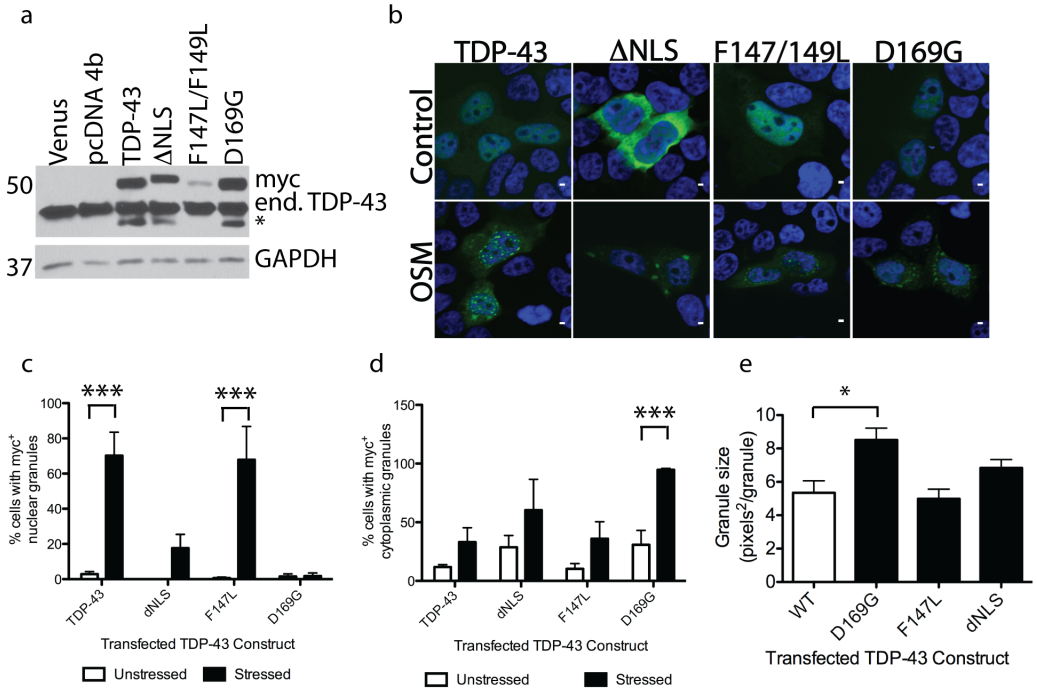

Figure 3.12, RNA-binding specificity is required for TDP-43 localization to stress granules. a. Expression of constructs in Hek293T cells by western blot. b. Immunofluorescence data of constructs before and after 1 hour of sorbitol stress. c. Two phenylalanine mutations (F147/149L) mutations ablate RNA specificity; mutation of these residues results in the inability of TDP-43 to form cytoplasmic granules. Interestingly, both the F147/149L mutant and wild-type TDP-43 localize to nuclear granules in response to stress. d and e. In contrast, the pathological mutant D169G localizes to large stress granules relative to wild-type TDP-43, although this mutation is not located in the GRR.

Interestingly, while the RNA-binding mutant is unable to generate cytoplasmic granules, nuclear granules were generated in response to 1 hour of sorbitol stress. We also observed nuclear granules in cells overexpressing wild-type TDP-43 (Figure 3.12 b and c), although some cells overexpressing this construct were able to generate cytoplasmic granules. In contrast, cells expressing the D169G variant of TDP-43 consistently formed cytoplasmic granules that were larger than the average granule size generated by wild-type TDP-43 in response to 1 hour of sorbitol stress (Figure 3.12 d and e). The presence of both nuclear and cytoplasmic granules in TDP-43 overexpressing cells is a fascinating observation, because as previously discussed, TDP-43 pathology is heterogeneous, and is found localized to both nuclear and cytoplasmic aggregates. How these findings relate to the cytoplasmic toxic GOF hypothesis are unknown, as further study is necessary, however it is tempting to speculate that aging (or senescence in a cellular model) may contribute to the rise of these nuclear granules, as their presence rose with higher passage numbers (my own personal, unquantified observations).

TDP-43's glycine rich region is critical for regulating both stress granule association and size

We next used our novel assay to investigate the structural regions that mediate TDP-43 association with cytoplasmic granules. To this end, I generated the following truncated constructs: 1-324 (removal of the distal glycine-rich region (GRR)), 1-267 (removal of the entire GRR), 1-179 (removal of the GRR

and RRM2) and 1-114 (removal of the GRR, RRM2 and RRM1) (Figure 3.13a). Transient transfection of these constructs did not show cytoplasmic granules in unstressed cells, and all constructs localized normally to the nucleus (Figure 3.13b).

Interestingly, wild-type TDP-43 (1-414) modestly clustered following 1 hr of stress, while the 1-324 construct robustly clustered at this time point; in contrast, shorter constructs failed to cluster (Figure 3.13b). Although wild-type TDP-43 failed to produce robust cytoplasmic clusters in response to 1 hr of stress, nuclear clusters were detected; interestingly, 1-324 also showed these nuclear clusters (Figure 3.13b). Importantly, even after 2 hours of stress, the truncated constructs were unable to form cytoplasmic granules, while cells expressing the 1-324 and 1-414 constructs did form cytoplasmic granules. Taken together, the above data indicates that the region mediating the association of TDP-43 with stress granules lies within residues 268-324.

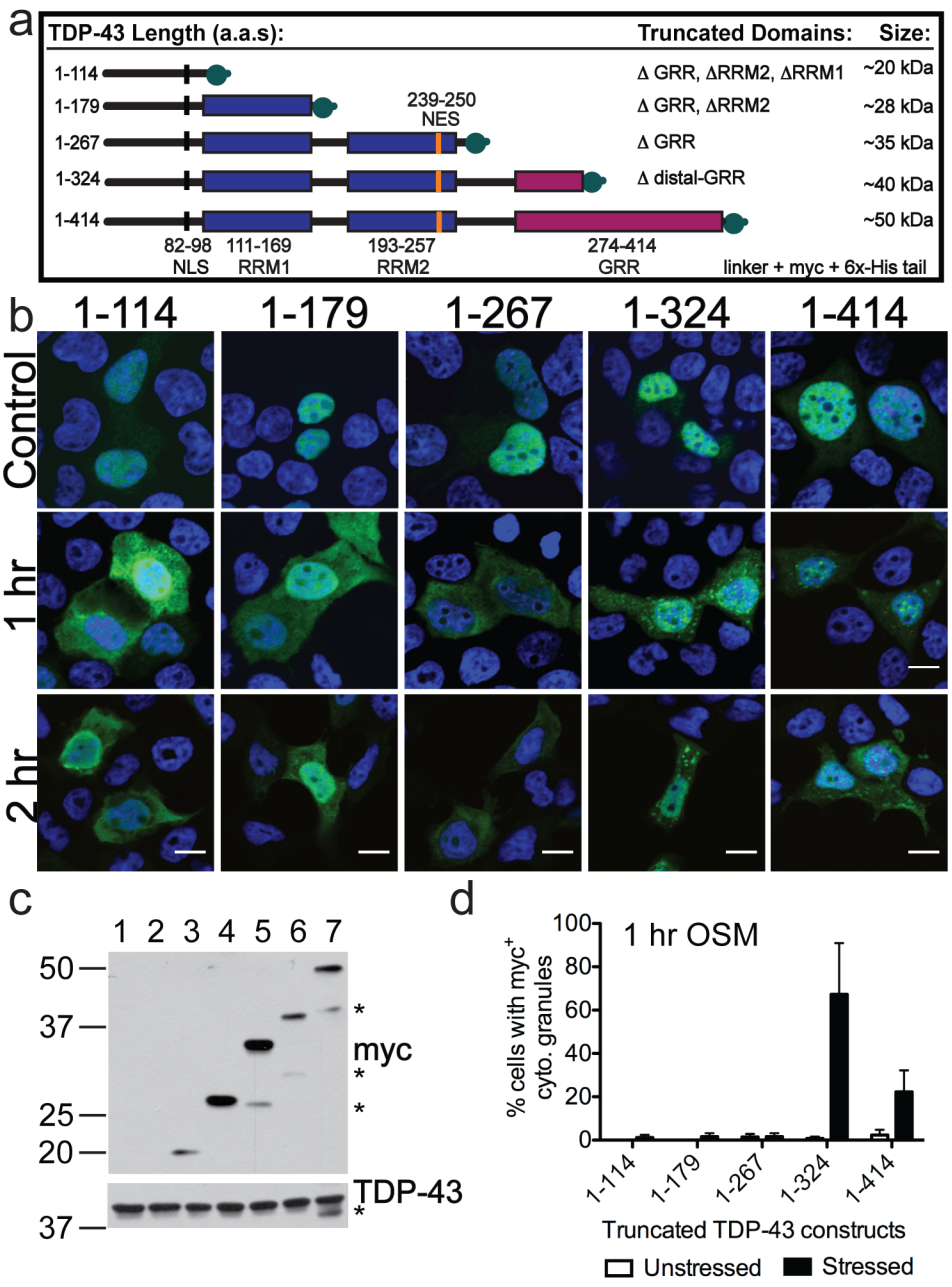

Figure 3.13, TDP-43 cytoplasmic clustering is mediated by residues 268-324. a. Schematic of truncated TDP-43 constructs with successive deletions in organized structural regions, including the distal C-terminus (1-324), the glycine-rich region (GRR) (1-267), the RRM2 (1-179) and the RRM1 (1-114). b. Nuclear localization of the transiently-transfected constructs from panel (a), and increased cytoplasmic localization following 1 and 2 hrs of sorbitol stress. c. Expression of constructs from panel (a) in Hek293T cells. Asterisks (*) indicate alternative C-terminal TDP-43 species detected by myc antibody. Lane 1, pcDNA4b-Venus; 2, empty vector; 3, 1-114; 4, 1-179; 5, 1-267; 6, 1-324; 7, 1-414. d. Quantification of cytoplasmic clustering of the truncation constructs following 1 hr of stress. Scale bars = 10 μm.

We should also note that although beyond the scope of this investigation, we noticed additional myc^{+} bands generated from constructs 1-267, 1-324 and 1-414 (*asterisks*; Figure 3.12c). Coincidentally, the size of these fragments are in agreement with proposed cleavage site/alternative TDP-43 isoforms starting at M(85)TED (103, 140) but could also indicate a novel protease that targets TDP-43. The role of these TDP-43 truncations in the sorbitol-induced stress response has been reserved for future study.

Hypothesis

Approximately ten pathological mutations lie within residues 268-324, yet nearly twenty pathological mutations lie outside of this region. In previous studies the overexpression of several pathological mutations *in vitro* resulted in no gross localization defects (A315T, G348C, A382T) (66), no effect on splicing (Q331K, M337V and G348C) (37) and no effect on protein:protein interactions (A315T, M337V) (49). Because the GRR was necessary for TDP-43 localization to cytoplasmic granules in our truncated study, and the majority of pathological mutations lie in the GRR, we hypothesized that wild-type and pathologically mutated TDP-43 have distinct stress responses, culminating in the generation of distinct stress granules in response to sorbitol stress.

Testing our hypothesis: do pathological mutations generate distinct cytoplasmic granules in response to stress relative to wild-type?

To examine the effect of sorbitol stress on pathological TDP-43, we selected the familial ALS (fALS) mutation A315T (55, 67), the sporadic (sALS) mutation G294A, and the fALS and sALS mutation G348C (39, 41, 67, 81) because they have no overt phenotype in unstressed cells (37, 49, 66). We also overexpressed the sporadic ALS mutation N390S, in addition to wild-type TDP-43, truncated (1-324) TDP-43 and vector control (Figure 3.14b). All these constructs predominantly localize to the nucleus in unstressed Hek293T cells (Figure 3.14a), consistent with previous results (66). However, following one hr of stress, robust cytoplasmic granules were formed by each pathological mutation, while wild type failed to generate this robust phenotype.

Quantification of these myc^{+} granules revealed that pathological TDP-43 mutations also formed significantly larger cytoplasmic granules relative to wild-type TDP-43 (Figure 3.14c), an observation consistent with the 1-324 truncated TDP-43 construct shown in Figure 3.14a and c.

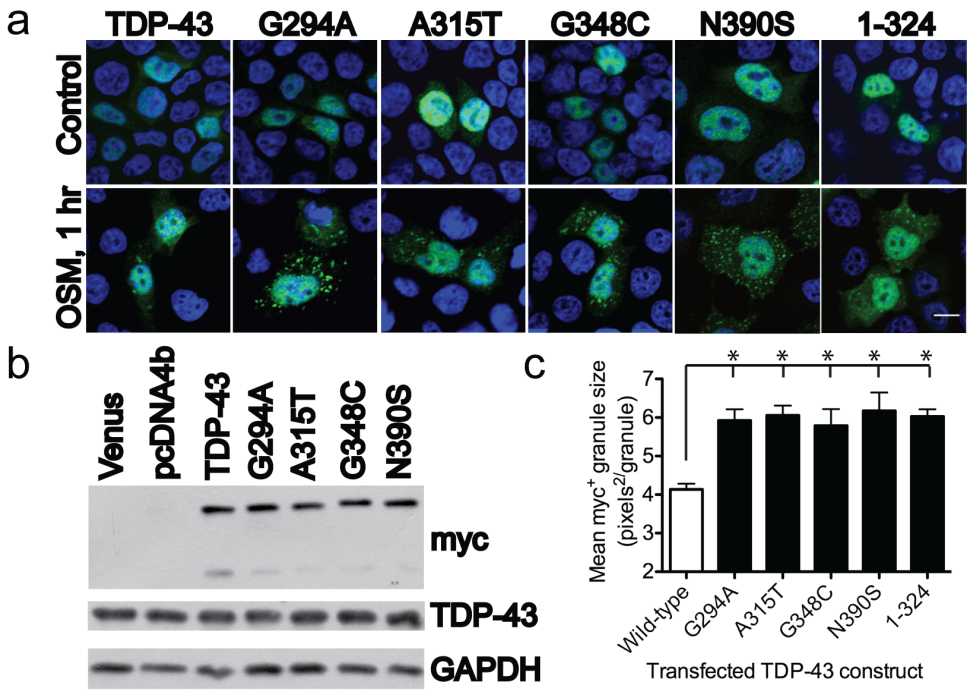

Figure 3.14, Alteration of the distal C-terminus generates larger cytoplasmic granules than does wild-type TDP-43 in response to stress. a. Localization of transiently expressed pathological TDP-43 mutants and TDP-43 lacking the distal C-terminus in Hek293T cells. Exogenous TDP-43 was stained with myc antibody; nuclei, with ToPro-3. Scale bar = 10 µm. b. Expression of constructs from panel (a). c. Quantification of cytoplasmic myc$^+$ granule size (pixels^2/granule) following 1 hr sorbitol stress. Shown is the mean granule size ± SEM for wild-type (white) and mutant (black) TDP-43 (*, $p < 0.05$).

Importantly, a non-pathological mutation outside the C-terminus (S242A) did not produce larger granules (Figure 3.15), confirming the specificity of this observation with pathological mutations in the C-terminus.

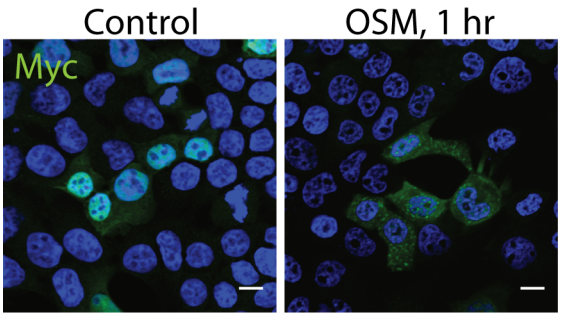

Figure 3.15, A non-pathological TDP-43 mutation (S242A) does not generate larger stress granules in response to sorbitol stress. The non-pathological TDP-43 mutation S242A localizes to the nucleus after transfection. After one

hour of sorbitol stress, S242A failed to localize to larger stress granules, although the construct localizes to cytoplasmic granules at this timepoint. Scale bar: 10 μm.

Taken together, our data show that pathological TDP-43 mutants localize more readily to larger cytoplasmic clusters than does wild type. We have determined that within one hour of stress administration, pathological and wild-type TDP-43 exhibit distinct stress responses. The most distinct change is the number and size of the TDP-43+ granules generated by the pathological mutants relative to the wild-type.

Mutant TDP-43 localizes to stress granules during stress

To further characterize the difference between wild-type- and mutant TDP-43-containing SGs, I established stable cell lines overexpressing either wild-type or mutant G348C TDP-43, using myc and C-terminal specific (748C) antibodies to assess the level of overexpression relative to endogenous protein, respectively (Figure 3.16a).

We selected the G348C mutation for further study because it is linked with both sALS and fALS, familial mutations are found in multiple families with distinct ancestry (39, 41, 67, 81) and because this mutation lies within a specific sub-region (residues 321-366) of the GRR that mediates interactions with hnRNP A2 (37). Interestingly, we observed a 1.5 fold difference in doubling frequency favoring the growth of wild-type stable overexpressing cell lines to mutant (mean ± SEM: 1.54 ± 0.05 (WT) vs. 1.27 ± 0.09 (G348C); $p<0.05$, *).

We next determined whether mutant TDP-43 localizes to SGs by treating cells with cycloheximide, a protein synthesis inhibitor that prevents SG assembly. We treated stable cell lines with cycloheximide (CHX, 40 μg mL^{-1}) or vehicle control (DMSO) followed by 1 hr of osmotic stress to examine whether granule size was affected by the treatments (Figures 3.16b and c). After 1 hr of stress, exogenous mutant TDP-43 was robustly directed to stress granules, whereas overexpressed wild-type TDP-43 was not. In stable wild-type TDP-43 overexpressing cell lines, stress granule size was consistent with that observed with transient overexpression, roughly 4 $pixels^2$/granule (Figure 3.16c). Cells expressing mutant TDP-43, however, had larger granules that shrunk upon treatment with CHX (**, $p<0.01$; Figure 6c). Additionally, we verified the colocalization of exogenous TDP-43 granules with stress granule markers hnRNP A1 (Figure 3.16d), HuR (Figure 3.16e) and TIAR (Figure 3.16f). Thus, mutant TDP-43 localizes to larger stress granules relative to wild-type TDP-43.

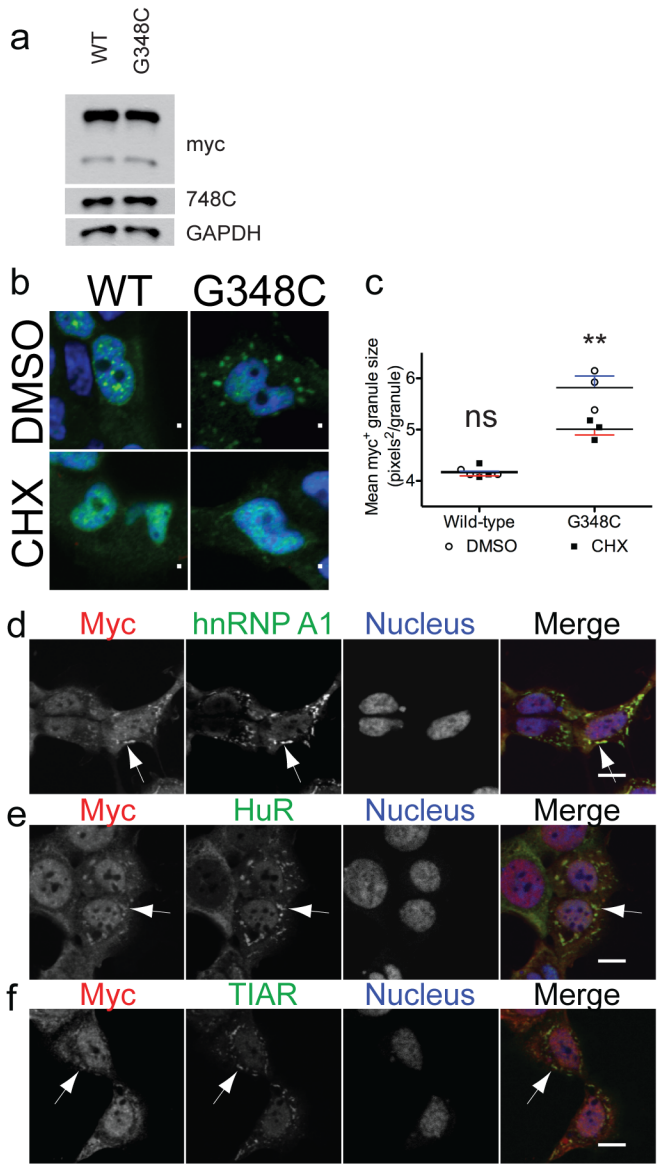

Figure 3.16, Pathological TDP-43 mutant G348C localizes to larger stress granules during osmotic stress. a. Expression level of myc-tagged wild-type and mutant (G348C) TDP-43 in stable cell lines. b. Localization of wild-type and mutant TDP-43 granule size in stressed cells (1 hr sorbitol) treated with (CHX) or without (DMSO) cycloheximide. c. Scatter plot of the mean granule size in cells as in panel (b). Horizontal bars depict the mean ± SEM (, $p < 0.01$). Each data point represents the individual mean of a single experiment; shown are three experiments per group. d-f. Co-localization of mutant (G348C) TDP-43 with hnRNP A1 (d), HuR (e) and TIAR (f) following 1 hr of stress. Exogenous mutant TDP-43 was detected using the myc antibody. Scale bars = 10 µm.**

Mutant TDP-43 localizes to progressively larger stress granules during stress

Next, stable cell lines overexpressing wild-type and mutant (G348C) TDP-43 were subjected to a time course of stress (0.4 M sorbitol for 0.5, 1, 2 and 4 hrs). In unstressed cells, both wild-type and mutant TDP-43 were primarily localized to the nucleus (Figure 3.17a). In both unstressed stable cell lines and in mixed primary glia cultures, we also detected similar background levels of other cytoplasmic granules that resemble the closely related P-bodies (Figure 3.17a). Quantification of the number of cells that generated myc^{+} granules in response to the stress showed that mutant and wild-type TDP-43 localization was not statistically different before stress (Figure 3.17b). However, following 0.5 and 1 hr of sorbitol stress, clustering of TDP-43 was found in more cells overexpressing mutant TDP-43 than wild type; moreover, this marked difference disappeared at 2 hrs of treatment (Figure 3.17b). Furthermore, while cells expressing wild-type TDP-43 gradually formed more clusters throughout all 4 hrs of stress, those expressing mutant TDP-43 showed a rapid accumulation of TDP-43 clusters at 0.5 hrs followed by a slow decline (Figure 3.17c). Importantly, overexpression of mutant TDP-43 resulted in larger sorbitol-induced clusters than wild type, this being the most striking difference between sorbitol-induced wild-type and mutant TDP-43 cytoplasmic clusters at all time points (Figure 3.17d).

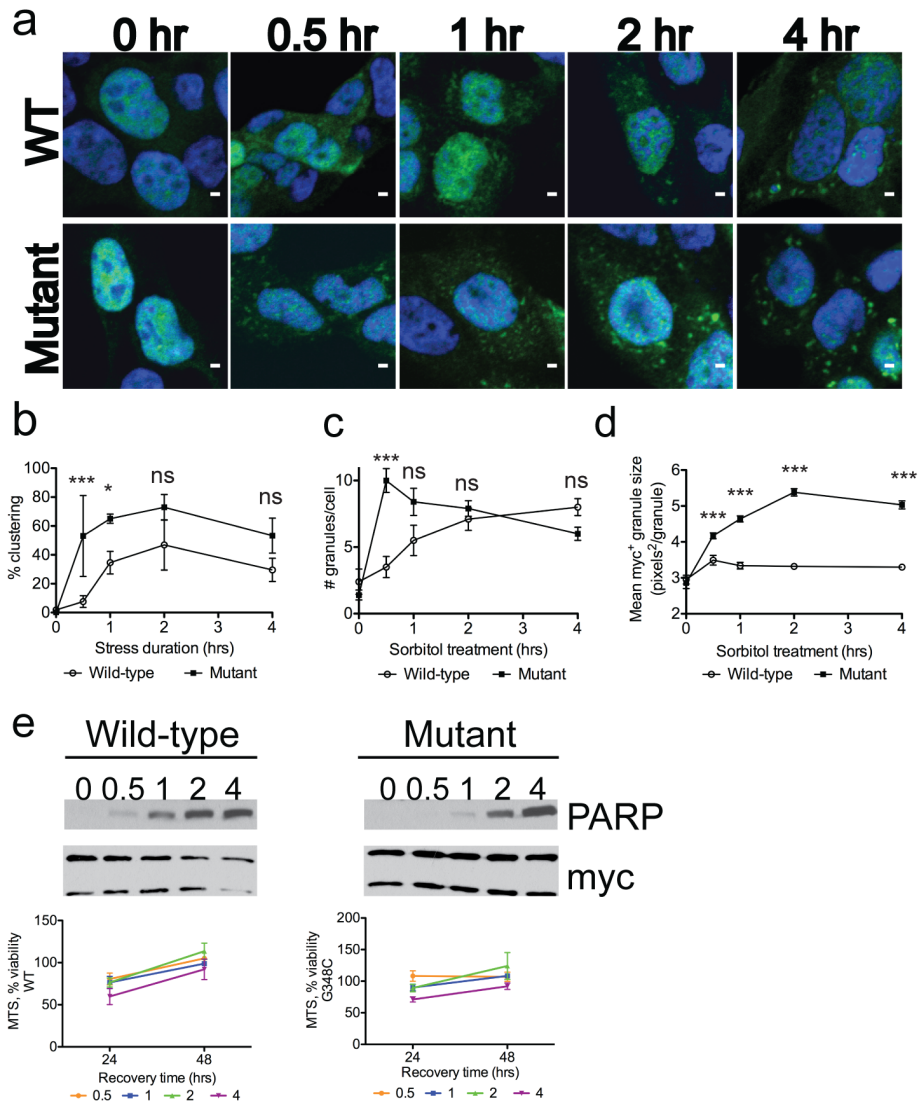

Figure 3.17, Wild-type TDP-43 and pathological TDP-43 (G348C) form unique stress granules. a. Localization of exogenous (anti-myc) wild-type and mutant (G348C) TDP-43 in stably-transfected Hek293T cells at the indicated times following sorbitol stress. b-d. Quantification of the percent, number, and size of clusters in stable cell lines as in panel (a). Each experiment was performed in triplicate; data is presented as mean ± SEM (*, $p < 0.05$; ***, $p < 0.001$). Scale bars = 2.5 mM. e. (Upper panel) PARP cleavage throughout 4 hrs of sorbitol stress. (Lower panel) Recovery of stably-transfected Hek293T cells expressing wild-type or mutant (G348C) TDP-43. Recovery was measured as in Figure 3e.

Enlarged stress granules produced by pathological TDP-43 is not toxic to the cell at the timepoints examined

Finally, mutant TDP-43 did not prematurely induce apoptosis, as judged by PARP cleavage (Figure 3.17e, *top*); moreover, overexpression of both wild-type and mutant TDP-43 equally allowed for the recovery of cells following up to 4 hrs of sorbitol stress (Figure 3.16e, *bottom*). This finding alone is very interesting, as it shows that the enlarged stress granule size is not sufficient to induce apoptotic pathways, rather these stress granules appear to function normally, ie preventing the activation of cell death pathways.

In future studies, it will be necessary to determine if/when these enlarged stress granules are ubiquitinated, and if this post-translational modification prevents the disassembly of the stress granules, or alters cellular signaling pathways leading to an induction of cell death pathways, instead of prevention of these pathways. Also, it will be necessary to address whether the toxicity of stress granules is dependent on their composition, not just size, and whether the convergence of multiple stressors (which would direct more cytoplasmic TDP-43 into a SG) may be a determinant in generating these larger granules leading to increased toxicity and cell death.

DISCUSSION

Although quickly expanding, our understanding of transient stress granule structures and their role in disease progression is at a primitive stage. Currently,

stress granules are known to contribute to the pathogenesis of several disorders, including fragile-X syndrome, spinal muscular atrophy and ischemia-reperfusion injury (6, 38, 40); like TDP-43 and FUS/TLS proteinopathies, these disorders are caused by altered RNA-binding proteins (5, 6, 36, 38, 40, 92, 135). In this study, we show that sorbitol is a novel stressor mediating TDP-43 and hnRNP A1 localization to $TIAR^+$ and HuR^+ stress granules; this was observed in both somatic (Hek293T cells) and nervous system cell types (primary cultured glia). Since colocalization of hnRNP A1 with TDP-43^+ granules was conserved between somatic cell lines and primary cultured glia (Figures 3.3-3.5), this indicates that the readily accessible and common Hek293T cell line can be used to model the stress response initiated in cortex-derived glia. We used this information to develop a cell culture model to quantitatively test the stress response mounted by wild-type and pathological TDP-43 mutants G294A, A315T, G348C and N390S, in conjunction with several truncated TDP-43 mutants.

Our analysis indicates that a 57-residue region (residues 268-324) spanning the first one-third of the glycine-rich region (GRR) is necessary for TDP-43's association with stress granules (Figure 3.13). Moreover, removal of the distal 90-residues of GRR (residues 325-414) renders TDP-43 to behave like a pathological mutant in terms of its ability to increase stress granule size and facilitate assembly. These observations are consistent with the model that the GRR harbors intrinsic determinants of stress granule formation: residues 268-324 are necessary for the association of TDP-43 with stress granules, while residues 325-414 are

necessary, but not sufficient, for regulating the association in a proper state. In this model, the pathological missense mutations -- both inside and outside the distal GRR -- negate this regulatory capability, perhaps by changing TDP-43's structure in a manner similar to distal truncation of TDP-43. Alternatively, mutations in TDP-43 may alter the interaction of the GRR domain with structural components of the stress granules to regulate their size.

Our work reinforces the notion that the GRR plays a crucial regulatory role for proper TDP-43 function. The GRR has been implicated in the regulation of splicing through hnRNP protein:protein interactions (80) and association with stress granules (35). This domain also harbors the vast majority of known pathological mutations in TDP-43 (and similarly in the pathologically related protein FUS/TLS) (85). The osmotic-stress-responsive sequence (residues 268-324, Figure 4) identified in our study overlaps with the oxidative-stress-responsive sequence (residues 216-315) previously identified by Colombrita et. al. (35). We note however that the osmotic stress responsive sequence identified here is only half the size of the oxidative stress responsive sequence. It is conceivable that the overlapping GRR region (residues 268-315) of these two stress responsive sequences in TDP-43 represents a conserved stress response sequence that mediates its association with stress granules in different cell types (both somatic and nervous system-specific) and with different stressors (oxidative and osmotic stressors). This region (residues 268-315) is particularly glycine-rich (Figure 3.18a) with multiple, putative GXXXG motifs; these motifs are believed to mediate hydrophobic helical protein:protein interactions and have also been

found in other proteins involved in neurodegenerative disorders (16, 59). Future studies will define the stress-responsive sequence motif in the GRR domain of TDP-43, which may include these GXXXG motifs, and test whether such a motif is conserved in other GRR containing proteins, in different cells, and for different stressors.

Since all missense mutations tested in our study mount similar stress responses, we analyzed one of these mutations (G348C) in more detail under progressively longer stress treatments. We found that a higher percentage of G348C-expressing cells directed the mutant protein into stress granules, that the number of granules formed peaked after short stress exposure, and that stress granule size progressively increased at the expense of granule number. Yet wild-type TDP-43-expressing cells coped with stress in the converse manner: instead of progressively forming larger granules over time, the wild-type protein progressively formed a greater number of smaller granules of relatively unchanged size (Figure 3.18b). Our results indicate that the pathological mutant handles stress in a markedly different way than the wild-type; these differences will be explored in future studies to understand how pathological TDP-43 mutants contribute to neurodegeneration and cell death.

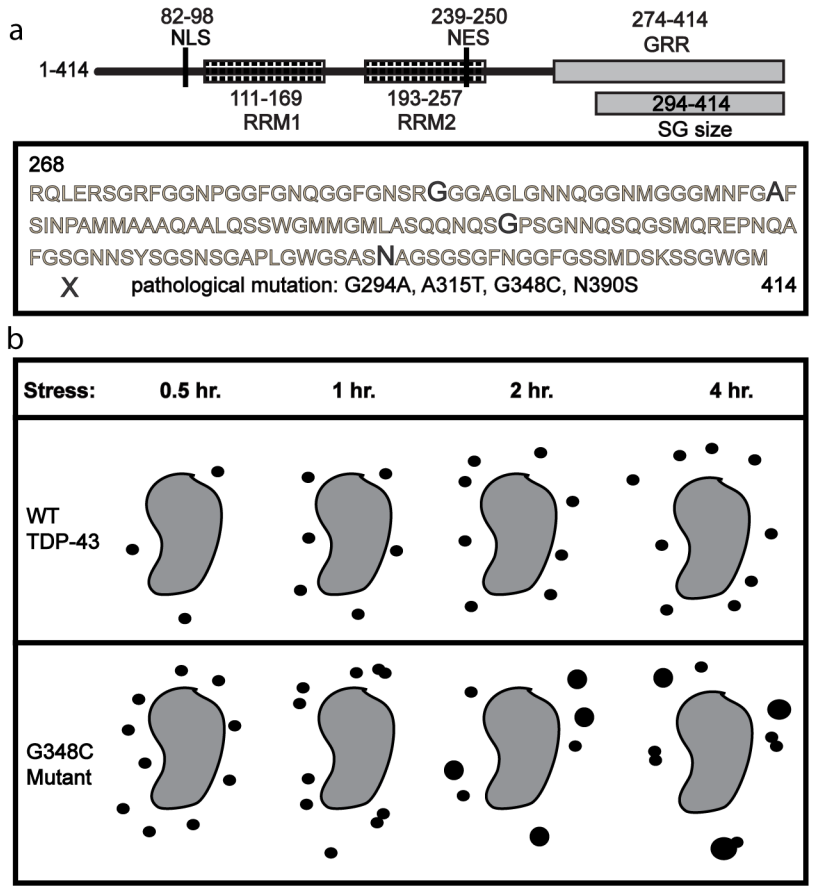

Figure 3.18, Model summarizing distinct stress granule species formed by wild-type and mutant (G348C) TDP-43. a. The GRR region harbors putative structural determinants for the association of TDP-43 with stress granules (box) and for control of stress granule (SG) size. b. Summary of the distinct stress-induced clusters of wild-type and mutant (G348C) TDP-43.

It has been suggested that formation of stress granules delays apoptosis by sequestering pro-apoptotic factors (such as RACK1 and ROCK1) (10, 46, 129). Our observation that cells recover after an initial stress response is compatible with this model. However, it is also expected that prolonged stress (beyond the cell's capability to handle such stress) would trigger cell death. Indeed, TDP-43, like PARP, is a target of caspase-3; multiple sites in TDP-43 are reportedly targeted by caspase-3 ($DEND_{10-13}$, $DETD_{85-88}$ and $DVMD_{216-219}$), producing 25 and 35 kDa species (43, 111, 112, 139).

In our study, we observed that prolonged sorbitol treatment reduces cell viability, which coincides with the formation of TDP-43^{+} stress granules in native Hek293T cells (Figure 3). In spite of drastically enlarged stress granule size in cells overexpressing pathological mutants (as compared to wild-type protein), we did not observe a premature induction of apoptosis in these cells (as indicated by PARP cleavage, data not shown). We interpret this observation as stress granule size not being a primary determinant of initiation of apoptosis and that mutants may actually delay the onset of cell death before the host cells commit suicide.

In interpreting our data, we consider that the effect and time course on stress granule formation in cells overexpressing a pathological mutant should best be compared to cells overexpressing a wild-type protein. This is particularly relevant when considering that overexpressing wild-type TDP-43 protein (or several other proteins implicated in neurodegenerative disorders) *in vivo* also promotes TDP-43 pathology and neuronal death over time. In this context, while the general effects are similar, there are subtle differences between the stress responses of overexpressed wild-type protein and that of endogenous TDP-43. Another related consideration is that TDP-43 protein levels are likely to be stringently regulated, such that overexpression of TDP-43 alone could cause cell death in some cell types (11). However, at our level of overexpression, we did not observe cell death in unstressed wild-type and mutant TDP-43 stable cell lines (Figure 7e).

Both neurons and glia display TDP-43^{+} cytoplasmic aggregates in ALS and FTLD-U spectrum neurodegenerative disorders, as well as in a subset of

Alzheimer's and Parkinson's disease (31, 48, 54, 84-86, 101). Degeneration and the eventual death of neurons in these diseases likely reflect a combined outcome of impaired neurons and their supporting glial cells. It is plausible that the neuronal and glial cytoplasmic aggregates in ALS or FTLD-U are end products of stress granules or derivatives of these structures generated after an unsuccessful response to stress. TDP-43 has previously been shown to localize to TIA-1^{+} stress granules in axotomized C57BL/6 mouse motor neurons (97). While previous studies failed to detect colocalization of TDP-43 with known stress granule markers in patient brain (99) and spinal cord (35), a more recent study indicates that TDP-43 pathology in ALS and FTLD-U human tissue colocalizes with SG markers eIF3 and TIA-1(88). Further investigation is needed to analyze the relationship of stress granule formation and TDP-43 proteinopathies in cellular and animal models and in human patients in order to understand the molecular and cellular mechanism by which TDP-43 and RNA-binding proteins respond to stress in health and disease.

CHAPTER FOUR
Discussion and Future Directions

Limitations of our model

400 mM sorbitol fails to direct TDP-43 to SGs in primary cultured neurons

As previously discussed, three hypotheses have been proposed to test TDP-43 mediated neurodegeneration: a nuclear LOF, a cytoplasmic toxic GOF and both a nuclear LOF and cytoplasmic GOF. In our study, we sought to test the cytoplasmic toxic gain of function hypothesis. To test this hypothesis, I developed a cell culture model where a physiological stressor (sorbitol) directs TDP-43 to SGs in Hek293T cells. I furthermore established that hyperosmotic stress directs TDP-43 to stress granules in multiple cell types, including additional immortalized cell lines (U343, HeLa) and primary cultured glia. Yet, my stressor failed to induce stress granules in primary cultured cortical neurons. Thus, a limitation of my cell culture model is that my stressor fails to induce TDP-43^{+} cytoplasmic aggregates in neurons.

The first argument as to why TDP-43 is not directed to SGs by 0.4 M sorbitol is that this sorbitol concentration is sub-optimal in neurons. I screened live neurons exposed to 0.4 M sorbitol and compared the morphology of unstressed to stressed neurons by phase contrast microscopy at different timepoints. After observing cellular morphology for 4.5 hours, I fixed the cells and used immunofluorescence to detect TDP-43 localization (in green, a). Neurons appeared pyknotic by this timepoint, as evidenced by TDP-43 nuclear staining in a. Also, neuronal somas clustered together in phase contrast microscopy images, a phenomenon often observed in unhealthy and/or dying

neuronal cultures. I failed to observe TDP-43^{+} cytoplasmic aggregates in dying neurons.

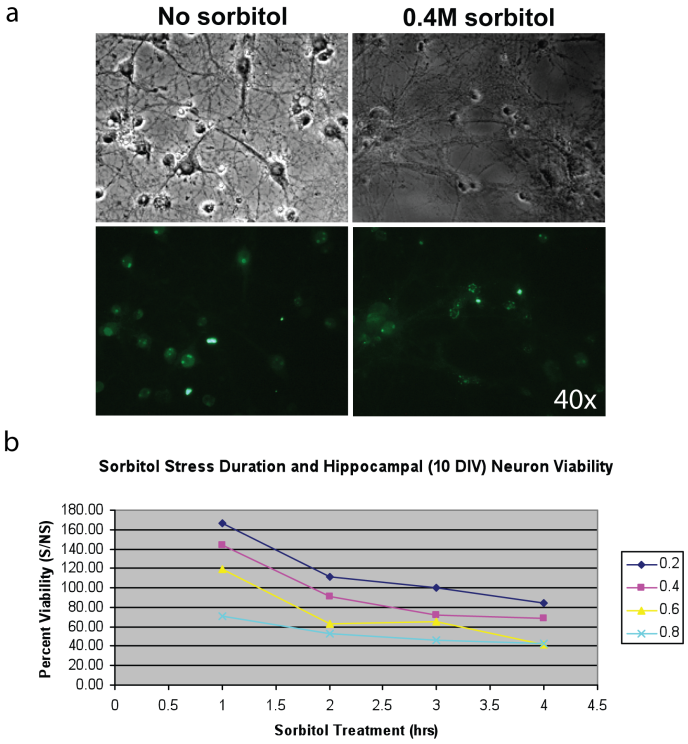

Figure 4.1, Neurons are viable after a one hour treatment with 0.2–0.6 M sorbitol. a. Neurons treated for up to 4.5 hours with 0.4 M sorbitol were imaged using phase contrast microscopy with a 40x objective. Untreated cells appear morphologically normal, while sorbitol-stressed neurons appear sickly at this timepoint. Immunofluorescent staining of TDP-43 (green) is shown under the phase contrast images. Nuclei appear pyknotic following stress treatment. b. MTS assay is used to analyze cell viability following treatment of neurons with 0.2, 0.4, 0.6 and 0.8 M sorbitol for 1-4 hours.

Neurons are sensitive cells, therefore induction of stress granules may occur at lower sorbitol concentrations, or at higher concentrations at shorter stress timepoints. I tested cellular viability by MTS assay (where %viability=(stressed neuronal viability/unstressed control) x 100) across a range of sorbitol concentrations (0.2-0.8 M, shown in blue, pink, yellow and blue, respectively) plotted against the timecourse of sorbitol stress (1-4 hours), as shown in Figure

4.1b. From this preliminary data, it seems that sorbitol concentrations spanning 0.2-0.6 M are viable after exposure to one hour of stress. Thus, my original timepoint (1 hr, 0.4 M sorbitol) should be viable. However, neuronal viability drops off dramatically after this timepoint. Although the percentage viability does not appear very low for some concentrations by 4 hours, the immunofluorescent data indicates that these timepoints are actually quite toxic. As such, in future experiments, I will test the effect of lower sorbitol concentrations (400, 200, 100 and 50 mM sorbitol) on cortical neuron viability. Additionally, future experiments will need to test whether any viable, lower concentrations are sufficient to induce stress granules in neurons.

Another argument is that 0.4 M sorbitol is the appropriate concentration to direct TDP-43 granules in cortical neurons, but this response requires glia. As such, a co-culture of neurons and glial cells would allow testing of this hypothesis. Finally, sorbitol may not induce stress granules at all in neurons because it fails to activate the appropriate kinases to induce the formation of stress granules in this cell type.

Stress granules are regarded as pro-survival structures – if true, how do they mediate a cytoplasmic toxic gain of function?

Another limitation of my cell culture model is that stress granules are regarded as pro-survival structures, yet my model is designed to test the cytoplasmic toxic GOF disease hypothesis. While it is true that stress granules are pro-survival structures, this finding may depend on the duration of stress. For

example, when cells are viable after a stress, stress granules disintegrate within a short time period (typically 15 minutes). Yet, in pathological tissues, ubiquitinated TDP-43^{+} granules are co-labeled by stress granule marker proteins. I have been unable to identify whether stress granules generated by sorbitol exposure are ubiquitinated at any point during the stress response. Another paper indicates that stress granules formed in the hippocampus in response to a 10 min global ischemic insult are ubiquitinated after a few days of reperfusion(40).

Treatment of cells overexpressing wild-type or mutant TDP-43 with sorbitol fail to decrease cellular viability

We detected no evidence that overexpression of either wild-type or mutant TDP-43 increased the susceptibility of transfected cells to sorbitol stress. In fact, an examination of PARP cleavage seemed to show that both wild-type and mutant TDP-43 overexpression increased viability in response to sorbitol stress, rather than reducing viability. However, recovery experiments indicate that despite this observation, no significant difference in viability exists between the wild-type and mutant stables following stress. These results can be interpreted in multiple ways, the first interpretation is that the stress granules in our assay are functioning as "normal" stress granules, hence pro-survival structures. This finding may be interpreted as a major flaw, as our hypothesis argues that stress granules are at the root of TDP-43-mediated neurodegeneration. Yet, an important difference between "physiological" and "pathological" TDP-43^{+} stress granules must be noted: stress granules are not typically modified by ubiquitin, yet disease

aggregates are clearly ubiquitin-modified. This raises the question of how ubiquitin-modified stress granules alter normal cellular functions, specifically through modulation of cellular signaling pathways?

Secondly, TDP-43 pathological granules are predominantly composed of TDP-43, whereas the stress granules in our assay stain for multiple RNA-binding proteins including TIAR, HuR and hnRNP A1. Previous results have indicated that pathological TDP-43 fails to costain with either hnRNP A1 or SMN(99). Hence, the composition of granules in my model, versus in the brain, are different, because TDP-43 is robustly colocalized with hnRNP A1 in stressed glial cells. One of the questions that remain then, is if TDP-43 is the primary component of these ubiquitinated aggregates, is TDP-43 really localizing to stress granules in most pathological tissues? -Or are other components of stress granules able to dissociate from the stress granule, while TDP-43 is unable to dissociate?

Finally, stress granules are reversible structures, but it appears that pathological aggregates are irreversibly "stuck" in the cytoplasm. Could this inability to dissociate from stress granules be the cytoplasmic toxic gain of function mediating the disease? In future experiments, I need to examine the ability of overexpressed wild-type and mutant TDP-43 to dissociate from stress granules following removal of the stressor.

Limitations of the cytoplasmic toxic gain of function disease hypothesis: the strengths of the nuclear loss of function hypothesis

How TDP-43 mediates neurodegeneration in ALS or FTLD-U is unknown. We cannot disregard the importance of other hypotheses being tested to understand TDP-43-mediated neurodegeneration. An alternate, very promising hypothesis is that a loss of nuclear TDP-43 function causes neuronal death. Polymenidou et. al. tested this hypothesis in adult mouse striatum following stereotactic injection of antisense oligonucleotides to TDP-43. Deep sequencing was used to determine RNA profile changes in knockdown and control samples. They found 601 mRNAs changed, and 965 altered splicing events were observed (knockdown vs. control). The authors conclude that nuclear depletion of TDP-43 leads to long pre-mRNA depletion and RNA mis-splicing culminating in neuronal vulnerability(110). In a similar study by Tollervey, the authors found that TDP-43 knockdown resulted in an increase of BIMs, the most cytotoxic isoform of BIM. Importantly, Tollervey et. al. found an increase in the BIMs isoform in FTLD-U patients relative to control(125). These papers offer important mechanistic insights into TDP-43-mediated cell death through mis-splicing.

Determinants of SG size: how does increased SG size affect the timecourse of TDP-43 disassembly?

It is now known that both TDP-43 and FUS localize to abnormally large stress granules during stress(19, 30, 42). Because both RNA binding proteins seem to generate larger stress granules, this argues in favor that increased SG size

somehow leads to the neurodegenerative phenotype. Yet, what accounts for this increased size? Previous studies have indicated that SG dynamics can be modulated by microtubule stability(32), the motor proteins dynein and kinesin(91, 128), RhoA/ROCK1(129) signaling and Grb7/FAK signaling(127). However, how TDP-43 feeds into these pathways, or modifies motor proteins is unknown. We discuss novel hypotheses proposed to explain SG size regulation by TDP-43.

TDP-43 is a determinant of SG size by regulating TIA-1 protein levels?

As for the involvement of TDP-43 in SG dynamics, a recent paper exploring TDP-43's function during stress found that knockdown of TDP-43 delayed the formation of stress granules(93). Also, TDP-43 was not necessary for SG formation, as TDP-43 knockdown cells formed SGs in response to arsenite stress(93). The authors argued that TDP-43 knockdown resulted in a reduction of TIA1, which is a seed for SG assembly(7, 74, 77, 93). Although no direct evidence of TDP-43's regulation of TIA-1 mRNA or protein was included in this report(93), the authors present a testable hypothesis of how TDP-43 modulates SG assembly.

TDP-43 pathological mutants alter stress granule size through novel protein:protein interactions?

As most pathological TDP-43 mutations span the GRR, one disease hypothesis is that these mutations disrupt protein:protein interactions, leading to altered splicing and cell death. Surprisingly, the TDP-43:hnRNP protein

interaction profile fails to change in response to overexpressed pathological TDP-43 in Hek293T cells(119). However, the lack of protein:protein interaction changes may be due to the use of Hek293T cells for this study, which cannot model a neuronal or glial-specific proteome(69).

Novel post-translational modifications on pathological TDP-43 mutants mediates increased SG size in response to stress?

At present, it is unknown how post-translational modifications alter TDP-43's protein:protein interaction profile, or its localization. If TDP-43 is modified similarly to other hnRNP family proteins, phosphorylation, acetylation and methylation may play roles in its localization(45). Phosphorylation of TDP-43 is of particular interest, as pathological TDP-43 is hyperphosphorylated in the hippocampus, neocortex and spinal cord(138). At present, it is known that TDP-43 is phosphorylated by casein-kinase-1(68). Additional studies are necessary to identify novel kinases targeting TDP-43. Of particular interest with respect to TDP-43 and stress granule dynamics is how and what modifications to TDP-43 affect the ability of it to disassemble from SGs.

Pathological TDP-43 mutants are more stable, so more TDP-43 is directed to stress granules in response to stress relative to control?

For reasons that are not yet understood, the pathological TDP-43 mutant is actually more stable than wild-type TDP-43(87). Therefore, one interpretation might be that increased cytoplasmic levels of TDP-43 means more TDP-43 bound

to mRNA transcript. And as previously shown and discussed, TDP-43 requires mRNA binding to localize to stress granules. Therefore, more mRNA-bound TDP-43 is directed to SGs in response to stress, resulting in larger stress granules.

Additional, testable hypotheses that might explain larger TDP-43 stress granules from pathological TDP-43 overexpression relative to wild-type

Additional hypotheses as to why the pathological mutants generate larger stress granules relative to wild-type include the following: first, that pathological TDP-43 mutants alter chaperone levels, facilitating more insoluble, aggregated and ubiquitinated TDP-43. Second, that pathological TDP-43 mutants alter degradative pathways of the cell, generating larger stress granules. Third, that pathological TDP-43 mutants alter microtubule stability, altering stress granule size. These hypotheses require further testing, although they make sense in the context of different disease hypotheses (as explained in Chapter 1: both ALS and FTLD-U may be caused by aberrations in the degradative capacity of the cell; the other genetic component of FTLD-U is caused by mutations in the microtubule protein tau).

Future Directions

As previously discussed, current TDP-43 research is focused on understanding its basic cellular functions. The TDP-43 field has come a long way since 2006, when very little was known about its localization or functions. With the understanding of where TDP-43 binds RNA, we have gathered an important

idea of the function of TDP-43 in the cell. Furthermore, because FUS (another RNA binding protein) is pathologically altered and genetically linked to both ALS and FTLD, this strongly implicates altered RNA metabolism in disease onset. It is necessary that a comparative approach between TDP-43 and FUS splicing targets be completed.

Yet, to understand disease onset, an important question remains: what initial cellular insult(s) signal TDP-43's nuclear depletion and cytoplasmic aggregation? I have significantly contributed to this question by defining a physiological stressor that directs TDP-43 to cytoplasmic aggregates called stress granules (SGs) in glial cells. As it is now recognized that pathological TDP-43 colabels with SG markers, this further reinforces the importance of my work. Also, I have addressed how pathological mutations alter stress granule assembly, culminating in abnormally large SGs with mutant overexpression relative to wild-type. Moreover, I have defined the temporal assembly of overexpressed wild-type and mutant TDP-43 during stress administration. Future studies will need to address why and how wild-type TDP-43 stress granule assembly is delayed relative to mutant TDP-43, in addition to how pathological mutants result in enlarged stress granule size relative to wild-type. Finally, future studies must also address when and how stress granules are ubiquitinated, and how this affects their assembly and disassembly.

Final Perspectives

Determining common etiologies of neurodegenerative diseases is integral to improving both the diagnosis and treatment of patients. Currently, patients are diagnosed after presenting common symptoms. Unfortunately, many symptoms arise only after catastrophic neuronal loss has already occurred. This complicates treatment options, etc. leading to bad outcomes for both patients and caregivers. To improve the system, it is essential to: 1. Develop more sensitive methods to detect the onset of neurodegeneration. 2. Identify lifestyle risk factors that lead to neurodegeneration. 3. Identify genetic risk factors that lead to neurodegeneration. 4. Identify common pathological changes before catastrophic neuronal loss.

As new diagnostics are developed, treatment options can be re-addressed. 1. If early diagnosis can be established, clinical trials can be repeated. Drugs that were not effective when administered at a later disease stage might be effective at a pre-symptomatic stage. 2. As novel lifestyle risk factors are identified, the public can be informed of preventative measures they can take to reduce their risks. 3. As novel genes are identified, novel drugs can be developed and tested in animal models and clinical trials.

The study of TDP-43, especially in the context of its most basic cellular functions, is a crucial new area of neurodegenerative research. The study of TDP-43 will allow scientists to bridge the gap in understanding how clinically diverse disorders may have common pathological etiologies. In this respect, the study of

TDP-43 offers the best potential for achieving the above goals, at a time when our population is aging and in need of new therapeutic options.

BIBLIOGRAPHY

1. **Abhyankar, M. M., C. Urekar, and P. P. Reddi.** 2007. A novel CpG-free vertebrate insulator silences the testis-specific SP-10 gene in somatic tissues: role for TDP-43 in insulator function. J Biol Chem **282:**36143-36154.
2. **Acharya, K. K., C. K. Govind, A. N. Shore, M. H. Stoler, and P. P. Reddi.** 2006. cis-requirement for the maintenance of round spermatid-specific transcription. Dev Biol **295:**781-790.
3. **Albert, T. C., E. Johnson, D. Gasperino, and P. Tokatli.** 2003. Planning for the baby boomers' healthcare needs: a case study. J Hosp Mark Public Relations **15:**77-88.
4. **Allemand, E., S. Guil, M. Myers, J. Moscat, J. F. Caceres, and A. R. Krainer.** 2005. Regulation of heterogenous nuclear ribonucleoprotein A1 transport by phosphorylation in cells stressed by osmotic shock. Proc Natl Acad Sci U S A **102:**3605-3610.
5. **Anderson, P., and N. Kedersha.** 2009. Stress granules. Curr Biol **19:**R397-398.
6. **Anderson, P., and N. Kedersha.** 2008. Stress granules: the Tao of RNA triage. Trends Biochem Sci **33:**141-150.
7. **Anderson, P., and N. Kedersha.** 2002. Visibly stressed: the role of eIF2, TIA-1, and stress granules in protein translation. Cell Stress Chaperones **7:**213-221.
8. **Aquilano, K., G. Filomeni, L. Di Renzo, M. Vito, C. Stefano, P. S. Salimei, M. R. Ciriolo, and G. Marfe.** 2007. Reactive oxygen and nitrogen species are involved in sorbitol-induced apoptosis of human erithroleukaemia cells K562. Free Radic Res **41:**452-460.
9. **Arai, T., M. Hasegawa, H. Akiyama, K. Ikeda, T. Nonaka, H. Mori, D. Mann, K. Tsuchiya, M. Yoshida, Y. Hashizume, and T. Oda.** 2006. TDP-43 is a component of ubiquitin-positive tau-negative inclusions in frontotemporal lobar degeneration and amyotrophic lateral sclerosis. Biochem Biophys Res Commun **351:**602-611.
10. **Arimoto, K., H. Fukuda, S. Imajoh-Ohmi, H. Saito, and M. Takekawa.** 2008. Formation of stress granules inhibits apoptosis by suppressing stress-responsive MAPK pathways. Nat Cell Biol **10:**1324-1332.
11. **Ayala, Y. M., T. Misteli, and F. E. Baralle.** 2008. TDP-43 regulates retinoblastoma protein phosphorylation through the repression of cyclin-dependent kinase 6 expression. Proc Natl Acad Sci U S A **105:**3785-3789.
12. **Ayala, Y. M., F. Pagani, and F. E. Baralle.** 2006. TDP43 depletion rescues aberrant CFTR exon 9 skipping. FEBS Lett **580:**1339-1344.
13. **Ayala, Y. M., S. Pantano, A. D'Ambrogio, E. Buratti, A. Brindisi, C. Marchetti, M. Romano, and F. E. Baralle.** 2005. Human, Drosophila,

and C.elegans TDP43: nucleic acid binding properties and splicing regulatory function. J Mol Biol **348:**575-588.

14. **Ayala, Y. M., P. Zago, A. D'Ambrogio, Y. F. Xu, L. Petrucelli, E. Buratti, and F. E. Baralle.** 2008. Structural determinants of the cellular localization and shuttling of TDP-43. J Cell Sci **121:**3778-3785.
15. **Balagopal, V., and R. Parker.** 2009. Polysomes, P bodies and stress granules: states and fates of eukaryotic mRNAs. Curr Opin Cell Biol **21:**403-408.
16. **Barnham, K. J., R. Cappai, K. Beyreuther, C. L. Masters, and A. F. Hill.** 2006. Delineating common molecular mechanisms in Alzheimer's and prion diseases. Trends Biochem Sci **31:**465-472.
17. **Beckham, C. J., and R. Parker.** 2008. P bodies, stress granules, and viral life cycles. Cell Host Microbe **3:**206-212.
18. **Borroni, B., C. Bonvicini, A. Alberici, E. Buratti, C. Agosti, S. Archetti, A. Papetti, C. Stuani, M. Di Luca, M. Gennarelli, and A. Padovani.** 2009. Mutation within TARDBP leads to frontotemporal dementia without motor neuron disease. Hum Mutat **30:**E974-983.
19. **Bosco, D. A., N. Lemay, H. K. Ko, H. Zhou, C. Burke, T. J. Kwiatkowski, Jr., P. Sapp, D. McKenna-Yasek, R. H. Brown, Jr., and L. J. Hayward.** 2010. Mutant FUS Proteins that Cause Amyotrophic Lateral Sclerosis Incorporate into Stress Granules. Hum Mol Genet.
20. **Bose, J. K., I. F. Wang, L. Hung, W. Y. Tarn, and C. K. Shen.** 2008. TDP-43 overexpression enhances exon 7 inclusion during the survival of motor neuron pre-mRNA splicing. J Biol Chem **283:**28852-28859.
21. **Buchan, J. R., and R. Parker.** 2009. Eukaryotic stress granules: the ins and outs of translation. Mol Cell **36:**932-941.
22. **Buchan, J. R., J. H. Yoon, and R. Parker.** 2011. Stress-specific composition, assembly and kinetics of stress granules in Saccharomyces cerevisiae. J Cell Sci **124:**228-239.
23. **Buratti, E., and F. E. Baralle.** 2001. Characterization and functional implications of the RNA binding properties of nuclear factor TDP-43, a novel splicing regulator of CFTR exon 9. J Biol Chem **276:**36337-36343.
24. **Buratti, E., and F. E. Baralle.** 2009. The molecular links between TDP-43 dysfunction and neurodegeneration. Adv Genet **66:**1-34.
25. **Buratti, E., and F. E. Baralle.** 2010. The multiple roles of TDP-43 in pre-mRNA processing and gene expression regulation. RNA Biol **7**.
26. **Buratti, E., A. Brindisi, M. Giombi, S. Tisminetzky, Y. M. Ayala, and F. E. Baralle.** 2005. TDP-43 binds heterogeneous nuclear ribonucleoprotein A/B through its C-terminal tail: an important region for the inhibition of cystic fibrosis transmembrane conductance regulator exon 9 splicing. J Biol Chem **280:**37572-37584.
27. **Buratti, E., A. Brindisi, F. Pagani, and F. E. Baralle.** 2004. Nuclear factor TDP-43 binds to the polymorphic TG repeats in CFTR intron 8 and causes skipping of exon 9: a functional link with disease penetrance. Am J Hum Genet **74:**1322-1325.

28. **Buratti, E., T. Dork, E. Zuccato, F. Pagani, M. Romano, and F. E. Baralle.** 2001. Nuclear factor TDP-43 and SR proteins promote in vitro and in vivo CFTR exon 9 skipping. EMBO J **20:**1774-1784.
29. **Cairns, N. J., M. Neumann, E. H. Bigio, I. E. Holm, D. Troost, K. J. Hatanpaa, C. Foong, C. L. White, 3rd, J. A. Schneider, H. A. Kretzschmar, D. Carter, L. Taylor-Reinwald, K. Paulsmeyer, J. Strider, M. Gitcho, A. M. Goate, J. C. Morris, M. Mishra, L. K. Kwong, A. Stieber, Y. Xu, M. S. Forman, J. Q. Trojanowski, V. M. Lee, and I. R. Mackenzie.** 2007. TDP-43 in familial and sporadic frontotemporal lobar degeneration with ubiquitin inclusions. Am J Pathol **171:**227-240.
30. **Cantoni, C., C. Fenoglio, F. Cortini, E. Venturelli, C. Villa, F. Clerici, A. Marcone, L. Benussi, R. Ghidoni, S. Gallone, D. Scalabrini, M. Franceschi, S. Cappa, G. Binetti, C. Mariani, I. Rainero, M. T. Giordana, N. Bresolin, E. Scarpini, and D. Galimberti.** 2010. FUS/TLS genetic variability in sporadic frontotemporal lobar degeneration. J Alzheimers Dis **19:**1317-1322.
31. **Chen-Plotkin, A. S., V. M. Lee, and J. Q. Trojanowski.** 2010. TAR DNA-binding protein 43 in neurodegenerative disease. Nat Rev Neurol **6:**211-220.
32. **Chernov, K. G., A. Barbet, L. Hamon, L. P. Ovchinnikov, P. A. Curmi, and D. Pastre.** 2009. Role of microtubules in stress granule assembly: microtubule dynamical instability favors the formation of micrometric stress granules in cells. J Biol Chem **284:**36569-36580.
33. **Chung, S. S., E. C. Ho, K. S. Lam, and S. K. Chung.** 2003. Contribution of polyol pathway to diabetes-induced oxidative stress. J Am Soc Nephrol **14:**S233-236.
34. **Cleveland, D. W., and J. D. Rothstein.** 2001. From Charcot to Lou Gehrig: deciphering selective motor neuron death in ALS. Nat Rev Neurosci **2:**806-819.
35. **Colombrita, C., E. Zennaro, C. Fallini, M. Weber, A. Sommacal, E. Buratti, V. Silani, and A. Ratti.** 2009. TDP-43 is recruited to stress granules in conditions of oxidative insult. J Neurochem **111:**1051-1061.
36. **Cooper, T. A., L. Wan, and G. Dreyfuss.** 2009. RNA and disease. Cell **136:**777-793.
37. **D'Ambrogio, A., E. Buratti, C. Stuani, C. Guarnaccia, M. Romano, Y. M. Ayala, and F. E. Baralle.** 2009. Functional mapping of the interaction between TDP-43 and hnRNP A2 in vivo. Nucleic Acids Res **37:**4116-4126.
38. **Dahm, R., and P. Macchi.** 2007. Human pathologies associated with defective RNA transport and localization in the nervous system. Biol Cell **99:**649-661.
39. **Daoud, H., P. N. Valdmanis, E. Kabashi, P. Dion, N. Dupre, W. Camu, V. Meininger, and G. A. Rouleau.** 2009. Contribution of

TARDBP mutations to sporadic amyotrophic lateral sclerosis. J Med Genet **46:**112-114.

40. **DeGracia, D. J., J. Rudolph, G. G. Roberts, J. A. Rafols, and J. Wang.** 2007. Convergence of stress granules and protein aggregates in hippocampal cornu ammonis 1 at later reperfusion following global brain ischemia. Neuroscience **146:**562-572.
41. **Del Bo, R., S. Ghezzi, S. Corti, M. Pandolfo, M. Ranieri, D. Santoro, I. Ghione, A. Prelle, V. Orsetti, M. Mancuso, G. Soraru, C. Briani, C. Angelini, G. Siciliano, N. Bresolin, and G. P. Comi.** 2009. TARDBP (TDP-43) sequence analysis in patients with familial and sporadic ALS: identification of two novel mutations. Eur J Neurol **16:**727-732.
42. **Dewey, C. M., B. Cenik, C. F. Sephton, D. R. Dries, P. Mayer, 3rd, S. K. Good, B. A. Johnson, J. Herz, and G. Yu.** 2011. TDP-43 is directed to stress granules by sorbitol, a novel physiological osmotic and oxidative stressor. Mol Cell Biol **31:**1098-1108.
43. **Dormann, D., A. Capell, A. M. Carlson, S. S. Shankaran, R. Rodde, M. Neumann, E. Kremmer, T. Matsuwaki, K. Yamanouchi, M. Nishihara, and C. Haass.** 2009. Proteolytic processing of TAR DNA binding protein-43 by caspases produces C-terminal fragments with disease defining properties independent of progranulin. J Neurochem **110:**1082-1094.
44. **Draper, B., and D. Anderson.** 2010. The baby boomers are nearly here - but do we have sufficient workforce in old age psychiatry? Int Psychogeriatr **22:**947-949.
45. **Dreyfuss, G., V. N. Kim, and N. Kataoka.** 2002. Messenger-RNA-binding proteins and the messages they carry. Nat Rev Mol Cell Biol **3:**195-205.
46. **Eisinger-Mathason, T. S., J. Andrade, A. L. Groehler, D. E. Clark, T. L. Muratore-Schroeder, L. Pasic, J. A. Smith, J. Shabanowitz, D. F. Hunt, I. G. Macara, and D. A. Lannigan.** 2008. Codependent functions of RSK2 and the apoptosis-promoting factor TIA-1 in stress granule assembly and cell survival. Mol Cell **31:**722-736.
47. **Ferrari, R., D. Kapogiannis, E. D. Huey, and P. Momeni.** 2011. FTD and ALS: A Tale of Two Diseases. Curr Alzheimer Res.
48. **Forman, M. S., J. Q. Trojanowski, and V. M. Lee.** 2007. TDP-43: a novel neurodegenerative proteinopathy. Curr Opin Neurobiol **17:**548-555.
49. **Freibaum, B. D., R. K. Chitta, A. A. High, and J. P. Taylor.** 2010. Global analysis of TDP-43 interacting proteins reveals strong association with RNA splicing and translation machinery. J Proteome Res **9:**1104-1120.
50. **Gassoumis, Z. D., K. H. Wilber, L. A. Baker, and F. M. Torres-Gil.** 2010. Who are the Latino baby boomers? Demographic and economic characteristics of a hidden population. J Aging Soc Policy **22:**53-68.
51. **Geser, F., N. J. Brandmeir, L. K. Kwong, M. Martinez-Lage, L. Elman, L. McCluskey, S. X. Xie, V. M. Lee, and J. Q. Trojanowski.**

2008. Evidence of multisystem disorder in whole-brain map of pathological TDP-43 in amyotrophic lateral sclerosis. Arch Neurol **65:**636-641.

52. **Geser, F., V. M. Lee, and J. Q. Trojanowski.** 2010. Amyotrophic lateral sclerosis and frontotemporal lobar degeneration: a spectrum of TDP-43 proteinopathies. Neuropathology **30:**103-112.
53. **Geser, F., M. Martinez-Lage, L. K. Kwong, V. M. Lee, and J. Q. Trojanowski.** 2009. Amyotrophic lateral sclerosis, frontotemporal dementia and beyond: the TDP-43 diseases. J Neurol **256:**1205-1214.
54. **Geser, F., M. Martinez-Lage, J. Robinson, K. Uryu, M. Neumann, N. J. Brandmeir, S. X. Xie, L. K. Kwong, L. Elman, L. McCluskey, C. M. Clark, J. Malunda, B. L. Miller, E. A. Zimmerman, J. Qian, V. Van Deerlin, M. Grossman, V. M. Lee, and J. Q. Trojanowski.** 2009. Clinical and pathological continuum of multisystem TDP-43 proteinopathies. Arch Neurol **66:**180-189.
55. **Gitcho, M. A., R. H. Baloh, S. Chakraverty, K. Mayo, J. B. Norton, D. Levitch, K. J. Hatanpaa, C. L. White, 3rd, E. H. Bigio, R. Caselli, M. Baker, M. T. Al-Lozi, J. C. Morris, A. Pestronk, R. Rademakers, A. M. Goate, and N. J. Cairns.** 2008. TDP-43 A315T mutation in familial motor neuron disease. Ann Neurol **63:**535-538.
56. **Gitcho, M. A., E. H. Bigio, M. Mishra, N. Johnson, S. Weintraub, M. Mesulam, R. Rademakers, S. Chakraverty, C. Cruchaga, J. C. Morris, A. M. Goate, and N. J. Cairns.** 2009. TARDBP 3'-UTR variant in autopsy-confirmed frontotemporal lobar degeneration with TDP-43 proteinopathy. Acta Neuropathol **118:**633-645.
57. **Grossman, M., E. M. Wood, P. Moore, M. Neumann, L. Kwong, M. S. Forman, C. M. Clark, L. F. McCluskey, B. L. Miller, V. M. Lee, and J. Q. Trojanowski.** 2007. TDP-43 pathologic lesions and clinical phenotype in frontotemporal lobar degeneration with ubiquitin-positive inclusions. Arch Neurol **64:**1449-1454.
58. **Guil, S., J. C. Long, and J. F. Caceres.** 2006. hnRNP A1 relocalization to the stress granules reflects a role in the stress response. Mol Cell Biol **26:**5744-5758.
59. **Harrison, C. F., V. A. Lawson, B. M. Coleman, Y. S. Kim, C. L. Masters, R. Cappai, K. J. Barnham, and A. F. Hill.** 2010. Conservation of a glycine-rich region in the prion protein is required for uptake of prion infectivity. J Biol Chem **285:**20213-20223.
60. **Haverkamp, L. J., V. Appel, and S. H. Appel.** 1995. Natural history of amyotrophic lateral sclerosis in a database population. Validation of a scoring system and a model for survival prediction. Brain **118 (Pt 3):**707-719.
61. **Heise, L.** 1988. China's baby boomers. World Watch **1:**10-11.
62. **Hu, W. T., and M. Grossman.** 2009. TDP-43 and frontotemporal dementia. Curr Neurol Neurosci Rep **9:**353-358.
63. **Iijima, M., M. Suzuki, A. Tanabe, A. Nishimura, and M. Yamada.** 2006. Two motifs essential for nuclear import of the hnRNP A1

nucleocytoplasmic shuttling sequence M9 core. FEBS Lett **580:**1365-1370.

64. **Izaurralde, E., A. Jarmolowski, C. Beisel, I. W. Mattaj, G. Dreyfuss, and U. Fischer.** 1997. A role for the M9 transport signal of hnRNP A1 in mRNA nuclear export. J Cell Biol **137:**27-35.
65. **Izawa, M., and K. Teramachi.** 2001. Down-regulation of protein kinase C activity by sorbitol rapidly induces apoptosis in human gastric cancer cell lines. Apoptosis **6:**353-358.
66. **Kabashi, E., L. Lin, M. L. Tradewell, P. A. Dion, V. Bercier, P. Bourgouin, D. Rochefort, S. Bel Hadj, H. D. Durham, C. Vande Velde, G. A. Rouleau, and P. Drapeau.** 2010. Gain and loss of function of ALS-related mutations of TARDBP (TDP-43) cause motor deficits in vivo. Hum Mol Genet **19:**671-683.
67. **Kabashi, E., P. N. Valdmanis, P. Dion, D. Spiegelman, B. J. McConkey, C. Vande Velde, J. P. Bouchard, L. Lacomblez, K. Pochigaeva, F. Salachas, P. F. Pradat, W. Camu, V. Meininger, N. Dupre, and G. A. Rouleau.** 2008. TARDBP mutations in individuals with sporadic and familial amyotrophic lateral sclerosis. Nat Genet **40:**572-574.
68. **Kametani, F., T. Nonaka, T. Suzuki, T. Arai, N. Dohmae, H. Akiyama, and M. Hasegawa.** 2009. Identification of casein kinase-1 phosphorylation sites on TDP-43. Biochem Biophys Res Commun **382:**405-409.
69. **Kamma, H., D. S. Portman, and G. Dreyfuss.** 1995. Cell type-specific expression of hnRNP proteins. Exp Cell Res **221:**187-196.
70. **Kedersha, N., and P. Anderson.** 2009. Chapter 4 Regulation of Translation by Stress Granules and Processing Bodies. Prog Mol Biol Transl Sci **90C:**155-185.
71. **Kedersha, N., and P. Anderson.** 2007. Mammalian stress granules and processing bodies. Methods Enzymol **431:**61-81.
72. **Kedersha, N., and P. Anderson.** 2002. Stress granules: sites of mRNA triage that regulate mRNA stability and translatability. Biochem Soc Trans **30:**963-969.
73. **Kedersha, N., S. Chen, N. Gilks, W. Li, I. J. Miller, J. Stahl, and P. Anderson.** 2002. Evidence that ternary complex (eIF2-GTP-tRNA(i)(Met))-deficient preinitiation complexes are core constituents of mammalian stress granules. Mol Biol Cell **13:**195-210.
74. **Kedersha, N., M. R. Cho, W. Li, P. W. Yacono, S. Chen, N. Gilks, D. E. Golan, and P. Anderson.** 2000. Dynamic shuttling of TIA-1 accompanies the recruitment of mRNA to mammalian stress granules. J Cell Biol **151:**1257-1268.
75. **Kedersha, N., G. Stoecklin, M. Ayodele, P. Yacono, J. Lykke-Andersen, M. J. Fritzler, D. Scheuner, R. J. Kaufman, D. E. Golan, and P. Anderson.** 2005. Stress granules and processing bodies are dynamically linked sites of mRNP remodeling. J Cell Biol **169:**871-884.

76. **Kedersha, N., S. Tisdale, T. Hickman, and P. Anderson.** 2008. Real-time and quantitative imaging of mammalian stress granules and processing bodies. Methods Enzymol **448:**521-552.
77. **Kedersha, N. L., M. Gupta, W. Li, I. Miller, and P. Anderson.** 1999. RNA-binding proteins TIA-1 and TIAR link the phosphorylation of eIF-2 alpha to the assembly of mammalian stress granules. J Cell Biol **147:**1431-1442.
78. **Kondo, T., T. Shirasawa, Y. Itoyama, and H. Mori.** 1996. Embryonic genes expressed in Alzheimer's disease brains. Neurosci Lett **209:**157-160.
79. **Kovacs, G. G., J. R. Murrell, S. Horvath, L. Haraszti, K. Majtenyi, M. J. Molnar, H. Budka, B. Ghetti, and S. Spina.** 2009. TARDBP variation associated with frontotemporal dementia, supranuclear gaze palsy, and chorea. Mov Disord **24:**1843-1847.
80. **Krecic, A. M., and M. S. Swanson.** 1999. hnRNP complexes: composition, structure, and function. Curr Opin Cell Biol **11:**363-371.
81. **Kuhnlein, P., A. D. Sperfeld, B. Vanmassenhove, V. Van Deerlin, V. M. Lee, J. Q. Trojanowski, H. A. Kretzschmar, A. C. Ludolph, and M. Neumann.** 2008. Two German kindreds with familial amyotrophic lateral sclerosis due to TARDBP mutations. Arch Neurol **65:**1185-1189.
82. **Kuo, P. H., L. G. Doudeva, Y. T. Wang, C. K. Shen, and H. S. Yuan.** 2009. Structural insights into TDP-43 in nucleic-acid binding and domain interactions. Nucleic Acids Res **37:**1799-1808.
83. **Kwong, L. K., M. Neumann, D. M. Sampathu, V. M. Lee, and J. Q. Trojanowski.** 2007. TDP-43 proteinopathy: the neuropathology underlying major forms of sporadic and familial frontotemporal lobar degeneration and motor neuron disease. Acta Neuropathol **114:**63-70.
84. **Kwong, L. K., K. Uryu, J. Q. Trojanowski, and V. M. Lee.** 2008. TDP-43 proteinopathies: neurodegenerative protein misfolding diseases without amyloidosis. Neurosignals **16:**41-51.
85. **Lagier-Tourenne, C., and D. W. Cleveland.** 2009. Rethinking ALS: the FUS about TDP-43. Cell **136:**1001-1004.
86. **Lagier-Tourenne, C., M. Polymenidou, and D. W. Cleveland.** 2010. TDP-43 and FUS/TLS: emerging roles in RNA processing and neurodegeneration. Hum Mol Genet **19:**R46-64.
87. **Ling, S. C., C. P. Albuquerque, J. S. Han, C. Lagier-Tourenne, S. Tokunaga, H. Zhou, and D. W. Cleveland.** 2010. ALS-associated mutations in TDP-43 increase its stability and promote TDP-43 complexes with FUS/TLS. Proc Natl Acad Sci U S A **107:**13318-13323.
88. **Liu-Yesucevitz, L., A. Bilgutay, Y. J. Zhang, T. Vanderwyde, A. Citro, T. Mehta, N. Zaarur, A. McKee, R. Bowser, M. Sherman, L. Petrucelli, and B. Wolozin.** 2010. Tar DNA binding protein-43 (TDP-43) associates with stress granules: analysis of cultured cells and pathological brain tissue. PLoS One **5:**e13250.

89. **Lomen-Hoerth, C., T. Anderson, and B. Miller.** 2002. The overlap of amyotrophic lateral sclerosis and frontotemporal dementia. Neurology **59:**1077-1079.
90. **Lomen-Hoerth, C., J. Murphy, S. Langmore, J. H. Kramer, R. K. Olney, and B. Miller.** 2003. Are amyotrophic lateral sclerosis patients cognitively normal? Neurology **60:**1094-1097.
91. **Loschi, M., C. C. Leishman, N. Berardone, and G. L. Boccaccio.** 2009. Dynein and kinesin regulate stress-granule and P-body dynamics. J Cell Sci **122:**3973-3982.
92. **Lukong, K. E., K. W. Chang, E. W. Khandjian, and S. Richard.** 2008. RNA-binding proteins in human genetic disease. Trends Genet **24:**416-425.
93. **McDonald, K. K., A. Aulas, L. Destroismaisons, S. Pickles, E. Beleac, W. Camu, G. A. Rouleau, and C. Vande Velde.** 2011. TAR DNA-binding protein 43 (TDP-43) regulates stress granule dynamics via differential regulation of G3BP and TIA-1. Hum Mol Genet **20:**1400-1410.
94. **Mercado, P. A., Y. M. Ayala, M. Romano, E. Buratti, and F. E. Baralle.** 2005. Depletion of TDP 43 overrides the need for exonic and intronic splicing enhancers in the human apoA-II gene. Nucleic Acids Res **33:**6000-6010.
95. **Michael, W. M., P. S. Eder, and G. Dreyfuss.** 1997. The K nuclear shuttling domain: a novel signal for nuclear import and nuclear export in the hnRNP K protein. EMBO J **16:**3587-3598.
96. **Miller, R. G., J. P. Bouchard, P. Duquette, A. Eisen, D. Gelinas, Y. Harati, T. L. Munsat, L. Powe, J. Rothstein, P. Salzman, and R. L. Sufit.** 1996. Clinical trials of riluzole in patients with ALS. ALS/Riluzole Study Group-II. Neurology **47:**S86-90; discussion S90-82.
97. **Moisse, K., K. Volkening, C. Leystra-Lantz, I. Welch, T. Hill, and M. J. Strong.** 2009. Divergent patterns of cytosolic TDP-43 and neuronal progranulin expression following axotomy: implications for TDP-43 in the physiological response to neuronal injury. Brain Res **1249:**202-211.
98. **Murray, M., D. Pullman, and T. H. Rodgers.** 2003. Social representations of health and illness among 'baby-boomers' in eastern Canada. J Health Psychol **8:**485-499.
99. **Neumann, M., L. M. Igaz, L. K. Kwong, H. Nakashima-Yasuda, S. J. Kolb, G. Dreyfuss, H. A. Kretzschmar, J. Q. Trojanowski, and V. M. Lee.** 2007. Absence of heterogeneous nuclear ribonucleoproteins and survival motor neuron protein in TDP-43 positive inclusions in frontotemporal lobar degeneration. Acta Neuropathol **113:**543-548.
100. **Neumann, M., L. K. Kwong, D. M. Sampathu, J. Q. Trojanowski, and V. M. Lee.** 2007. TDP-43 proteinopathy in frontotemporal lobar degeneration and amyotrophic lateral sclerosis: protein misfolding diseases without amyloidosis. Arch Neurol **64:**1388-1394.

101. **Neumann, M., L. K. Kwong, A. C. Truax, B. Vanmassenhove, H. A. Kretzschmar, V. M. Van Deerlin, C. M. Clark, M. Grossman, B. L. Miller, J. Q. Trojanowski, and V. M. Lee.** 2007. TDP-43-positive white matter pathology in frontotemporal lobar degeneration with ubiquitin-positive inclusions. J Neuropathol Exp Neurol **66:**177-183.
102. **Neumann, M., D. M. Sampathu, L. K. Kwong, A. C. Truax, M. C. Micsenyi, T. T. Chou, J. Bruce, T. Schuck, M. Grossman, C. M. Clark, L. F. McCluskey, B. L. Miller, E. Masliah, I. R. Mackenzie, H. Feldman, W. Feiden, H. A. Kretzschmar, J. Q. Trojanowski, and V. M. Lee.** 2006. Ubiquitinated TDP-43 in frontotemporal lobar degeneration and amyotrophic lateral sclerosis. Science **314:**130-133.
103. **Nishimoto, Y., D. Ito, T. Yagi, Y. Nihei, Y. Tsunoda, and N. Suzuki.** 2010. Characterization of alternative isoforms and inclusion body of the TAR DNA-binding protein-43. J Biol Chem **285:**608-619.
104. **Obrosova, I. G.** 2005. Increased sorbitol pathway activity generates oxidative stress in tissue sites for diabetic complications. Antioxid Redox Signal **7:**1543-1552.
105. **Ou, S. H., F. Wu, D. Harrich, L. F. Garcia-Martinez, and R. B. Gaynor.** 1995. Cloning and characterization of a novel cellular protein, TDP-43, that binds to human immunodeficiency virus type 1 TAR DNA sequence motifs. J Virol **69:**3584-3596.
106. **Pasinelli, P., and R. H. Brown.** 2006. Molecular biology of amyotrophic lateral sclerosis: insights from genetics. Nat Rev Neurosci **7:**710-723.
107. **Pesiridis, G. S., V. M. Lee, and J. Q. Trojanowski.** 2009. Mutations in TDP-43 link glycine-rich domain functions to amyotrophic lateral sclerosis. Hum Mol Genet **18:**R156-162.
108. **Pinol-Roma, S., and G. Dreyfuss.** 1992. Shuttling of pre-mRNA binding proteins between nucleus and cytoplasm. Nature **355:**730-732.
109. **Pollard, V. W., W. M. Michael, S. Nakielny, M. C. Siomi, F. Wang, and G. Dreyfuss.** 1996. A novel receptor-mediated nuclear protein import pathway. Cell **86:**985-994.
110. **Polymenidou, M., C. Lagier-Tourenne, K. R. Hutt, S. C. Huelga, J. Moran, T. Y. Liang, S. C. Ling, E. Sun, E. Wancewicz, C. Mazur, H. Kordasiewicz, Y. Sedaghat, J. P. Donohue, L. Shiue, C. F. Bennett, G. W. Yeo, and D. W. Cleveland.** 2011. Long pre-mRNA depletion and RNA missplicing contribute to neuronal vulnerability from loss of TDP-43. Nat Neurosci **14:**459-468.
111. **Rohn, T. T.** 2008. Caspase-cleaved TAR DNA-binding protein-43 is a major pathological finding in Alzheimer's disease. Brain Res **1228:**189-198.
112. **Rohn, T. T., and P. Kokoulina.** 2009. Caspase-cleaved TAR DNA-binding protein-43 in Pick's disease. Int J Physiol Pathophysiol Pharmacol **1:**25-32.

113. **Rowland, L. P., and N. A. Shneider.** 2001. Amyotrophic lateral sclerosis. N Engl J Med **344:**1688-1700.
114. **Rutherford, N. J., Y. J. Zhang, M. Baker, J. M. Gass, N. A. Finch, Y. F. Xu, H. Stewart, B. J. Kelley, K. Kuntz, R. J. Crook, J. Sreedharan, C. Vance, E. Sorenson, C. Lippa, E. H. Bigio, D. H. Geschwind, D. S. Knopman, H. Mitsumoto, R. C. Petersen, N. R. Cashman, M. Hutton, C. E. Shaw, K. B. Boylan, B. Boeve, N. R. Graff-Radford, Z. K. Wszolek, R. J. Caselli, D. W. Dickson, I. R. Mackenzie, L. Petrucelli, and R. Rademakers.** 2008. Novel mutations in TARDBP (TDP-43) in patients with familial amyotrophic lateral sclerosis. PLoS Genet **4:**e1000193.
115. **Seelaar, H., H. J. Schelhaas, A. Azmani, B. Kusters, S. Rosso, D. Majoor-Krakauer, M. C. de Rijik, P. Rizzu, M. ten Brummelhuis, P. A. van Doorn, W. Kamphorst, R. Willemsen, and J. C. van Swieten.** 2007. TDP-43 pathology in familial frontotemporal dementia and motor neuron disease without Progranulin mutations. Brain **130:**1375-1385.
116. **Sephton, C. F., C. Cenik, A. Kucukural, E. B. Dammer, B. Cenik, Y. Han, C. M. Dewey, F. P. Roth, J. Herz, J. Peng, M. J. Moore, and G. Yu.** 2011. Identification of neuronal RNA targets of TDP-43-containing ribonucleoprotein complexes. J Biol Chem **286:**1204-1215.
117. **Sephton, C. F., S. K. Good, S. Atkin, C. M. Dewey, P. Mayer, 3rd, J. Herz, and G. Yu.** 2010. TDP-43 is a developmentally regulated protein essential for early embryonic development. J Biol Chem **285:**6826-6834.
118. **Sephton, C. F., D. Zhang, T. M. Lehmann, P. R. Pennington, M. P. Scheid, and D. D. Mousseau.** 2009. The nuclear localization of 3'-phosphoinositide-dependent kinase-1 is dependent on its association with the protein tyrosine phosphatase SHP-1. Cell Signal **21:**1634-1644.
119. **Seyfried, N. T., Y. M. Gozal, E. B. Dammer, Q. Xia, D. M. Duong, D. Cheng, J. J. Lah, A. I. Levey, and J. Peng.** 2010. Multiplex SILAC analysis of a cellular TDP-43 proteinopathy model reveals protein inclusions associated with SUMOylation and diverse polyubiquitin chains. Mol Cell Proteomics **9:**705-718.
120. **Siomi, H., and G. Dreyfuss.** 1995. A nuclear localization domain in the hnRNP A1 protein. J Cell Biol **129:**551-560.
121. **Sreedharan, J., I. P. Blair, V. B. Tripathi, X. Hu, C. Vance, B. Rogelj, S. Ackerley, J. C. Durnall, K. L. Williams, E. Buratti, F. Baralle, J. de Belleroche, J. D. Mitchell, P. N. Leigh, A. Al-Chalabi, C. C. Miller, G. Nicholson, and C. E. Shaw.** 2008. TDP-43 mutations in familial and sporadic amyotrophic lateral sclerosis. Science **319:**1668-1672.
122. **Strong, M. J., K. Volkening, R. Hammond, W. Yang, W. Strong, C. Leystra-Lantz, and C. Shoesmith.** 2007. TDP43 is a human low molecular weight neurofilament (hNFL) mRNA-binding protein. Mol Cell Neurosci **35:**320-327.

123. **Teramachi, K., and M. Izawa.** 2000. Rapid induction of apoptosis in human gastric cancer cell lines by sorbitol. Apoptosis **5:**181-187.
124. **Thomas, M. G., L. J. Martinez Tosar, M. A. Desbats, C. C. Leishman, and G. L. Boccaccio.** 2009. Mammalian Staufen 1 is recruited to stress granules and impairs their assembly. J Cell Sci **122:**563-573.
125. **Tollervey, J. R., T. Curk, B. Rogelj, M. Briese, M. Cereda, M. Kayikci, J. Konig, T. Hortobagyi, A. L. Nishimura, V. Zupunski, R. Patani, S. Chandran, G. Rot, B. Zupan, C. E. Shaw, and J. Ule.** 2011. Characterizing the RNA targets and position-dependent splicing regulation by TDP-43. Nat Neurosci **14:**452-458.
126. **Tolnay, M., and S. Frank.** 2007. Pathology and genetics of frontotemporal lobar degeneration: an update. Clin Neuropathol **26:**143-156.
127. **Tsai, N. P., P. C. Ho, and L. N. Wei.** 2008. Regulation of stress granule dynamics by Grb7 and FAK signalling pathway. EMBO J **27:**715-726.
128. **Tsai, N. P., Y. C. Tsui, and L. N. Wei.** 2009. Dynein motor contributes to stress granule dynamics in primary neurons. Neuroscience **159:**647-656.
129. **Tsai, N. P., and L. N. Wei.** 2010. RhoA/ROCK1 signaling regulates stress granule formation and apoptosis. Cell Signal **22:**668-675.
130. **Van Deerlin, V. M., J. B. Leverenz, L. M. Bekris, T. D. Bird, W. Yuan, L. B. Elman, D. Clay, E. M. Wood, A. S. Chen-Plotkin, M. Martinez-Lage, E. Steinbart, L. McCluskey, M. Grossman, M. Neumann, I. L. Wu, W. S. Yang, R. Kalb, D. R. Galasko, T. J. Montine, J. Q. Trojanowski, V. M. Lee, G. D. Schellenberg, and C. E. Yu.** 2008. TARDBP mutations in amyotrophic lateral sclerosis with TDP-43 neuropathology: a genetic and histopathological analysis. Lancet Neurol **7:**409-416.
131. **Wang, H. Y., I. F. Wang, J. Bose, and C. K. Shen.** 2004. Structural diversity and functional implications of the eukaryotic TDP gene family. Genomics **83:**130-139.
132. **Wang, I. F., N. M. Reddy, and C. K. Shen.** 2002. Higher order arrangement of the eukaryotic nuclear bodies. Proc Natl Acad Sci U S A **99:**13583-13588.
133. **Wang, I. F., L. S. Wu, H. Y. Chang, and C. K. Shen.** 2008. TDP-43, the signature protein of FTLD-U, is a neuronal activity-responsive factor. J Neurochem **105:**797-806.
134. **Wicklund, M. P.** 2005. Amyotrophic lateral sclerosis: possible role of environmental influences. Neurol Clin **23:**461-484.
135. **Wilkinson, M. F., and A. B. Shyu.** 2001. Multifunctional regulatory proteins that control gene expression in both the nucleus and the cytoplasm. Bioessays **23:**775-787.
136. **Winston, N. A., and J. Barnes.** 2007. Anticipation of retirement among baby boomers. J Women Aging **19:**137-159.

137. **Wu, L. S., W. C. Cheng, S. C. Hou, Y. T. Yan, S. T. Jiang, and C. K. Shen.** 2010. TDP-43, a neuro-pathosignature factor, is essential for early mouse embryogenesis. Genesis **48:**56-62.
138. **Zhang, H., C. F. Tan, F. Mori, K. Tanji, A. Kakita, H. Takahashi, and K. Wakabayashi.** 2008. TDP-43-immunoreactive neuronal and glial inclusions in the neostriatum in amyotrophic lateral sclerosis with and without dementia. Acta Neuropathol **115:**115-122.
139. **Zhang, Y. J., Y. F. Xu, C. Cook, T. F. Gendron, P. Roettges, C. D. Link, W. L. Lin, J. Tong, M. Castanedes-Casey, P. Ash, J. Gass, V. Rangachari, E. Buratti, F. Baralle, T. E. Golde, D. W. Dickson, and L. Petrucelli.** 2009. Aberrant cleavage of TDP-43 enhances aggregation and cellular toxicity. Proc Natl Acad Sci U S A **106:**7607-7612.
140. **Zhang, Y. J., Y. F. Xu, C. A. Dickey, E. Buratti, F. Baralle, R. Bailey, S. Pickering-Brown, D. Dickson, and L. Petrucelli.** 2007. Progranulin mediates caspase-dependent cleavage of TAR DNA binding protein-43. J Neurosci **27:**10530-10534.